University of Alberta

DEM Modelling, Vegetation Characterization and Mapping of Aspen Parkland Rangeland Using LIDAR Data

by

Guangquan Su

A thesis submitted to the Faculty of Graduate Studies and Research in partial fulfillment of the requirements for the degree of Doctor of Philosophy

in

Rangeland and Wildlife Resources

Department of Agricultural, Food and Nutritional Science

Edmonton, Alberta

Spring, 2004

Library and Archives Canada

Published Heritage Branch

395 Wellington Street
Ottawa ON K1A 0N4
Canada

Bibliothèque et Archives Canada

Direction du Patrimoine de l'édition

395, rue Wellington
Ottawa ON K1A 0N4
Canada

Your file Votre référence
ISBN: 0-612-96322-5
Our file Notre référence
ISBN: 0-612-96322-5

The author has granted a non-exclusive license allowing the Library and Archives Canada to reproduce, loan, distribute or sell copies of this thesis in microform, paper or electronic formats.

The author retains ownership of the copyright in this thesis. Neither the thesis nor substantial extracts from it may be printed or otherwise reproduced without the author's permission.

L'auteur a accordé une licence non exclusive permettant à la Bibliothèque et Archives Canada de reproduire, prêter, distribuer ou vendre des copies de cette thèse sous la forme de microfiche/film, de reproduction sur papier ou sur format électronique.

L'auteur conserve la propriété du droit d'auteur qui protège cette thèse. Ni la thèse ni des extraits substantiels de celle-ci ne doivent être imprimés ou aturement reproduits sans son autorisation.

In compliance with the Canadian Privacy Act some supporting forms may have been removed from this thesis.

While these forms may be included in the document page count, their removal does not represent any loss of content from the thesis.

Conformément à la loi canadienne sur la protection de la vie privée, quelques formulaires secondaires ont été enlevés de cette thèse.

Bien que ces formulaires aient inclus dans la pagination, il n'y aura aucun contenu manquant.

Canada

Abstract

Detailed geographic information system (GIS) studies on plant ecology, animal behavior and soil hydrologic characteristics across spatially complex landscapes require an accurate digital elevation model (DEM). Following interpolation of last return LIDAR data and creation of a LIDAR-derived DEM, a series of 260 points, stratified by vegetation type, slope gradient and off-nadir distance, were ground-truthed using a total laser station, GPS, and 27 interconnected benchmarks. Despite an overall mean accuracy of +2 cm across 8 vegetation types, it created a RMSE (square root of the mean square error) of 1.21 m. DEM elevations were over-estimated within forested areas by an average of 20 cm with a RMSE of 1.05 m, under-estimated (-12 cm, RMSE = 1.36 m) within grasslands. Vegetation type had the greatest influence on DEM accuracy, while off-nadir distance ($P=0.48$) and slope gradient ($P=0.49$) did not influence DEM accuracy; however, the latter factors did interact ($P<0.10$) to effect accuracy.

Vegetation spatial structure (i.e., physiognomy) including plant height, cover, and vertical or horizontal heterogeneity, are important factors influencing biodiversity. Vegetation over and understory were sampled for height, canopy cover, and tree or shrub density within 120 field plots, evenly stratified by vegetation formation (grassland, shrubland, and aspen forest). Results indicated that LIDAR data could be used for estimating the maximum height, cover, and density, of both closed and semi-open stands of aspen ($P<0.001$). However, LIDAR data could not be used to assess understory (< 1.5 m) height within aspen stands, nor grass height and cover.

Recognition and mapping of vegetation types are important for rangelands as they provide a basis for the development and evaluation of management policies and actions.

In this study, LIDAR data were found to be superior to digital classification schedules for their mapping accuracy in aspen forest and grassland, but not shrubland. No single classification schedule created a high classification accuracy map for all types; however, the integration of LIDAR data and digital images achieved maps with corresponding overall accuracies of 91% and 83.9% with 3 and 8 classes of vegetation.

Acknowledgements

I would like to express sincere appreciation to Dr. Edward Bork for his time, effort on my behalf, and contributions to the successful completion of this research throughout my 4 years of graduate program study. I would also like to thank the members of my supervisory committee, Dr. Evelyn Merrill, Dr. Peter Crown, Dr. Ed Korpela, Dr. Subhash Lele and Dr. Yuguang Bai for their support and contributions in improving this research.

I would like to express my sincere appreciation to Dr. Evelyn Merrill for her enormous effort on polishing my writing, as well as her extra help on my daily life. I am also grateful to Dr. Peter Crown for his invaluable advice on the methodology of RS and GIS research and kindness in lending me literature from his lab. I also thank Dr. Ed Korpela for his support and guidance in collecting field data at University of Alberta Kinsella Ranch, including his generosity in lending me a laptop for assisting during data collection. Special thanks are expressed to Dr. Subhash Lele for his valuable insights into the modelling and computational aspects of this dissertation. Sincere thanks are also extended to Dr. YuGuang Bai for his time reviewing my thesis and invaluable advice on the research.

My very special thanks are given to Graduate Student Administrator - Jody Forslund. Without her kind help, it would have been impossible for me to come to Canada in year 2000. Also, it was Jody who went many extra miles and provided me with tons of kind help on solving all kinds of issues I encountered throughout my graduate program, including but not limited to correcting financial mistakes, maintaining

scholarships and coordinating related communications among my Supervisor, AFNS and FGSR.

Appreciation is owed to Brent Finnestad for his tremendous help with data collection in operating the Total Laser Station and GPS in extreme hot summer season. Thank you Dr. Barry Irving for helping identify plant species and providing a convenient home for data collection on the Ranch, as well as your extra help on solving mechanical problems of our data collection vehicle. Special thanks to Rick Pelletier for his effort on maintaining the Spatial Information Systems Laboratory and enormous help on solving various kinds of technical issues in our analysis process. Eternal gratitude goes to Shirley Ross, Linda Hunt, Jennifer Walker, and particularly, Carla Marin for sharing their knowledge on Canadian plant science, as well as friendship on dealing with everyday life.

I would also like to thank my fellow graduate students George Powell, Chad Grekul, Angela Bogen, Hillary Page, Steven Asamoah, Brian Lambert, Jody Best, Laura Blonski, Amanda Bogen, and Trevor Lennox for their friendship and support throughout the program.

Many thanks are given to AFNS Department, University FGSR, Alberta Research Council, FS Chia (Scholarship), Alberta Innovation & Science Research Investments Program, Mary Louise Imrie, Butter Survey Supplies Ltd. and Hodgeson Beef Endowment Fund for providing financial support for the research as well as related conferences.

Finally, I owe a deep debt of gratitude to my beautiful wife for her steadfast support over the years. It was her encouragement, inspiration and sacrifice for the family that made this dissertation a reality.

Table of Contents

1 Introduction 1

1.1 Research Background 1

1.2 LIDAR System Description 5

1.3 Research Objectives 7

1.4 Literature Cited 10

2 Literature Review of the Application of LIDAR Technology 12

2.1 Introduction 12

2.2 Terrain Modelling 13

2.3 Land Cover Classification 15

2.4 Application in Forestry 16

2.4.1 Canopy Height 18

2.4.2 Vertical Distribution of Intercepted Surfaces 23

2.4.3 Aboveground Biomass 24

2.4.4 Other Forest Characteristics 26

2.5 Application of LIDAR Data in Rangeland Management 26

2.6 Problems and Challenges of LIDAR Data Use 29

2.7 Conclusion 29

2.8 Literature Cited 31

3 Influential Factors on LIDAR-derived DEM Accuracy 35

3.1 Introduction 35

3.2 Materials and Methods 37

3.2.1 Study Area 37

3.2.2 LIDAR Data Acquisition and Processing 40
3.2.3 DEM Ground Truthing 42
3.3 Analysis 45
3.4 Results 47
3.4.1 Off-Nadir Distance 47
3.4.2 Slope Gradient 47
3.4.3 Vegetation Types 48
3.4.4 Interaction Effects 48
3.5 Discussion 49
3.5.1 Non-Vegetation Factors 49
3.5.2 Vegetation Factors 50
3.6 Conclusion 52
3.7 Literature Cited 54
3.8 Tables and Figures 56
4 Characterization of Aspen Parkland Vegetation Using LIDAR Data 63
4.1 Introduction 63
4.2 Study Area 66
4.3 Materials and Methods 69
4.3.1 LIDAR Data Acquisition 69
4.3.2 Experimental Design 70
4.3.3 Field Vegetation Sampling 71
4.3.4 LIDAR Data Compilation 72
4.4 Analysis 72

4.4.1 Vegetation Height Characterization Using LIDAR Data 72
4.4.2 Vegetation Cover Characterization Using LIDAR Data 75
4.4.3 Vegetation Density Characterization Using LIDAR Data 76
4.4.4 Assessment of LIDAR Intensity Data 77
4.5 Results 78
4.5.1 Vegetation Height Assessment Using LIDAR Data 78
4.5.2 Vegetation Cover Characterization Using LIDAR Data 79
4.5.3 Density Analysis Using LIDAR Data 80
4.5.4 Assessment of LIDAR Intensity Data 80
4.6 Discussion 82
4.7 Conclusion 88
4.8 Literature Cited 90
4.9 Tables and Figures 94
5 Vegetation Mapping 104
5.1 Introduction 104
5.2 Materials and Methods 108
5.2.1 Study Area 108
5.2.2 LIDAR Data Acquisition 111
5.2.3 Digital Image Acquisition 112
5.2.4 Experimental Design 113
5.3 Analysis 114
5.3.1 Digital Image Classification Schedules 114
5.3.2 LIDAR Data Classification Schedule 117

5.3.3 Classification Schedules Integrating LIDAR Data and Digital Images.. 120
5.4 Results 121
5.4.1 Digital Image Classification Schedules 121
5.4.2 LIDAR Data Classification Schedule 123
5.4.3 Classification Schedules Integrating LIDAR Data and Digital Images.. 124
5.5 Discussion 126
5.6 Conclusion 129
5.7 Literature Cited 132
5.8 Tables and Figures 136
6 Synthesis/Conclusion 150
6.1 Literature Cited 156

List of Tables

Table 3-1 Comparison of interpolation accuracy among the 4 interpolation methods. 56

Table 3-2 Effects of influential factors on the accuracy of a LIDAR-derived DEM. 56

Table 3-3 Comparison among the 4 general vegetation types of their influence on the accuracy of a LIDAR-derived DEM. 57

Table 3-4 Results of the interaction analysis among factors (vegetation, slope and nadir distance) on their influence on the accuracy of the LIDAR-derived DEM. 57

Table 3-5 Comparison among the 8 vegetation types with respect to their influence on accuracy of a LIDAR-derived DEM. 58

Table 4-1 Height and cover characteristics of the 8 vegetation types based on field sampling in July 2001. 94

Table 4-2 Association between LIDAR measured and field sampled mean vegetation height (m). 94

Table 4-3 Mean LIDAR sampling intensity among different vegetation types. 95

Table 4-4 Association of LIDAR sampling intensity with field measured vegetation patchiness. 95

Table 5-1 Height characteristics [mean (range)] of the 8 detailed vegetation types based on field sampling in July 2001. 136

Table 5-2 Contingency table validating accuracy of the 3-class (vegetation) classification schedule using digital images and LIDAR data. 136

Table 5-3 Contingency table assessing classification accuracy of the 3 digital images and a LIDAR data classification schedule for 8 classes of vegetation. 137

List of Figures

Figure 3-1 Field layout for obtaining elevation measurements on ground truthed points using a total laser station. 59

Figure 3-2 The distribution of 27 inter-connected benchmarks and 260 ground truthed data points around those benchmarks. 60

Figure 3-3 Digital elevation model of the study area with a spatial resolution of 1.5 m obtained using IDW 0.3 interpolation 61

Figure 3-4 The relationship between mean vertical accuracy and integrated vegetation characteristics to the over (a) or underestimation (b) of a LIDAR-derived DEM. [*Woodland integrated height and cover value = (understory cover)·(understory height) + (overstory cover) · (overstory height); **Grassland integrated height and cover value = (grass height) · (grass cover)]. The square brackets represent the std. dev. of the integrated values 62

Figure 4-1 Field vegetation and LIDAR data sampling diagram in 2-dimension (a) and 3- dimension (b). 96

Figure 4-2 Estimated height division lines between herb and shrub layers, and between shrub and tree layers in closed (a) and semi-open (b) aspen forest. 97

Figure 4-3 Association of LIDAR estimated height with field measured vegetation height within closed (a) and semi-open (b) aspen forest. The field measured vegetation height on the Y-axis was the mean of 6 field height measurements; the LIDAR estimated vegetation height on the X-axis was the mean of 6 tallest LIDAR data points within the same plot. 97

Figure 4-4 Plot by plot comparison between LIDAR estimated and field measured vegetation height within the 4 herbaceous communities, including fescue (a) and mixed prairie (b) grasslands, as well as fresh (c) and saline (d) riparian meadows. 98

Figure 4-5 Plot by plot comparison between LIDAR estimated and field measured vegetation cover within the 2 shrublands, including herbaceous (a) and shrub (b) layers in the silverberry community, and herbaceous (c) and shrub (d) layers in the western snowberry community. 99

Figure 4-6 Plot by plot comparison between LIDAR estimated and field measured vegetation cover within the 4 herbaceous vegetation types,

including mixed prairie (a) and fescue (b) grasslands, as well as fresh (c) and saline (d) riparian meadows. 100

Figure 4-7 Association between LIDAR estimated vegetation height (m) and individual LIDAR intensity return characteristics. 101

Figure 4-8 Association between variation in field measured vegetation height and variation in LIDAR intensity for the fescue grassland (a) and fresh riparian meadow (b). (X: standard deviation of the 40 field measured vegetation heights in 1 plot; Y: standard deviation of all the LIDAR data points within the same plot). 103

Figure 5-1 Flowchart of digital image classification schedules on original mosaic image, color composite image from band ratioing and intensity-hue-saturation image with 3 and 8 classes of vegetation. 138

Figure 5-2 Hybrid color composite image of the study area from red/blue ratio, green and green/blue ratio. 139

Figure 5-3 Intensity-hue-saturation image of the study area. 140

Figure 5-4 Flowchart of LIDAR data classification schedule. 141

Figure 5-5 Surface elevation model of the study area. 142

Figure 5-6 Slope gradient map of the study area. 143

Figure 5-7 Aspect map of the study area. 144

Figure 5-8 Relative relief map of the study area. 145

Figure 5-9 Upland and lowland map of the study area. 146

Figure 5-10 Land cover map of the study area produced by integrating LIDAR data and digital image classification schedules with 3 classes of vegetation. 147

Figure 5-11 Land cover map of the study area produced by integrating LIDAR data and digital image classification schedules with 7 classes of vegetation. 148

Figure 5-12 Final land cover map of the study area produced by integrating LIDAR data and digital image classification schedules with 11 classes of land cover (including 8 classes of vegetation). 149

Appendix

Appendix 1 Target calendar of data collection at Kinsella UA Ranch.....157

Appendix 2 The mean brightness and std. dev. of the 120 signatures within the 8 vegetation types and bare ground.....158

Appendix 3 The effect of vegetation on LIDAR-derived DEM accuracy (RMSE in parentheses). 158

Appendix 4 Comparison between LIDAR-derived and field measured veg. cover. 159

1 Introduction

1.1 Research Background

Rangelands comprise 60-70% of the global land surface (Everitt 1992). These diverse ecosystems produce a broad array of tangible and intangible products. Physical commodities include those such as forage and habitat for livestock and wildlife, water, minerals, energy, forest products, recreational opportunities, and plant and animal genetics, with many of these being economically important rangeland outputs. Rangelands also produce intangible products such as natural beauty and wilderness that satisfy important societal values, many of which can also be economically important (Cox *et al.* 1994).

Regardless of the type of land-use taking place, rangeland degradation through excessive or improperly timed livestock or wildlife grazing reduces the diversity of commodities and values that these areas provide. In many cases, severe degradation may be irreversible without intensive rehabilitation efforts, at least within the current time frames relevant for contemporary land managers. For this reason, ranchers, land administrators, and range and wildlife conservationists, are collectively interested in monitoring the current condition of rangelands, including their ability to sustainably provide key outputs, which in most areas, include either the provision of high quality livestock forage (Waer *et al.* 1997), wildlife habitat (Weber *et al.* 2002), or both (Arsenault and Norman 2002).

Precision Ranching is a new concept encapsulating the need to limit and/or control animal impacts in rangeland landscapes. In essence, it is an analogue to precision farming, which strives to more closely match external inputs (e.g., fertilizers, herbicides, etc) with basic crop requirements across spatially variable agronomic fields, thereby promoting biologic and cost efficiencies (Friend 2002, Long *et al.* 2002). Given that the major causes of rangeland degradation are typically associated with excessive animal numbers, improperly timed grazing, or poor animal distribution (Perevolotsky and Seligman 1998, Turbak 2001), Precision Ranching is an attempt to understand, and in turn regulate, animal behaviour, by ensuring that, "the right animal is in the right place at the right time". Meeting the latter objective will ensure plant communities are not overgrazed, averting long-term reductions in herbage production and rangeland sustainability. In order to implement the notion of Precision Ranching, however, in either a research or practical (e.g., commercial) framework, detailed spatial information of vegetation types is needed to interpret animal movement and grazing activities within rangeland landscapes.

Historical methods of rangeland inventory (i.e., a process of collecting information about rangeland resources to facilitate their proper management (National Research Council 1994)) and condition assessment largely emphasized the use of point- or plot-based inventories, intended to collect detailed information on the species composition and productivity of individual plant communities. With this method, primary, representative sampling units were selected from the entire rangeland, with sub-sampling used to obtain select data from a few, stratified locations within the entire land base. While the use of this point-based inventory is highly effective at providing

information on localized plant communities, several problems exist. These problems largely stem around the inability of managers to safely extrapolate local sampling points to the larger, its all real, and more spatially variable landscape scale at which management actually occurs, as well as the very laborious and costly nature of point-based data collection. Together, these factors have limited the application of point-based sampling for rangeland managers, including the potential for large-scale rangeland condition and trend assessment. In reality, reductions to both the budget and labour pool in many rangeland management, advisory, and regulatory agencies, along with a restricted field season, renders the intensive, prolonged sampling of plant communities unrealistic.

Remote sensing is a potential alternative rangeland monitoring method to gather site-specific data from vast and inaccessible areas (Tueller 1989). Primary benefits include synoptic (e.g., spatially complete) coverage, high cost-effectiveness (i.e., reducing the cost per unit area examined), and lower labour requirements relative to point-based sampling. In addition, remote sensing can provide data on areas that are often inaccessible, as well as highly heterogeneous landscapes where complex mosaics of vegetation with frequent transitional areas may preclude the effective use of point sampling. Remote sensing data also facilitates, though its complete coverage, additional forms of analysis such as landscape metrics (e.g., vegetation distribution). The spatially complete nature of remotely-sensed information on rangelands provides a top-down strategy for rangeland management, and as a result, provides a potential complementary data source to the collection of detailed point-based plant community information.

With the increasing public scrutiny of rangeland uses and their management, it is

likely that emphasis will continue to be placed on the collection of detailed plant community information (e.g., vegetation types) capable of evaluating the merits of a particular management tactic. Nevertheless, specific information about a plant community (and its soils) such as location, topography, vegetation type and biomass are also critical for monitoring an area's ecosystem functioning and/or biological integrity (Angermeier and Karr 1994, National Research Council 1994). Moreover, this information will be needed across entire landscapes, including range allotments and pastures, as these are the scale at which actual management occurs. To gather this information, it may be necessary to make increasing use of precisely located, high spatial (e.g., greater than 1 meter) and/or spectral resolution remotely-sensed data.

In addition to vegetation attributes, spatial information on topography and soils are important to enable implementation of the Precision Ranching concept. Remotely-sensed data may also facilitate creation of a digital elevation model (DEM). A DEM is described as "an ordered array of numbers that represents the spatial distribution of elevation above some arbitrary datum in the landscape" (Moore *et al.* 1991). These models have become widely used in geological, hydrological, and biological modelling, and have replaced contour maps as a vital tool for understanding site landform types, surface geology, soil class, vegetation community, land-use and population density (United States Dept. of the Interior 1990). Traditional elevation data were collected using manual or automated digitizing techniques from photographic sources. Raw elevations are usually weighted with additional information such as drainage, water, and observed elevations at set points during the interpolation process. Interpolation method can have a large influence on the final accuracy of the DEM. Unfortunately,

photographic and other passive sensors are unable to penetrate through aboveground objects (e.g., trees) through gaps, with the resulting DEM erroneously constructed. In addition, the interval spacing (i.e., spatial resolution) of DEMs currently available are usually greater than 30m (airborne) and may even exceed 1km (satellite borne). The result is that the existing standard DEMs are often insufficient to meet the increasing demands for more accurate exploration of terrain, particularly where total landscape relief may fall below this resolution.

Recent developments in Light Detection and Ranging (LIDAR) and laser terrain mapping systems, however, dramatically reduce the time and effort needed to achieve the goal of effective rangeland management. Advances in timing technology have allowed laser pulses of a LIDAR system to be measured in fractions of a nanosecond and create vertical accuracy up to 10 centimetres (Krabill *et al.* 1995). Because of its active sensor system, a LIDAR system offers unique capabilities and distinct advantages for penetrating vegetation through gaps to allow the terrain surface to be remotely mapped from the air. LIDAR data can be used to manage effectively detailed rangeland characteristics such as plant species composition, the biomass of a single species and vegetation structure, which have been less successful when traditional remote sensing systems are used (Ritchie *et al.* 2001).

1.2 LIDAR System Description

A LIDAR collection system basically functions like RADAR, except that it uses laser light instead of microwave. It has a powerful laser sensor comprised of a laser transmitter and receiver, an Inertial Navigation System (INS) unit and a geodetic-quality

Global Positioning System (GPS) receiver. The laser sensor is precision mounted to the underside of an aircraft. Once airborne, the sensor emits rapid pulses of infrared laser light, which are used to determine distances to points on the terrain below. The pulse rate of LIDAR systems range from 2,000 to 33,000 pulses per second (Serr 2000) depending on the manufacturer's design and intended application. Even at these high pulse rates, light has enough time to travel from the sensor to the ground and back before the next pulse is sent. A scanning mirror is used to direct laser pulses back and forth across a wide swath underneath the path of the airplane. The swath width is dependent on the altitude of the aircraft and the scan angle. Recorded data include intensity values of light reflected from ground objects. Aircraft for land mapping typically fly at an altitude of 700 meters, which allows elevation recording across a swath about 300 meters wide. A series of overlapping, parallel swaths are conducted so the entire study area is mapped.

Inertial systems essentially consist of a minimum of several gyroscopes, each of which spins a globular mass within a gimbal or cage. To reduce the spinning friction of such devices, today these objects are electro-magnetically held in suspension. One of the gyros is oriented in a vertical direction, with a second fixed at right angles to it. Because of the effects of gravity, spinning objects in the near vertical will orient themselves to true vertical. If the object on which the device is located tilts over (as happens when you bank during an aircraft turn) the gimbal cage turns with the aircraft while the spinning mass remains vertical. This allows for measurement of the angle of tilt. Coupled with a very high-accuracy timing device and the gyroscope, the inertial system can tell how far, how fast, and in what direction the airplane is moving relative to the point where it started (Fowler 2000). However, with the combined effects of motion, acceleration, turns

and so on, errors will accumulate and the inertial system begins to lose accuracy. This is where developments in GPS (Global Positioning Systems) come in.

The GPS component is an extension of a technique typically used for photogrammetric mapping, eliminating the amount of ground survey control required for a projected area. The GPS antenna is ideally situated directly above the place where the laser is located (to reduce the effects of crab), and specific equipment and software are used to survey the position accurately. A *minimum* of 4--optimally 6 or more--satellites are required to compute a sensor's exact position. GPS data are typically recorded at a rate of 0.5Hz or 1Hz (Sapeta 2000). 2 or more GPS receivers, logging data at the same rate, are deployed at known ground locations during each flying mission. After a laser sensor head is rigidly fixed inside an aircraft, the distance between antenna and sensor unit must be measured. This is accomplished via a "total station" that measures the relative offset between sensor and GPS antenna to within centimeter accuracy.

The integration of all these components (laser sensor, IMU and GPS) forms a network of points with accurate location (coordinates X and Y), height (Z) and I (intensity) values throughout the sampled area.

1.3 Research Objectives

LIDAR has been used for years with a variety of applications, including measuring distances between fixed points of known location and other objects (e.g., the moon) and calculating the atmosphere's water vapor levels and volumes. More recently, LIDAR has become a feasible platform due to the maturation of 2 associated

technologies: GPS products and IMUs. Current LIDAR applications involve mounting lasers in moving platforms, for example aircraft. In these conditions, the accurate distance, position and orientation of the laser device are measured by integrating these 3 components and technologies. The new applications mainly include development of high resolution DEMs, mapping vegetation structure and land surface change detection. As a new technology, LIDAR's application on vegetation mostly concentrates on structure characterization. Utilization of the laser return intensity data has been least explored and little research has been done on vegetation mapping (Narayanan and Guenther 1998, Ni-Meister *et al.* 2001). Similarly, few investigations have been made on DEM construction, vegetation characterization and other applications on rangelands (Ritchie *et al.* 1992, Rango *et al.* 2000).

This thesis research focuses on: (1) construction of a DEM by extracting (and separating) "bare" ground information from LIDAR data and a vegetation surface elevation model (SEM) from the first return of the LIDAR data for a native rangeland environment; (2) comparison of the effects of vegetation type (forests, shrublands, grasslands and riparian meadows), slope gradient and off-nadir sampling distances on DEM accuracy, as well as exploring the spatial (i.e., landscape) variability on the accuracy of a DEM derived from LIDAR data; (3) estimation of ecologically important vegetation characteristics such as height, cover, density and vertical structure, and (4) comparison of LIDAR with multi-spectral digital photography for their ability to map complex vegetation in the Aspen Parkland. All these objectives will help fulfil the goal of evaluating the overall utility of using LIDAR data for landscape and vegetation assessment. A secondary goal is to provide a high resolution DEM and associated

vegetation maps for use by the Precision Ranching Center at Kinsella.

1.4 Literature Cited

Angermeier, P.L and J.R. Karr. 1994. Biological integrity versus biological diversity as policy directives. *BioScience* 44:690-697.

Arsenault, R. and O. S. Norman. 2002. Facilitation versus competition in grazing herbivore assemblages. *Oikos* 97:313-18.

Cox W.J., Cherney J.H., Cherney D.J.R., and Pardee W.D. 1994. Forage quality and harvest index of corn hybrids under different growing conditions. *Agronomy Journal* 86:277-282.

Everitt, J.1992. Overview of remote sensing for rangeland management. *Geocarto International* 7:1-15.

Fowler, R. A. 2000. The lowdown on LIDAR. *Earth Observation Magazine* 9:1-7.

Friend, D. 2002. What to do with all the maps. *Journal of Soil and Water Conservation* 57:110A.

Krabill, W.B., R.H. Thomas, C.F. Martin, R.N. Swift, and E.B. Frederick. 1995. Accuracy of airborne laser altimetry over the Greenland ice-sheet. *International Journal of Remote Sensing* 16:1211-1222.

Long, D. S, J. M. Wraith, and G. Kegel. 2002. A heavy-duty time domain reflectometry soil moisture probe for use in intensive field sampling. *Soil Science Society of America Journal* 66:396-401.

Moore, I. D., R. D. Grayson, and A. R. Ladson. 1991. Digital terrain modeling: a review of hydrological, geomorphological and biological applications. *Hydrological Processes*. 5:3-30.

Narayanan, R. M. and B. R. Guenther. 1998. Effects of emergent grass on mid-infrared laser reflectance of soil. *Photogrammetric Engineering and Remote Sensing* 64: 407-13.

National Research Council. 1994. Rangeland health: New methods to classify, inventory and monitor rangelands. National Academy Press, Washington, D. C.

Ni-Meister, W., D. L. B. Jupp, and R. Dubayah. 2001. The modelling LIDAR waveforms in heterogeneous and discrete canopies. *IEEE Transactions on Geoscience and Remote Sensing* 39:1943-58.

Perevolotsky, A. and N. G. Seligman. 1998. Role of grazing in Mediterranean rangeland ecosystems. *BioScience* 48:1007-17.

Rango, A., M. J. Chopping, J. C. Ritchie, K. M. Havstad, W. P. Kustas, and T. J. Schmugge. 2000. Morphological characteristics of shrub-coppice dunes in desert grasslands of southern New Mexico derived from scanning LIDAR. *Remote Sensing of Environment* 74:26–44.

Ritchie, J. C., H. J. Everitt, , E. D. Escobar, J. T. Jackson, and R. M. Davis. 1992.

Airborne laser measurements of rangeland canopy cover and distribution. *Journal of Range Management* 45:189-193.

Ritchie, J. C., M. S. Seyfried, M. J. Chopping, and Y. Pachepsky 2001. Airborne laser technology for measuring rangeland conditions. *Journal of Range Management* 54:A8-21.

Sapeta, K. 2000. Have you seen the light-LIDAR Technology is creating believers. *Geo World* 13:32-4.

Serr, D. 2000. Use of LIDAR in Creating Accurate Terrain Elevation Models for Floodplain Mapping (term project). http://www.emporia.edu/earthsci/student /serr1/abstract.htm.

Tueller, P. T. 1989. Remote Sensing technology for rangeland management. *Journal of Range Management* 42:442-453.

Turbak, G. 2001. The good, the bad and the wapiti. *National Wildlife* 39:46-53.

United States Dept. of the Interior/U.S. Geological Survey. 1990. Digital Elevation Models (3rd ed). Reston, Virginia.

Waer, N. A, H. L. Stribling, and M. K. Causey. 1997. Cost efficiency of forage plantings for white-tailed deer. *Wildlife Society Bulletin* 25:803-8.

Weber, W. L., J. L. Roseberry, and A. Woolf. 2002. Influence of the conservation reserve program on landscape structure and potential upland wildlife habitat. *Wildlife Society Bulletin* 30:888-98.

2 Literature Review of the Application of LIDAR Technology

2.1 Introduction

Light detection and ranging (LIDAR) is an active remote sensing system, analogous to RADAR, but using laser light. LIDAR instruments measure the roundtrip time for a pulse of laser energy to travel between the sensor and a target. This incident pulse of energy reflects off the vegetation canopy (branches, leaves) or ground surface and back to the instrument where it is collected by a telescope. The travel time of the pulse, from initiation until it returns to the sensor, provides a distance or range from the instrument to the object (hence the common use of the term "laser altimetry" which is synonymous with LIDAR). There are a number of different LIDAR systems made by different manufacturers. To obtain best reflections over land, LIDAR data are generated with wavelengths in the infrared/near infrared frequencies (Fowler 2000). The elapsed time from when a laser is emitted from a sensor and intercepts an object can be measured using either (i) scanning LIDAR, where the travel time of a laser pulse from a sensor to a target object is recorded; or (ii) profiling LIDAR, where the phase change in a transmitted sinusoidal signal produced by a continuously emitting laser is converted into travel time (Wehr and Lohr 1999). At present, the majority of systems in use belongs to small footprint ($\leq$10 m in diameter) scanning LIDAR. Profiling and scanning airborne laser altimeters have been typically used for terrain mapping, land cover classification and the identification of forest structure, although few applications have been done in

rangelands.

2.2 Terrain Modelling

Collecting accurate elevation data to describe the terrain can be difficult and is often time consuming. Traditionally, elevation data were generated by derivation from aerial photogrammetry, scanning pre-existing maps, or by a field survey using standard elevation survey techniques (Flood and Gutelius 1997). These methods, though well-developed and often highly advanced, require substantial effort and long processing times following data acquisition. A laser-based mapping system, however, is synoptic and more accurate (up to 10 cm, Krabill *et al.* 1995) for gathering the required data. Because the laser-based sensor relies on active rather than passive illumination, shadow effects (e.g., from buildings or trees) are not a concern. Rural and remote areas can be surveyed, even when forested. Because each laser point is individually georegistered, aerial triangulation or orthorectification of the data are not required. Currently, terrain mapping surveys are typically carried out using a small-footprint LIDAR system (Lim *et al.* 2003) except within densely vegetated areas.

White and Wang (2003) studied an approximately 70-km stretch of the southern North Carolina coastline using a DEM derived from small footprint LIDAR data. The high-resolution DEM data allowed for a comprehensive visual/quantitative investigation into the spatial patterns of morphologic change that occurred to the barrier islands' oceanfront beaches between 1997 and 2000. This study also demonstrated the utility of using laser altimetry to examine coastline response to tropical storm activity, and led to

the discovery that over-wash was recognized as an integral component of coastline landward migration.

Hodgson *et al.* (2003) assessed 4 different remote sensing based methods for deriving digital elevation models (DEMs) in a flood-prone watershed. New airborne small footprint LIDAR and IFSAR [interferometric synthetic aperture RADAR (SAR)] data were collected and corresponding DEMs created. These new sources were compared to 2 traditional methods: Gestalt Photomapper (GPM) and contour-to-grid, both used by the U.S. Geological Survey (USGS) for creating DEMs. Survey-grade points (1470) for 5 different land cover classes (approximately 60% deciduous and pine forest) were used as reference points. One unique aspect of this study was the LIDAR and IFSAR data were collected during leaf-on conditions. The LIDAR- and contour-to-grid derived DEMs exhibited the greatest overall absolute elevation accuracies.

The difficulty of penetrating dense and complex forest canopies through gaps has promoted the use of large footprint (>10 m in diameter) laser altimetry to measure sub-canopy topography during leaf-on conditions. Hofton *et al.* (2002) mapped a ~800 km^2 area of Costa Rica using 25 m-diameter footprints as part of the pre-launch activities of the Vegetation Canopy LIDAR (VCL) Mission. Crossover analysis using laser shots, whose recorded waveforms contained more than 50% of the total returned energy within their lowest reflections, showed the elevations had an accuracy of better than 1 m. Comparison of the VCL elevations with coincident *in-situ* ground elevation data revealed that the measurements were within ~1.5 m of each other on slopes less than 3°. All measurements were within ~5 m of each other (on slopes ranging up to 30°). These were very encouraging results given that forests of this region are some of the densest, most

complex on Earth, and that mapping their sub-canopy topography is near-impossible using any other remote sensing technique. Overall these results suggested that the topographic measurements made by the VCL would meet stated accuracy goals under the majority of measurement conditions.

In modeling digital elevation, discrete LIDAR data points are required to be interpolated to a continuous surface. Lloyd and Atkinson (2002) assessed inverse distance weighting (IDW), ordinary kriging (OK) and kriging with a trend model (KT) for the construction of DEMs from LIDAR data. Their results indicated that the advantages of KT and OK became more apparent as the number of data points decreased (and the sample spacing increased). However, where the sample space was very small, it was recommended that simpler approaches such as IDW be used.

2.3 Land Cover Classification

Recognition of land cover types is important for land use management agencies as it provides a basis for the development and evaluation of management policies and actions. Land cover classification is the process of identifying and describing areas of relatively homogeneous land cover formation (e.g., water in a resource inventory), and subsequently mapping the resulting spatial distribution of various land cover types across the area of interest.

Lee (2003) studied the effect of airborne LIDAR elevation data on the classification of multispectral IKONOS images over a coastal area. The LIDAR elevation data was first resampled and stretched to the same spatial resolution and

radiometric range as the IKONOS images. An unsupervised classification based on the ISODATA algorithm was then used to identify 6 classes: road, water, marsh, roof, tree, and sand. Training and validation sites were selected over the LIDAR-IKONOS merged data set for the subsequent supervised classification and accuracy assessment. He claimed that the inclusion of LIDAR elevation data benefited the separation of classes that had similar spectral characteristics, such as roof and road, water and marsh. The overall classification errors, especially the false positive errors, were reduced by up to 50%. Moreover, by using the LIDAR elevation data, the classification results showed more realistic and homogeneous distribution of geographic features.

Song *et al.* (2002) assessed the possibility of conducting land-cover classifications using LIDAR intensity data. In their study, LIDAR point data were converted to a grid and then assessed for the separability of intensity data based on surface features such as asphalt road, grass lands, house roofs, and trees. After removing noisy patterns through resampling and filtering algorithms, the authors claimed that LIDAR intensity data had the potential to classify the above 4 land cover types.

2.4 Application in Forestry

Vertical and horizontal patterns of forest canopy, and the heterogeneous distribution of canopy components (i.e., leaves, twigs, branches, trunks, epiphytes, etc.) and spaces (i.e., structural openings between components occasionally from broken branches or treefall gaps) produce microclimatic (e.g., light, temperature, humidity) gradients (Weishampel *et al.* 2000). These gradients feed back into biological/ecological processes (e.g., growth, competition, mortality) thereby further defining organizational

properties. The complexity of this architecture is classically described as cathedral-like and has often been misrepresented as being stratified or layered (Halle *et al.* 1978, Richards 1996). These canopies provide the primary surfaces of energy and matter exchange between the atmosphere and the largest reserves of aboveground carbon (Perry 1994). As a result, the 3- and 4-dimensional characterization and visualization of these dynamic systems have been deemed an essential avenue of future forest canopy research (Nadkarni and Cushing 1995).

Various remote sensing systems and techniques have been explored for forestry applications and are reviewed by Weishampel *et al.* (1996), Wulder (1998), and Lefsky *et al.* (2001) with a comparison of various remotely-sensed data sources with LIDAR. Typically, most optical sensors are only capable of providing detailed information on the horizontal distribution and not the vertical distribution of vegetation in forests. LIDAR remote sensing is unique in its capability of providing both horizontal and vertical information with the horizontal and vertical sampling dependent on the type of LIDAR system used and its configuration (i.e., discrete small footprint with diameter < 10 m or full waveform LIDAR with diameter > 10 m) (Lim *et al.* 2003).

Small-footprint (scanning) LIDAR systems may not be optimal for mapping forest structure. First, small diameter beams frequently over-sample crown shoulders and miss the tops of trees (Nelson 1997), so that unless many LIDAR points are taken (e.g., at an increasing density), the true canopy topography must be reconstructed statistically. Secondly, because of their small beam size, mapping large areas requires extensive flying and large data handling capability. Finally, with systems that only record first and/or last returns, it is difficult to determine whether or not a particular point has fully penetrated

the canopy through gaps all the way to the ground. If this topography cannot be reconstructed, accurate height determination is impossible because canopy height is measured relative to the ground. In contrast, large-footprint systems (e.g., Blair *et al.* 1999) have several advantages that help avoid these problems. First, by increasing the footprint size to at least the average crown diameter of a canopy-forming tree (10-25 m), laser energy consistently reaches the ground even in dense forests. The larger footprint size also avoids the biases of small-footprint sensors that may frequently miss the tops of trees altogether. Secondly, large-footprint systems enable a wide image swath, which reduces the expense of mapping large forested areas (Blair *et al.* 1999). Finally, large-footprint LIDAR systems not only digitize the first and last return, but the entire return signals (e.g., in ~30 cm vertical bins) thus providing a more comprehensive vertical distribution of intercepted surfaces (or "waveform") from the top of the canopy to the ground. However, full waveform large-footprint LIDAR systems are primarily used by researchers for scientific applications and have yet to be fully commercialized.

Given the capability of using LIDAR data to accurately measure topography, it may be possible to quantify certain forest attributes from forest canopy profiles derived from LIDAR data, such as canopy height, basal area, above-ground biomass, mean stem diameter, vertical foliar profiles and canopy volume (Means *et al.* 1999, Lefsky *et al.* 1999a and 1999b, Dubayah and Drake 2000).

2.4.1 Canopy Height

A strong link between vegetation height and other biophysical characteristics

(e.g., cover, density) (Dubayah and Drake 2000) suggests vegetation height may be used to model many of the forest structural characteristics that are not directly recovered from optical sensor systems such as LIDAR. In addition, vegetation height is a function of species composition, climate and site quality, and can therefore be used for land cover classification or in conjunction with vegetation indices from passive optical sensors (Dubayah *et al.* 1997 and 2000).

A requirement for calculating canopy heights using both discrete small footprint and full waveform LIDAR data is the ability to identify some ground reference level below the canopy. In the case of discrete small-footprint LIDAR data, canopy height estimates are calculated by subtracting the elevations of the first and last returns from the LIDAR signal. With large-footprint systems, canopy height is calculated by converting the elapsed time difference between the highest and lowest peaks of the 2 most prominent modes in the amplitude waveform into range (Roberts 1998).

Popescu *et al.* (2002) discussed processing algorithms for estimating tree heights by using a multiple return, high–density, small-footprint LIDAR data set in deciduous, coniferous, and mixed stands of varying age classes in the south-eastern US. 2 LIDAR processing algorithms are discussed - the first based on single tree crown identification using a variable window size for local filtering, and the second based on the height of all laser pulses within the area covered by the ground truthed data. The maximum height on each plot was predicted with the greatest accuracy (R^2 = 85 and 90%, respectively) for the first and the second algorithm. Ritchie *et al.* (1993) claimed that mean LIDAR heights from a first return LIDAR were significantly related to mean target heights in pine forest and grassland sites in Niger. Nilsson (1996) had also investigated the effects

of different beam divergences (i.e., 2.5, 5.0, 7.5 and10.0 mrad) on LIDAR tree height measurements (Scots pine stands) and concluded that differences in measurements were negligible and that all beam divergences were usable for measuring tree height. These beam divergences equate to footprint diameters ranging from 0.75 m to 3.0 m.

Nelson *et al.* (1988b), while studying a southern pine stand using LIDAR data, observed that the mean LIDAR height measurements from 2 distinct flight lines underestimated ground measurements by approximately 30% or 4 m. During his studies of a Scots pine stand using an airborne scanning laser mounted on a helicopter, Nilsson (1996) found that mean tree height was underestimated by 2.1–3.7 m. Næsset (1997) studied 36 stands covered by Norway spruce, Scots pine, or both using an Optech ALTM and also found that mean LIDAR canopy heights within each stand were underestimated relative to ground-based estimates by 4.1–5.5 m. Although not explicitly stated, the influence of canopy structure on the laser response was considered by incorporating Lorey's height in the calculations for each plot. Lorey's height is a weighted mean of canopy height based on the basal area of individual trees to account for the influence of larger trees on mean canopy height. Despite this change, the weighted mean of the LIDAR canopy height still underestimated ground-based estimates by 2.1–3.6 m. This approach implicitly assumed that the laser response was related to the largest trees during LIDAR remote sensing of forest structure and resulted in mean differences between –0.4 m and 1.9 m. Regression of the LIDAR stand heights against ground reference stand heights accounted for 91% of the variation.

The majority of LIDAR studies have focused on coniferous rather than deciduous forests. More gaps (needle leaf shape) and stronger LIDAR ability to penetrate through

over-story layers might promote utilization of LIDAR data more often within coniferous species. However, studies have shown that tree heights are underestimated by small footprint LIDAR because of the low probability of a small-footprint laser pulse intercepting the apex of a conical crown (Nilsson 1996, Næsset 1997, Nelson *et al.* 1988b). Underestimates of tree heights given conical crown shapes should not be a deterrent for the use of small-footprint LIDAR, because the differences between LIDAR canopy height and actual canopy height can be modelled (Magnussen and Boudewyn 1998).

Of the 36 Douglas-fir plots studied by Magnussen and Boudewyn (1998), mean LIDAR canopy heights were found to be 3.1 m lower than mean field heights. In their study, they outlined why simple grid approaches, where only the maximum canopy heights within cells are retained for analysis (e.g., Næsset 1997) provided the closest matches to target heights. Magnussen and Boudewyn (1998: 1017) state that 'the essence of the grid-based system is in the selection of a certain quantile of the LIDAR canopy height that best matches a known target height'. On the basis of this concept, they supported their hypothesis that 'the quantile of the LIDAR canopy heights matching in probability the fraction of leaf area above a desired height would be an unbiased estimator ' (Magnussen and Boudewyn 1998: 1030). Using these results, Magnussen *et al.* (1999) presented 2 tree height recovery models. The assumption of one of the models was that 'observations are sampled with a probability proportional to displayed crown area', while the second was 'derived from the probability that a laser beam penetrates to a given canopy depth' (Magnussen *et al.* 1999: 407). Both models were shown to eliminate the underestimation bias of mean LIDAR estimated canopy heights.

The work by Magnussen and Boudewyn (1998) and Magnussen *et al.* (1999) is significant as it provides an explanation of laser response to forest canopy structure and how it can be dealt with to ensure accurate measurements of forest attributes derived from LIDAR data. Furthermore, evidence in support for Magnussen and Boudewyn's (1998) concept that a certain quantile of LIDAR canopy heights is a best estimate of actual tree height can be found in the work done by Ritchie *et al.* (1993) where the inclusion of the highest 10% of LIDAR measurements did not produce significant differences between LIDAR measurements and ground measurements, while significant differences were produced when the highest 15% of LIDAR measurements were used.

Beyond measuring mean tree heights for study plots and forest stands, some attention has been directed towards delineating individual tree crowns in LIDAR data and predicting individual tree heights. St-Onge *et al.* (2000) used small-footprint LIDAR data acquired from an ALTM to study individual trees. The authors used a combined spatial filter and edge detection operator - Laplacian of Gaussian (LoG) and applied it to a canopy height model to delineate individual tree crowns. The LoG requires the input of a spread parameter(s), equivalent to the standard deviation of a distribution. This parameter is typically selected in an *ad-hoc* fashion and the results are visually compared with the original images. The heights of 36 delineated trees in a canopy height model corresponding to the highest LIDAR hit in the delineated crowns, were compared with corresponding ground measurements using a linear model ($R^2 = 0.90$, $P<0.01$).

Coupled with the recent work by Magnussen and Boudewyn (1998) and Magnussen *et al.* (1999), this evidence clearly suggests that tree height can be recovered from LIDAR data just as accurately as from ground measurements, if not more

accurately. St-Onge *et al.* (2000) demonstrated that the focus of the application of LIDAR may be shifting from the landscape/stand scale (e.g., forest inventories) to a local/tree scale (e.g., forest inventories stratified by species). The potential of LIDAR for forestry is slowly coming to fruition and as a result, others have begun to explore LIDAR as an operational forestry tool (e.g., Tickle *et al.* 1998 and 2001).

2.4.2 Vertical Distribution of Intercepted Surfaces

In addition to the first and last returns, large-footprint systems digitize the complete return signal of the laser pulse between the canopy surface and ground, thus recording a waveform that is related to the vertical distribution of canopy structure. Specifically, a large-footprint LIDAR waveform records reflections from the nadir-projected vertical distribution of the surface area of canopy components such as foliage, trunk, twigs, and branches. Like canopy height, the vertical distribution of intercepted surfaces provides a new means to classify vegetation, and provides the basis for estimating other important canopy descriptors, such as aboveground biomass. It also functions as a predictor of the successional state of a forest (Dubayah *et al.* 1997).

Hardling *et al.* (2001) studied a successional sequence of 4, closed-canopy, deciduous forest stands in eastern Maryland using a waveform-recording laser altimeter. The 10-m-diameter footprint laser system revealed vertical variations in vegetation within and between stands in their canopy height profiles. Their results demonstrated that the laser observations reliably provide a measure of canopy vertical structure that reveals ecologically interesting structural variations. Lefsky *et al.* (1999b) also successfully

modelled "canopy height profiles" and vertical distribution of intercepted surfaces using assumptions from methods developed to estimate vertical foliage profiles from optical point quadrats.

As a stand ages and grows, the vertical distribution of canopy components changes relative to younger stands (Dubayah *et al.* 1997, Lefsky *et al.* 1999b). Older stands are characterized by canopy gaps and trees of multiple ages, and sizes exhibit a more even vertical distribution of canopy components compared to younger, even-aged stands, which have a majority of their biomass in the top portion of the canopy. Lefsky *et al.* (1999b) demonstrated that LIDAR waveforms are sensitive to these structural changes and were able to identify forest succession.

2.4.3 Aboveground Biomass

Taller trees contain more wood and typically support more foliage and roots than shorter trees of the same species and diameter. Additionally, because of the mechanical properties of trees, stem diameter and canopy area typically increase as trees become taller, further increasing wood volume and mass. Remotely-sensed measurements from LIDAR instruments can exploit these biological constraints to model biomass from height and canopy area.

Dubayah *et al.* (2000) found that LIDAR measured heights were highly correlated with aboveground biomass in mixed deciduous-coniferous, pine, Douglas fir/western hemlock, and in dense tropical forests. In recent studies, metrics from large-footprint LIDAR systems were able to explain over 90% of the variation in aboveground biomass

in forests with extremely high (up to 1300Mg/ha, in Means *et al.* 1999) biomass and canopy closure (~99% canopy closure, in Drake *et al.* in review) levels.

Using 113 sample plots, Nelson *et al.* (1988a) tested 2 logarithmic equations for estimating biomass and volume with 6 LIDAR-derived canopy measurements to determine which model could best describe the variation in observed ground measurements. The LIDAR height variables examined included average LIDAR canopy height of the 3 largest trees, mean plot height, mean canopy height, and modified canopy profiles with a 2 m, 5 m and 10 m exclusion level. From the 12 models tested, those applying the mean plot height metric derived from all LIDAR pulses as an input parameter were identified as the best models.

MacLean and Krabill (1986) demonstrated that a LIDAR-generated canopy profile area was a significant variable in estimating gross merchantable timber volume. Multiple regression relating the natural log of timber volume to the full profile area and a profile area with a 10 m exclusion level produced promising results ($R^2 = 0.72$, $P<0.01$). By considering the profile area with a 10 m exclusion level and the predominant species of each plot expressed as a ratio of the volume of the predominant species to total volume, an R^2 value approaching 0.90 was obtained. Furthermore, they demonstrated that an overall R^2 value of 0.92 could be achieved if the LIDAR data were stratified by species within plots of the study area. However, Nelson *et al.* (1988a) showed that stratification of southern conifers only slightly improved the accuracy of their volume and biomass estimation (1.0% and 0.4% improvements, respectively).

2.4.4 Other Forest Characteristics

LIDAR metrics (e.g., canopy height) have also been used to accurately estimate basal area (e.g., Drake *et al.* in review, Means *et al.* 1999) and mean stem diameter (Drake *et al.* in review). The distributions of basal area and mean stem diameter may then be used to infer the density of large trees. In addition, the vertical distribution of intercepted surfaces has been used to examine the volumetric nature of Douglas fir/western hemlock (Lefsky *et al.* 1999b) and tropical (Weishampel *et al.* 2000) forest canopy structure. These kinds of measurements provide extraordinary new data for forest wildlife management and habitat mapping.

2.5 Application of LIDAR Data in Rangeland Management

Land surface and vegetation properties are key for understanding range and habitat conditions, as well as understanding vegetation susceptibility and response to disturbance. Ground-based measurements of these properties are difficult and time-consuming. Profiling and scanning airborne laser altimeter systems provide an alternative method to synoptically measure land surface and vegetation features over large land areas. The agreement between airborne laser altimeter and field measurements is favorable for both topographic features and vegetation properties (i.e., height, cover) (Ritchie *et al.* 2001). Laser measurements improve our understanding of the effect of canopy and landscape roughness on rangeland conditions.

Ritchie *et al.* (2001) collected laser profile and ground data from 5 different vegetation types in the Reynolds Creek Watershed. Most of the canopy heights (74.2%)

were less than 0.5 m in their profile. Only 12.5% of the height measurements were greater than 1 m. Vegetation sites were Mountain big sagebrush (*Artemisia tridentata* subsp. *vaseyana* [Rydb.] Beetle), low sagebrush (*Artemisia arbuscula* Nutt.), Wyoming big sagebrush (*Artemisia tridentata* subsp. *wyomingensis* Beetle & A. L. Young), bitterbush (*Purshia tridentata* [Pursh] DC.), and greasewood (*Sarcobatus vermiculatus* [Hook.] Torr.). The ground data were averages of 6, 30-m transects along an approximate 1 km line, using the line intercept method. The laser data were averages of 3, 1-km transects over the same area. Their analysis found that differences in the average heights between the ground and laser measurement of the transects ranged from 2.0 to 8.7 cm, with the laser measured heights always being lower. However, there was no statistical difference between the ground and laser height measurements at the 5% level of probability.

In a comparison of canopy cover measured by laser and ground techniques, Ritchie *et al.* (2001) found the measurements to be significantly different. While there was agreement between the 2 techniques in the Bitterbrush (cover differences less than 4%) and Low sagebrush (cover differences less than 6%) communities, the greatest difference was at the Wyoming big sagebrush community where the laser estimate of cover was twice that of the ground measurement. This might be the inconsistency of the 2 datasets -- the ground data was an average for 6, 30-m transects while the laser data was the average of 3, 1-km transect (Ritchie *et al.* 2001).

Weltz *et al.* (1994) used a laser altimeter mounted in a small airplane to measure surface patterns of the landscape in the Walnut Gulch Experimental Watershed (N 31° 44.3', W 110° 1.4') of Arizona. The area was representative of the Chihuahuan desert

scrub and semi-desert grasslands. The lower two-thirds of the watershed were dominated by shrubby vegetation with little herbaceous understory vegetation. The upper third of the watershed was dominated by grassland. Their analysis indicated that the laser-measured vegetation properties of plant height and canopy cover (>0.3 m) were not significantly different than field measurements made using the line-intercept transect method at 7 of the 8 sites evaluated. Although the laser measurements of canopy height were not significantly different from the ground measurements, the laser consistently overestimated canopy cover in those areas where the height of the canopy was less than 0.3 m and underestimated cover in areas of vegetation taller than 0.5 m. The overestimation might be the background noise and underestimation the LIDAR interception of the shoulder of vegetation, not the top of the canopy.

Finally, studies in rangeland of a South Texas (N 26° 11.5', W 97° 59.2') mesquite stand (Ritchie *et al.* 1992) and a Mississippi (N 33° 15.6', W 88° 52.8') pine forest (Ritchie *et al.* 1993) indicated that laser altimeter measurements of vegetation height and cover were highly correlated with ground measurements. These studies demonstrated the potential of using airborne laser to measure vegetation characteristics such as height and cover. However, these studies also indicated new techniques were necessary to discriminate background noise in the laser return signal within grass and low stature shrub communities before the laser technology would be suitable for more widespread use in estimating vegetation characteristics on rangelands.

2.6 Problems and Challenges of LIDAR Data Use

The use of LIDAR and other optical remote sensing systems may be restricted by the limited availability of the most current technology. Additionally, clouds and dense atmospheric haze can attenuate the signal before it reaches the ground. Moreover, commercial airborne small-footprint systems are only now becoming available on a cost-effective basis and large-footprint systems are still in the research phase. The lack of algorithms and data processing expertise also limits operational use of the data. These limitations will likely decline with the continuing maturation of the technology and fusion with information from other remote sensing systems such as passive optical, thermal and RADAR remote sensing.

2.7 Conclusion

LIDAR remote sensing is a rapidly developing and expanding technology. The direct measurement of elevation and subcanopy topography, canopy height, and the vertical distribution of intercepted surfaces provide a wealth of data for terrain mapping, vegetation characterization, and forest or rangeland management. In addition, the strong relationships between these direct measurements and other biophysical parameters, such as aboveground biomass, provide critical information about the function and productivity of forest and rangeland ecosystems. Such measurements will improve our understanding of the effects of these factors on hydrological systems of natural and agricultural landscapes, and facilitate forest and rangeland wildlife/livestock management and habitat mapping, so that improved management practices and structures can be developed to

manage our natural resources better.

2.8 Literature Cited

Blair, J. B., D. L. Rabine, and M. A. Hofton. 1999. The Laser Vegetation Imaging Sensor (LVIS): A medium-altitude, digitization-only, airborne laser altimeter for mapping vegetation and topography. *ISPRS Journal of Photogrammetry and Remote Sensing* 54:115-122.

Drake, J., D. Clark, R. Dubayah, R. Knox, J. B. Blair, and R. L. Chazdon. (In review). Estimation of tropical forest structural characteristics using large-footprint LIDAR. *Remote Sensing of Environment.*

Dubayah, R. O., R. G. Knox, M. A. Hofton, J. B. Blair, and J. B. Drake. 2000. Land surface characterization using LIDAR remote sensing (pp25-38), in M. Hill and R. Aspinall (eds) *Spatial Information for Land Use Management.* International Publishers Direct, Singapore.

Dubayah, R., J. B. Blair, J. L. Bufton, D. B. Clark, J. JaJa, R. G. Knox, S. B. Luthcke, S. Prince, and J. F. Weishampel. 1997. The vegetation canopy LIDAR mission (pp100-112), in *Land Satellite Information in the Next Decade II: Sources and Applications.* American Society for Photogrammetry and Remote Sensing, Bethesda Maryland.

Dubayah, R.O. and J.B. Drake. 2000. LIDAR remote sensing for forestry. *Journal of Forestry* 98:44–46.

Flood, M and B. Gutelius. 1997. Commercial implications of topographic terrain mapping using scanning airborne laser RADAR. *ISPRS Journal Photogrammetry and Remote Sensing* 63:327-66.

Fowler R. A. 2000. The low down on LIDAR. *Earth Observation Magazine* 9:1-7.

Halle, F., R. A. A. Oldeman, and P. B. Tomlinson. 1978. *Tropical Trees and Forests: an Architectural Analysis.* Springer-Verlag, New York, New York.

Harding, D.J., M.A. Lefsky, G.G. Parker, and J.B. Blair. 2001. Laser altimeter canopy height profiles: methods and validation for closed-canopy, broadleaf forests. *Remote Sensing of Environment* 76:283-297.

Hodgson, M., J. R. Jensen, L. Schmidt, S. Schill, and D. Bruce. 2003. An evaluation of LIDAR- and IFSAR-derived digital elevation models in leaf-on conditions with USGS Level 1 and Level 2 DEMs. *Remote Sensing of Environment* 84:295-308.

Hofton, M. A., L. E. Rocchio, J. B. Blair, and R. Dubayah. 2002. Validation of vegetation canopy LIDAR sub-canopy topography measurements for a dense tropical forest. *Journal of Geodynamics* 34:491-502.

Krabill, W.B., R.H. Thomas, C.F. Martin, R.N. Swift, and E.B. Frederick. 1995. Accuracy of airborne laser altimetry over the Greenland ice-sheet. *International Journal of Remote Sensing* 16:1211-1222.

Lee, D. S. 2003. Combining LIDAR elevation data and IKONOS multispectral imagery for coastal classification mapping. *Marine Geodesy* 26:117-127.

Lefsky, M., W. Cohen, and T. Spies. 2001. An evaluation of alternate remote sensing products for forest inventory, monitoring, and mapping of Douglas-fir forests in western Oregon. *Canadian Journal of Forest Research* 31:78–87.

Lefsky, M.A., D. Harding, W.B. Cohen, G. Parker, and H.H. Shugart. 1999a. Surface LIDAR remote sensing of basal area and biomass in deciduous forests of Eastern Maryland, USA. *Remote Sensing of Environment* 67:83–98.

Lefsky, M.A., W.B. Cohen, S.A. Acker, G.G. Parker, T.A. Spies, and D. Harding. 1999b. LIDAR remote sensing of the canopy structure and biophysical properties of Douglas-fir western hemlock forests. *Remote Sensing of Environment* 70:339–61.

Lim, K., P. Treitz, M. Wulder, B. St-Onge, and M. Flood. 2003. LIDAR remote sensing of forest structure. *Progress in Physical Geography* 27:88–106.

Lloyd, C. D. and P. M. Atkinson. 2002. Deriving DSMs from LIDAR data with kriging. *International Journal of Remote Sensing* 23:2519-2524.

MacLean, G.A. and W.B. Krabill. 1986. Grossmerchantable timber volume estimation using an airborne LIDAR system. *Canadian Journal of Remote Sensing* 12:7–18.

Magnussen, S. and P. Boudewyn. 1998. Derivations of stand heights from airborne laser scanner data with canopy-based quantile estimators. *Canadian Journal of Forest Research* 28:1016–31.

Magnussen, S., P. Eggermont, and V.N. LaRiccia. 1999. Recovering tree heights from airborne laser scanner data. *Forest Science* 45:407–22.

Means, J.E., S.A. Acker, D.J. Harding, D.B. Blair, M.A. Lefsky, W.B. Cohen, M.E. Harmon,and W.A. McKee. 1999. Use of largefootprint scanning airborne LIDAR to estimate forest stand characteristics in the Western Cascade of Oregon. *Remote Sensing of Environment* 67:298–308.

Nadkarni, N. M. and J. B. Cushing. 1995. Designing the forest canopy researcher's workbench: computer tools for the 21st century (final report). International Canopy Network, Olympia, Washington.

Næsset, E. 1997. Determination of mean tree height of forest stands using airborne laser scanner data. *ISPRS Journal of Photogrammetry and Remote Sensing* 52:49–56.

Nelson, R. 1997. Modeling forest canopy heights: The effects of canopy shape. *Remote Sensing of Environment* 60:327-334.

Nelson, R., R. Swift, and W. Krabill. 1988b. Using airborne lasers to estimate forest canopy and stand characteristics. *Journal of Forestry* 86:31–38.

Nelson, R., W. Krabill, and J. Tonelli. 1988a. Estimating forest biomass and volume using airborne laser data. *Remote Sensing of Environment* 24:247–67.

Nilsson, M. 1996. Estimation of tree heights and stand volume using an airborne LIDAR system. *Remote Sensing of Environment* 56:1-7.

Perry, D. A. 1994. *Forest Ecosystems.* Johns Hopkins University Press, Baltimore, Maryland.

Popescu, S. C., R. H. Wynne, and R. F. Nelson. 2002. Estimating plot-level tree heights with LIDAR: local filtering with a canopy-height based variable window size. *Computers & Electronics in Agriculture* 37:71.

Ritchie, J. C., M. S. Seyfried, M. J. Chopping, and Y. Pachepsky. 2001. Airborne laser technology for measuring rangeland conditions. *Journal of Range Management* 54:A8-21.

Ritchie, J.C., D.L. Evans, D.M. Jacobs, J.H. Everitt, and M.A. Weltz. 1993. Measuring canopy structure with an airborne laser altimeter. *Transactions of the ASAE* 36:1235-38.

Ritchie, J.C., J.H. Everitt, D.E. Escobar, T.J. Jackson, and M.R. Davis. 1992. Airborne laser measurements of rangeland canopy cover. *Journal of Range Management* 2:189-193.

Roberts, G. 1998: Simulating the vegetation canopy LIDAR: an investigation of the waveform information content. University College London, M.Sc. *Thesis* 74 pp.

Song, J. H., S. H. Han, K. Yu, and Y. Kim. 2002. Assessing the possibility of land cover classification using LIDAR intensity data (pp 259-62). In *The International Archives of the Photogrammetry, Remote Sensing and Spatial Information Science,* Commission III, PCV02. September 9-13, Graz, Austria.

St-Onge, B., J. Dufort, and R. Lepage. 2000. Measuring tree height using scanning laser altimetry (pp425-32). In *Proceedings of the 22nd Annual Canadian Remote Sensing Symposium.* August 21-25, Victoria, B.C.

Tickle, P., C. Witte, T. Danaher, and K. Jones. 1998. The application of large-scale video and laser altimetry to forest inventory (pp20-24). In *Proceedings of the 9th Australasian Remote Sensing and Photogrammetry Conference*. Sydney, Australia.

Tickle, P.K., C. Witte, A. Lee, K. Jones, R. Denham, R.M. Lucas, and J. Austin. 2001. The use of airborne scanning LIDAR and large scale photography within a strategic forest inventory and monitoring framework (pp9-13). In *Proceedings, International Geoscience and Remote Sensing Symposium*, Sydney, Australia.

Wehr, A. and U. Lohr. 1999. Airborne laser scanning – an introduction and overview. *ISPRS Journal of Photogrammetry and Remote Sensing*, 54:68-82.

Weishampel, J. F., J. B. Blair, R. G. Knox, R. Dubayah, and D. B. Clark. 2000. Volumetric LIDAR return patterns from an old-growth tropical rainforest canopy. *International Journal of Remote Sensing* 21: 409-415.

Weishampel, J.F., K.J. Ranson, and D.J. Harding. 1996. Remote sensing of forest canopies. *Selbyana* 17:6–14.

Weltz, M.A., J.C. Ritchie, and H.D. Fox. 1994. Comparison of laser and field measurements of vegetation heights and canopy cover. *Water Resources Res.* 30:1311-20.

White, S. and Y. Wang 2003. Utilizing DEMs derived from LIDAR data to analyze morphologic change in the North Carolina coastline. *Remote Sensing of Environment* 85:39-48.

Wulder, M. 1998. Optical remote-sensing techniques for the assessment of forest inventory and biophysical parameters. *Progress in Physical Geography* 22:449–76.

3 Influential Factors on LIDAR-derived DEM Accuracy

3.1 Introduction

Detailed geographic information system (GIS) studies on plant ecology, animal behavior and soil hydrologic characteristics across spatially complex landscapes require a highly accurate digital elevation model (DEM). Although few technologies have been available in the past to generate DEMs that meet these criteria, the use of light detection and ranging (LIDAR) data may provide a suitable alternative. Few studies, however, have evaluated whether LIDAR data can be used to provide a DEM of superior quality (e.g., accuracy) across all areas of complex rangeland landscapes, as well as evaluating the role of external factors (equipment and environment) in influencing DEM accuracy.

LIDAR inertial systems are supposed to point perpendicularly to the ground surface, but can generate attitude (i.e., shifting angle) to 0.1 degree in a fast turning or tilting flight, changing the positional/horizontal accuracy depending on flying height. Timing electronics (recording precision) of a laser receiver can generate a vertical resolution error up to 5 cm. However, vertical accuracy of LIDAR systems are typically more accurate compared to other remote sensing systems (videography, RADAR, etc.), and are postulated to be in the order of 15 cm given the current data used (Sapeta 2000, Serr 2000, Thomas and Hutton 2000, Eagle Scan Inc. 2000, Renslow 2001). Krabill (1995) showed the maximum vertical resolution detectable with LIDAR data was 10 cm when researching ice sheet thickness in the Arctic.

Most researchers have claimed 15 cm vertical accuracy using LIDAR data

regardless of where the work was done or what the surface conditions (e.g., vegetation type) might be. However, limited research has quantified the influence of specific ground characteristics such as the type and density of vegetation (Narayanan and Guenther 1998, Ni-Meister *et al.* 2001) and slope gradient (Bufton *et al.* 1991), or other external factors such as off-nadir distance (Tsutsui *et al.* 1998), on the accuracy of LIDAR data.

Many rangeland landscapes, including the Aspen Parkland of western Canada, consist of complex topography with frequent and rapid changes in slope, aspect, and elevation (Ayad and Dix 1964, Acton 1965). These factors in turn, interact to alter the type of plant communities found across the landscape (Wheeler 1976, Sheffler 1976), as well as the magnitude of disturbances such as grazing and fire. As a result, meaningful ecological information for the management of land use activities can only be obtained if the relative influence of topography and vegetation can be distinguished from one another. Furthermore, the use of existing DEM models with a spatial resolution coarser than 30m (through manual or automated digitizing techniques from photographic sources) are clearly insufficient to accurately represent the local topographic variability occurring within these areas, where average relief is much less than this resolution (e.g., 5-10m).

This research quantified the accuracy of a high resolution DEM generated from LIDAR data within the Aspen Parkland of central Alberta. Additionally, this investigation evaluated the influence of external factors on the accuracy of the resulting DEM, including environmental characteristics such as vegetation type and slope gradient, as well as equipment characteristics such as off-nadir distance during LIDAR sampling.

It was hypothesized that any factors responsible for reducing the density or uniformity of sampling points would reduce the overall accuracy of a LIDAR-derived DEM. For example, more complex vegetation (shrub or forest) was hypothesized to reduce DEM accuracy due to a reduction in the density of LIDAR "last return" data points reaching the ground. Similarly, increasing slope gradients along with an increasing distance from nadir would reduce sampling densities (points/unit area) and associated DEM accuracy. Furthermore, the uneven distribution (distance deviation) of sampling points within similar density areas would also reduce the overall accuracy of a LIDAR-derived DEM. Finally, it was hypothesized that these factors (slope, off-nadir distance or vegetation type) may also interact with each other to affect LIDAR sampling of the soil surface and compound errors in DEM generation.

3.2 Materials and Methods

3.2.1 Study Area

This research was conducted at the University of Alberta Ranch (53° 0' N; 111°31' W) located 150 km SE of Edmonton, Alberta, Canada, within the Aspen Parkland natural sub-region. The Ranch is 2700 ha in size and has a general topography of rolling hills (i.e., knob and kettle terrain) with 5-15 m relief arising from its glacial moraine landform origin. The region has a temperate continental climate, with mean annual precipitation of 433mm and 100-120 frost-free days (University's Meteorological Station at Kinsella Ranch). North-facing slopes are capable of supporting plant species with greater moisture requirements such as aspen forest and shrublands due to snow

accumulation, while south-facing slopes typically support plant communities tolerant of drier conditions such as grasslands (Coupland 1961, Wheeler 1976). The most common soil type of the area is a Black Chernozem, although Dark Gray Chernozems and Eluviated Chernozems are present as well (Bailey and Wroe 1974, Scheffler 1976). Gleysols and Solonetzic soils also occur, the former confined to poorly drained lowlands. Herbage production is 2251 ± 747 and 2886 ± 993 ($kg \cdot ha^{-1}$, dry matter) in its first and second rotation, respectively (Asamoah *et al.* 2003), and the major vegetation types at the Ranch are as follows:

(1) Riparian meadows

Meadows are mesic to hygric habitats occupied by grass (*Poaceae* family) and grasslike species primarily of the genera *Carex* and *Juncus*. The primary environmental characteristic affecting meadow vegetation is the high water table during all or part of the year (Benedict 1982, Ratliff 1985, Allen-Diaz 1991). 2 major types of wetlands exist at Kinsella, which include:

A. Saline riparian meadows (SRM) dominated by salt grass [*Distichlis spicata* (L.) Greene], alkali grass [*Puccinellia nuttalliana* (Schultes) Hitchc] and numerous forbs. They were found bordering salt covered lakebeds of discharge origin.

B. Freshwater riparian meadows (FRM) dominated by aquatic sedges (e.g,, *Carex atherodes* Spreng., etc), tufted hairgrass [*Deschampsia caespitose* (L.) Beauv.], and some marsh reedgrass [*Calamagrostis canadensis* (Michx.) Beauv.]. These meadows occurred at slightly greater elevations as ground water recharge areas.

(2) Upland grasslands

Grasslands were historically maintained by a combination of periodic fire (Wright

and Bailey 1982) coupled with grazing by ungulates including bison (*Bison bison*) (Campbell *et al.* 1994). 2 major upland grassland types at Kinsella Ranch were described by Coupland (1961), and include:

A. Mixed prairie grassland [Stipa-Elymus (SEG)] dominated by western speargrass (*Stipa comata* Trin. & Rupr.), and northern wheatgrass [*Elymus lanceolatus* (Scribn. & J.G. Sm.) Gould], these xeric grasslands can be found on steep, south-facing slopes (>5°) and hilltops.

B. Fescue grassland [Festuca-Stipa (FSG)] dominated by plains rough fescue [*Festuca hallii* (Vasey) Piper] and western porcupine grass [*Stipa curtiseta* (A.S. Hitchc.) Barkworth], fescue grassland once covered much of the Aspen Parkland. Today, most fescue grasslands have been broken for cereal production or have been overgrazed (Trottier 1986). At Kinsella, remnants of unbroken or moderately grazed fescue grasslands remain abundant on mesic uplands with gentle slopes (<5°).

(3) Shrublands

Upland shrublands are ecotonal between grassland and adjacent aspen forest. 2 major types of shrublands occur at Kinsella and include (after Wheeler 1976):

A. Western snowberry (*Symphoricarpos occidentalis* Hook.) (SPS).

B. Silverberry (*Elaeagnus commutata* Bernh. ex Rydb.) (ENS).

Both snowberry and silverberry reproduce extensively by suckering from creeping underground roots, resulting in dense, closed canopy patches.

(4) Aspen forest

Generally, forested areas at Kinsella are represented by trembling aspen (*Populus tremuloides* Michx.) communities, with an understory of saskatoon [*Amelanchier*

alnifolia (Nutt.) Nutt. ex M. Roemer], chokecherry (*Prunus virginiana* L.) and wild rose (*Rosa woodsii* Lindl) shrubs along with a well-developed herbaceous component. Aspen forest has expanded considerably over the last 60+ years (Bailey and Wroe 1974, Scheffler 1976), although periodic outbreaks of tent caterpillars and drought, coupled with prescribed burning have resulted in aspen stands of varied condition across the Ranch. Young (5-30yr) and mature (30-60yr) aspen communities are characterized by closed canopy stands of relatively uniform tree age, height and diameter (Stelfox, 1995). In contrast, old and decadent aspen communities (>60yr) have often undergone significant canopy break-up and subsequent understory release as well as the emergence of secondary young aspen and shrubs. As a result, aspen communities at Kinsella can be classified into closed (young or mature) (CAF) and semi-open (decadent) aspen forest (OAF) types.

3.2.2 LIDAR Data Acquisition and Processing

Airborne scanning laser data were collected over the study area by Optech, a company specializing in the design of laser-based ranging, mapping and detection systems. The laser system was flown at 1700m above sea level, with an average above ground elevation of 1005m (but ranging from 989m to 1027m) in the afternoon of 3 October 2000 during leaf-on conditions (Appendix 1). LIDAR sampling used an across-track scanning system with a Z-shaped ground target path. The wavelength and frequency of the laser pulse were 1.04 μm and 25 KHz, respectively. The mean intensity was 42% and maximum off-nadir angle 15°. Flight lines were approximately 500m apart,

with a total of 19 north-south flight lines covering the entire area (2700ha). Laser measurements are sometimes but not usually affected by other reflections such as sunlight. Optech's scanning laser instruments scan laser pulses within a preferred range of angles. Instruments are designed to operate in daylight (Optech Incorporated 2003).

Initial LIDAR data files consisted of 2 components including the realtime geo-corrected coordinates (UTM easting and northing, as well as Z-elevation) for each laser point on the ground (last return) and the top of the vegetation (first return), as well as the associated intensity readings. LIDAR intensity is the ratio of strength of reflected light to that of emitted light (unit: %). An elevation was calculated by knowing the speed of light (approximately 0.3 metres per nanosecond) and distance to (start pulse) and from (return pulse) the object being measured. The average laser footprint diameter was 0.3m ($0.071m^2$) directly below the aircraft, which increased to 0.31m ($0.075m^2$) at a distance of 250 m off-nadir. The average sampling interval was 1.5m between footprints in the across-track direction and 1.3m in the along-track (i.e., forward) direction. Final LIDAR data sampling densities across the area averaged 0.54 points/m^2, but ranged from 0.28 to 1.35 points/m^2.

The discontinuous last return ground LIDAR data points were subsequently interpolated into a continuous DEM surface to facilitate comparison of the LIDAR data to individual ground-truthed locations. Several interpolation methods, including kriging, inverse distance weighting (IDW, with a 0.3 and 3.0 coefficient), and splining (regular spline and tension spline), were initially used to determine the most accurate method for establishing a continuous LIDAR data surface. Kriging was subsequently dropped due to the excessive computational time required to process the data.

4 areas, each 4 km^2, were randomly selected from the LIDAR data to assess the remaining interpolation methods. Prior to interpolation, 0.1% of the original LIDAR points in each file (total of 6959 points for all 4 files) were extracted for comparison with the interpolated values to evaluate interpolation error. Analysis of variance (ANOVA) indicated that the 4 interpolation techniques did not differ significantly from each other in their mean interpolation accuracy (df=3, 27832; F=1.43 and P=0.23). Although mean differentiation levels among interpolation methods were similar (Table 3-1), the differential minima and maxima, as well as the standard deviation revealed the 2 splining methods produced greater distortions relative to the original data. Based on the smallest standard deviation, IDW with weight 0.3 was used for development of a final DEM for the study area.

3.2.3 DEM Ground Truthing

Ground truthing was conducted in relation to the treatment variables, namely vegetation type, slope gradient, and off-nadir distance. Due to limitations in the time and logistics (i.e., accessibility) of ground truthing, a preliminary power analysis (Thomas and Juanes 1996) was conducted to determine the minimum sample sizes needed to detect significant effects due to the external factors. This analysis indicated approximately 250 data points were needed to detect treatment affects on DEM accuracy.

Ground truthed data points were distributed across the study area in a stratified random pattern across the landscape (Appendix 1). Points were stratified by both vegetation type and slope gradient to ensure adequate sample sizes, but were randomly

located around a series of benchmarks (BMs) distributed throughout the study area. The vegetation categories included fescue (*Festuca-Stipa*) and mixed prairie (*Stipa-Elymus*) grasslands, closed and semi-open aspen forest, silverberry (*Elaeagus*) and western snowberry (*Symphoricarpos*) shrublands, as well as freshwater and saline riparian meadows. Slope gradient was stratified by low (<5 degree), moderate (5-10 degree), and steep (>10 degree) slopes. Although data points could not be readily stratified by off-nadir distance because of difficulty in identifying these classes within the landscape prior to sampling, the widespread spatial distribution of points (i.e., nearly random) ensured that all these categories were represented. Categories of off-nadir distance used for analysis were from 0 to 200 m in increments of 50 m, with a final category of 200-260m. Distances beyond 260m were not present because the total distance between adjacent flight lines was limited to about 500m.

The relative elevation of each ground truthed point was recorded using a Leica TCR 703 total laser station. Relative elevations were first used for the convenience of elevation transfer. Sampled points (n=260) were connected to one another using a series of 27 interconnected benchmarks set up across the study area (Figure 3-1). These BMs were used for transferring vertical elevations from one point to another using the "block station" (BS) (Leica 2000) transfer method (Figure 3-1, a and b). This method does not require the actual coordinates of the station. The total station calculates automatically the relative elevation of a target (e.g., BM) and is then passed to calculate the relative elevation between 2 targets. Adjacent BMs were approximately 500m apart (n=27) to avoid exceeding the capability of the laser station. Each BM was set up on top of a hill with a flat ground surface for convenient and accurate elevation transfer. Each time a

new BM was established, backsighting was used to validate the initial change in elevation (Figure 3-1, c→k). Cumulative backsight errors never exceeded 5cm. Finally, relative elevations were transferred to the absolute elevations based on BM #1, which was also a ground control point with centimeter elevation accuracy (<10 cm). This technical sampling design ensured centimeter accuracy of absolute elevations of both 27 BMs and the associated ground truthed points.

Each ground truthed point was located between two-BMs up to 250 m away from either adjacent BM. At each of the 27 BMs, between 6 and 12 ground truthed data points were sampled using the "free-station technique" (Leica 2000). This method requires a minimum of 2 known BMs and a maximum of 5 to determine the elevation of a single ground truthed point (Figure 3-1, a, c, e, then to d). The free-station technique averaged the orientation and elevation of the laser station, and produced more reliable elevation measurements of the ground truthed points.

There were 2 additional situations in which the height transfer method (Figure 3-1, f→g→h) was used to determine the ground elevation of a location. This included when the ground truthed points were more than 500m away from the BMs; or when the ground truthed points were located inside closed aspen forest. In both situations, a transfer point was set up at first with the laser station located between the transfer point and the targeted ground truthed point in order to transfer the ground elevation from the transfer point to the targeted point. Corresponding positional coordinates of each ground truthed point were sampled through the assistance of a differential-GPS (DGPS) system (mean horizontal accuracy 0.53 m). The distribution of all ground truthed points, as well as those BMs established on the study area, is illustrated in Figure 3-2.

3.3 Analysis

The IDW0.3 interpolation method was applied to the LIDAR data from the study area and created a digital elevation model with a spatial resolution of 1.5 m (Figure 3-3). All 254 ground truthed points (originally there were 260 GPS measurements, but 6 were excluded because their horizontal accuracy based on the DGPS exceeded 1 m) were applied to the DEM in order to determine their estimated elevations. Corresponding data points were extracted from the interpolated surface (i.e., DEM) and subsequently compared to the ground truthed points for testing the influence of off-nadir distance, slope gradient, and vegetation type, as well as their interaction effects, on the resulting accuracy of the DEM derived from the LIDAR data.

In order to assess effects of off-nadir distance, LIDAR data points along the flight lines were first converted to continuous lines with a swath interval of about 500m. Lines were then buffered with off-nadir distance intervals 50 m wide up to 200m. The final category was greater than 200m, and included all points beyond that but before the mid-point between successive flight lines. In order to test for the effect of off-nadir distance on DEM and LIDAR data accuracy, the predicted elevations (i.e., elevations from the DEM) were compared to the 254-ground truthed points. Sample sizes per class varied from 34 to 63 (Table 3-2). Where the mean differentiation of one group differed from that of another, it indicated off-nadir distance influenced DEM accuracy from the LIDAR data.

The same 254 points were used to test if slope gradient influenced LIDAR-derived DEM accuracy. We hypothesized that with the increase of slope gradient, LIDAR data accuracy would decrease because of the decrease in density of LIDAR

points. Slope categories were then classified into 3 classes. The corresponding sample sizes among the 0-5°, 5-10° and >10° slope classes varied from 156 to 43 respectively, likely in proportion to their abundance in the landscape. The predicted LIDAR data elevations of the 254 points were subsequently differentiated among slope classes using their corresponding ground measurements.

Vegetation types of the study area were first classified into upland grasslands, shrublands, forested areas and lowland meadows, and their corresponding ground truthed data points compared and differentiated with the predicted LIDAR data points. The comparatively smaller number (27) of ground truthed points of lowland meadows was due to the small portion of that vegetation type within the study area (about 5%).

A Paired-Sample T Test was first used to identify whether the LIDAR-derived elevations differed significantly from the ground-truthed elevations. Where they did, the mean differentiation, standard deviation and ANOVA analysis were applied to individual influential factors (e.g., slope gradient, off-nadir distance or vegetation type), interaction effects (e.g., slope gradient by vegetation types), as well as sub-vegetation factors (e.g., forested areas vs. grasslands) to identify whether those influential factors significantly influenced LIDAR-derived DEM accuracy. Tukey HSD comparisons (min. $P<0.10$) were applied to sub-vegetation categories with 4 and 8 classes of vegetation, respectively, to identify the quantitative over/under-estimation of elevations of vegetation types on LIDAR-derived DEM accuracy. Positive values indicated DEM elevation over-estimation and negative values under-estimation. Square root of the mean square error (RMSE) was also calculated to identify the deviation of LIDAR prediction from field measured vegetation heights.

3.4 Results

A Paired-Sample T Test (t=-33.78, df=253 and Sig<0.01) indicated that the LIDAR-derived elevations differed significantly from ground-truthed measurements. Either vegetational or non-vegetational influential factors or both created elevation differences.

3.4.1 Off-Nadir Distance

The mean of differences, standard deviations of mean as well as the ANOVA analysis (df=4, 249; F=0.87, P=0.48) all indicated there were no significant differences in DEM accuracy associated with the 5 off-nadir distance categories (Table 3-2). No significant difference existed even at the most extreme off-nadir distance (200-250 m). As an individual factor, off-nadir distance did not influence the accuracy of the LIDAR-derived DEM.

3.4.2 Slope Gradient

The mean of differences and standard deviations of mean in the second part of Table 3-2 and the ANOVA analysis (df=2, 251; F=0.72 and P=0.49) indicated slope gradient also did not significantly influence the LIDAR-derived DEM accuracy. No significant influence existed even if slope gradient exceeded 10 degrees.

3.4.3 Vegetation Types

The mean of differences (third part of Table 3-2) and the ANOVA analysis (df=3, 250; F=7.49 and p<0.001) indicated the vegetation types had a significant influence on accuracy of the LIDAR-derived DEM. Although the overall mean estimation was very accurate (+2 cm), it created a RMSE of 1.21 m. Table 3-2 also indicates that the elevations were over-estimated within forested areas by an average of 20 cm (with a RMSE of 1.05 m), under-estimated (-12 cm, RMSE = 1.36) within grasslands (upland and lowland), and mostly accurate in shrublands (+7 cm, RMSE = 1.15 m). Forested areas differed significantly from both upland grasslands and lowland meadows with respect to their influence on accuracy of the LIDAR-derived DEM (Table 3-3).

Further exploration of the 8 detailed vegetation types revealed that the forested areas (closed and semi-open) differed from the fescue grasslands and fresh riparian meadows with respect to differences in LIDAR-derived DEM accuracy. Closed aspen forest resulted in the greatest over-estimation of ground elevations, followed by the semi-open aspen forest. Fresh riparian meadows had the greatest under-estimation of ground elevations, with the fescue grassland second. The mixed prairie grasslands, saline riparian meadows and 2 shrublands (silverberry and western snowberry) did not significantly influence (P>0.10) accuracy of the LIDAR-derived DEM relative to the other vegetation types (Table 3-5).

3.4.4 Interaction Effects

Although the individual factors of off-nadir distance and slope gradient did not

significantly influence DEM and LIDAR data accuracy, when integrated, these factors resulted in a significant effect (P=0.05). Accuracy normally increased at positions with shorter off-nadir distances and flatter slope gradient. Other interaction effects including vegetation by slope and vegetation by off-nadir distance were not significant (P=0.43 and 0.96, respectively) (Table 3-4).

3.5 Discussion

Most studies have claimed maximum 15 cm vertical accuracy of LIDAR data regardless of where the work was done or what the surface conditions (e.g., vegetation type) might be. This research created a DEM with a mean overall accuracy of +2 cm and RMSE of 1.21 m. It supported the hypothesis that a laser-based system can provide synoptic (i.e., landscape-based complete coverage) and relatively accurate for elevation mapping (Krabill *et al.* 1995). However, accuracy of the LIDAR-derived DEM also created an overall RMSE of 1.21m and did vary with a number of external factors.

3.5.1 Non-Vegetation Factors

2 possible explanations may account for the lack of influence of off-nadir distance on LIDAR-derived DEM accuracy, including tilt angle of the laser camera, and the spatial distribution of LIDAR data sampling. By randomly selecting 1 data file (4 km^2) and calculating the laser point density with increasing off-nadir distance (<50m, 50-100m, 100-150m, 150-200m and >200m, respectively), this research found that contrary to our expectations, the intensity of LIDAR sampling increased with off-nadir distance

(e.g., densities of 0.42, 0.47, 0.59, 0.69 and 0.71 points/m^2, respectively). This trend might compensate for the sensor tilt angle effects of the laser camera during data collection, especially under windy conditions, by increasing the surface sampling intensity at greater off-nadir distances.

The insignificant influence of slope gradient on DEM and LIDAR data accuracy may lie in the comparatively negligible variation in ground slope gradient and relief relative to the sampling distance from plane to ground. The aircraft with LIDAR equipment flew at an elevation of about 1700m, and the ground elevation varied from 680m to 720m. Thus, the distance from the LIDAR equipment to ground was about 1000 m. Most of the slope gradients on the Ranch do not exceed 10^o, and the relief is less than 15m. This type of moderately rolling landscape may have limited overall variation in LIDAR sampling density across different slopes and reliefs.

However, the interaction of slope gradient and off-nadir distance reflected an increase in LIDAR sampling density at positions with shorter off-nadir distances and smaller slope gradient, which also created higher accuracies than positions with larger off-nadir distance and bigger slope gradient. Interpolated DEM accuracy normally increases in locations where more LIDAR data sampling points are available. Therefore, this may therefore account for the significant influence of these 2 integrated effects on LIDAR-derived DEM accuracy.

3.5.2 Vegetation Factors

Ni-Meister *et al.* (2001) indicated leaf orientation and shape contributed to the

change of foliage profile and their influences on LIDAR data collection accuracy. Grasslands at the study area have largely vertical oriented leaves, due to their domination by monocots. The repeated bouncing back and forth of incoming LIDAR signals may have made the peak values of the waveforms for grasslands consistently greater than their actual peak waves, resulting in under-estimation of grassland elevations. Background noise in sparsely populated shrublands and herbaceous grasslands (Weltz *et al.* 1994) might also contribute to the underestimation. In contrast, the leaves of trees and shrubs (i.e., dicots) are usually more horizontally oriented, and oval shaped. This kind of vegetation can attenuate the laser beam irradiance passing through the canopy more readily. As a result, attenuated peak signals of the last return would reflect back more rapidly than from grasses. Moreover, the last return is less likely to come from the true ground, but rather from somewhere within the understory layers. Combined, these effects may have resulted in the over-estimation of ground elevations in forests and shrublands, opposite to the former.

Comparisons within each plant functional group (i.e., woodland vs. grassland type) and its influential factors, revealed that increasing woody species height and cover increased the over-estimation of ground elevations (Figure 3-4 a). In contrast, increasing grass height and cover had the opposite tendency of increasing the under-estimation of ground elevations (Figure 3-4 b). The integrated values represent volume information or vegetational "denseness" of woodlands and grasslands. These values were calculated using Equations 3.1 and 3.2, respectively, and were visually displayed on Figure 3-4 (a and b):

Woodland (integrated) denseness = (understory cover)*(understory height) +

(Overstory cover)*(Overstory height) ..... (Eq. 3.1)

Grassland (integrated) denseness = (grass cover)*(grass height) .....(Eq. 3.2)

These non-linear regressions indicated that closed forest areas (greatest volume and density within the shrub/aspen group) had the greatest over-estimation and the fresh riparian meadows (greatest volume and density within the grassland group) had the greatest under-estimation of the LIDAR-derived DEM accuracy. LIDAR signals are influenced by both the vertical distribution (i.e., physiognomy) and plant morphology of vegetation (Ni-Meister *et al.* 2001), but had opposite effects within grasslands and woody vegetation types.

In addition to canopy structure influences on laser responses and DEM accuracy, the inherent characteristics of small footprint laser systems limit their application in dense and complex forest areas. Hofton *et al.* (2002) mapped a ~800 km^2 area of Costa Rica using 25 m-diameter footprints as part of the pre-launch activities of the Vegetation Canopy LIDAR (VCL) Mission. Crossover analysis using laser shots, whose recorded waveforms contained more than 50% of the total returned energy within their lowest reflections, showed elevation accuracy more than 50% greater compared to a corresponding small footprint LIDAR system. The difficulty of penetrating dense and complex forest canopies through gaps will promote the use of large footprint (>10 m in diameter) laser altimetry to measure sub-canopy topography.

3.6 Conclusion

LIDAR data can provide synoptic quantification of landscape topography and

roughness for large areas by building DEMs within the Aspen Parkland. Measurements of micro and macro surface features contribute to the quantification of water retention, infiltration, evaporation, and movement from landscape surfaces. Estimation of soil condition and development can also benefit from an understanding of study area topography. The distribution of some vegetation communities, as well as animal movement and grazing is also dependent on specific topographic features.

Accuracy assessment indicated that as an individual factor neither slope gradient nor off-nadir distance significantly influenced accuracy of a LIDAR-derived DEM. However, the interaction of slope gradient and off-nadir distance did significantly influence accuracy. Different vegetation types had the greatest influence on accuracy of a LIDAR-derived DEM within this Aspen Parkland environment. Despite an overall mean accuracy of +2 cm across the 8 vegetation types, this accuracy included an overall RMSE of 1.21 m. Also, elevations were over-estimated within forested areas by an average of 20 cm with a RMSE of 1.05 m, under-estimated (-12 cm, RMSE = 1.36 m) within grasslands (upland and lowland), and most accurate in shrublands (+7 cm, RMSE = 1.15 m), potentially necessitating DEM correction for vegetation type influences. Overall, results of this research highlight the potential of using LIDAR data to effectively model landscape DEM properties over large areas of the Aspen Parkland. Such measurements will improve our understanding of the effects of complex landscape characteristics on hydrological systems, vegetation distribution, animal movement and grazing, so that improved management practices and structures can be developed to sustain our natural resources.

3.7 Literature Cited

Acton, D. F. 1965. The relationship of patterns and gradients of slopes to soil type. *Canadian Journal of Soil Science* 45:96-101.

Allen-Diaz, B., R.D. Jackson, and J. Fehmi. 1998. Detecting channel morphology change in California's hardwood rangeland spring systems. *Journal of Range Management* 51:514-18.

Anderson, M.L. and A.W. Bailey. 1979. Effect of fire on a *Symphoricarpos occidentalis* shrub community in cental Alberta. *Canadian Journal of Botany* 57:2819-23.

Asamoah, S. A., E. W. Bork, B. D. Irving, M. A. Price, and R. J. Hudson. 2003. Cattle herbage utilization patterns under high-density rotational grazing in the Aspen Parkland. *Canadian Journal of Animal Science*. 83:541-550.

Ayad, M.A.G. and R.L. Dix. 1964. Analysis of a vegetation micro environmental complex on prairie slopes in Saskatchwon. *Ecological Monographs* 34:421-442.

Bailey, A.W. 1978. Effects of fire on the mixed prairie vegetation (pp5). In *Proc, Prairie Prescribed Burning Symposium and Workshop.* U.S. Forest Services, Burning Land Management, and USFWS, Jamestown, North Dakota.

Bailey, A.W. and R.A. Wroe. 1974. Aspen invasion in a portion of the Alberta parklands. *Journal of Range Management* 27:263-266.

Bailey, A.W., B.D. Irving, and R.D. Fitzgerald. 1990. Regeneration of woody species following burning and grazing in aspen parkland. *Journal of Range Management* 43: 212-215.

Benedict, N.B. 1982. Mountain meadows: stability and change. *Madroño* 29:148-53.

Bufton, J.L., J.B. Garvin, J.F. Cavanaugh, L. Ramos-Izquierdo, T.D. Clem, and W.B. Krabill. 1991. Airborne LIDAR for profiling of surface topography. *Optical Engineering* 30:72-78.

Eagle Scan Inc. 2000. 3D perspective views of Kosciusko Island, Southeast Alaska, generated from LIDAR DEM data. http://www.3dillc.com/rem-LIDAR-off-the-shelf-data.html, March.

Krabill, W.B., R.H. Thomas, C.F. Martin, R.N. Swift, and E.B. Frederick. 1995. Accuracy of airborne laser altimetry over the Greenland ice-sheet. *International Journal of Remote Sensing* 16:1211-1222.

Leica. 2000. Leica Geosystems TC(R)702/703/705-1.1.Oen User's Manual pp39-69.

Narayanan, R.M. and B.D. Guenther. 1998. Effects of emergent grass on mid-infrared laser reflectance of soil. *Photogrammetric Engineering and Remote Sensing* 64:407-13.

Ni-Meister, W., D.L.B. Jupp, and R. Dubayah. 2001. Modeling LIDAR waveforms in heterogeneous and discrete canopies. *IEEE transactrions on Geoscience and Remote Sensing* 39:1943-58.

Optech Incorporated. 2003. About laser RADAR. http://www.optech.on.ca /aboutlaser.htm.

Ratliff, R.D.1985. Meadows in the Sierra Nevada of California: state of knowledge. Forest Service, Pacific Southwest Forest and Range Experiment Station. Berkeley, California, U.S.

Renslow, M.S. 2001. Applications of advanced LIDAR for DEM applications. http://www.sbgmaps.com/LIDAR_apps.htm.

Sapeta, K. 2000. Have you seen the light-LIDAR technology is creating believers. *Geo World* 13:32-4.

Serr, David. 2000. Use of LIDAR in Creating Accurate Terrain Elevation Models for Floodplain Mapping (term project). http://www.emporia.edu/earthsci/student/ serr1/abstract.htm. December 7.

Thomas and Hutton Engineering Inc. 2000. LIDAR. http://thomas-button.com /LIDAR.html.

Thomas, L. and F. Juanes. 1996. The importance of statistical power analysis: an example from Animal Behaviour. *Animal Behaviour* 52: 856-859.

Tsutsui, K., K. Koya, and T. Kato. 1998. An investigation of continuous-angle laser light scattering. *Review of Scientific Instruments* 69:3482-86.

3.8 Tables and Figures

Table 3-1 Comparison of interpolation accuracy among the 4 interpolation methods.

Interpolation Method[1]	Number of Points (0.1%)	Mean Differentiation (m)	Std. Deviation	95% Confidence Interval for Mean		Differentiation Minimum (m)	Differentiation Maximum (m)
				Lower Bound	Upper Bound		
IDW3.0	6959	-0.002	0.391	-0.012	0.007	-3.24	3.00
IDW0.3	6959	-0.002	0.385	-0.011	0.007	-3.10	3.12
Reg-Spline	6959	-0.070	4.173	-0.169	0.028	-129.79	104.21
Ten-Spline	6959	0.009	2.818	-0.058	0.075	-24.99	221.20
Total	27836	-0.017	2.533	-0.046	0.013	-129.79	221.20

[1] IDW 3.0 and IDW0.3 – Inverse distance weighted interpolation with weight 3 and 0.3, respectively; Reg-Spline and Ten-Spline – Regular and tension interpolation, respectively.

Table 3-2 Effects of influential factors on the accuracy of a LIDAR-derived DEM.

Influential Factor	Category	Number of Points	Mean Differentiation (m)	Std. Deviation	95% Confidence Interval for Mean		Differentiation Minimum (m)	Differentiation Maximum (m)
					Lower Bound	Upper Bound		
Off-Nadir Distance (m)	<50	63	0.055	0.572	-0.089	0.199	-0.988	2.415
	50~100	54	-0.061	0.514	-0.201	0.079	-2.125	0.61
	100~150	46	-0.037	0.447	-0.17	0.096	-1.407	1.118
	150~200	57	0.071	0.484	-0.057	0.199	-1.146	1.28
	>200	34	0.098	0.557	-0.097	0.292	-1.691	1.33
	Total	254	0.023	0.517	-0.041	0.087	-2.125	2.415
Slope Gradient (°)	<5	156	-0.055	0.405	-0.069	0.058	-1.18	1.809
	5~10	55	0.09	0.455	-0.033	0.213	-0.974	1.372
	>10	43	0.041	0.854	-0.222	0.303	-2.125	2.415
	Total	254	0.023	0.517	-0.041	0.087	-2.125	2.415
Vegetation Type	Upland Grasslands	74	-0.118	0.526	-0.24	0.035	-2.125	1.118
	Shrub Lands	79	0.068	0.463	-0.035	0.172	-1.146	1.809
	Forested Areas	74	0.203	0.515	0.084	0.322	-1.691	2.415
	Lowland Meadows	27	-0.215	0.466	-0.399	-0.031	-1.049	0.37
	Total	254	0.023	0.517	-0.041	0.087	-2.125	2.415

Table 3-3 Comparison among the 4 general vegetation types of their influence on the accuracy of a LIDAR-derived DEM.

Vegetation Type (I)	Vegetation Type (J)	Mean Difference (I-J) (m)	Std. Error	Sig. (P)	95% Confidence Interval Lower Bound (m)	95% Confidence Interval Upper Bound (m)
Upland Grasslands (1)	2	-0.187	0.081	**0.094**	-0.394	0.020
	3	**-.321**[1]	0.082	**0.001**	-0.532	-0.111
	4	0.097	0.112	0.824	-0.191	0.384
Shrub Lands (2)	1	0.187	0.081	**0.094**	-0.020	0.394
	3	-0.135	0.081	0.339	-0.342	0.072
	4	0.283	0.111	**0.052**	-0.002	0.569
Forested Areas (3)	1	**.321**[1]	0.082	**0.001**	0.111	0.532
	2	0.135	0.081	0.339	-0.072	0.342
	4	**.418**[1]	0.112	**0.001**	0.130	0.706
Lowland Meadows (4)	1	-0.097	0.112	0.824	-0.384	0.191
	2	-0.283	0.111	**0.052**	-0.569	0.002
	3	**-.418**[1]	0.112	**0.001**	-0.706	-0.130

[1] Mean difference is significant at the .10 level.

Table 3-4 Results of the interaction analysis among factors (vegetation, slope and nadir distance) on their influence on the accuracy of the LIDAR-derived DEM.

Interaction Factors	Sum of Squares	Degree of Freedom	Mean Square	F-test	Sig. (P)
Vegetation * Slope	.159	1	.159	.637	.426
Vegetation*Off-nadir Distance	0.001	1	0.001	.005	.942
Slope * Off-nadir Distance	.938	1	.938	3.752	**.054**
Vegetation * Slope * Off-nadir Distance	0.039	1	0.039	.155	.694

Table 3-5 Comparison among the 8 vegetation types with respect to their influence on accuracy of a LIDAR-derived DEM.

(I) Focal Vegetation Type[1]	(J) Focal Vegetation Type[1]	Mean Difference (I-J) (m)	Std. Error	Sig.	95% Confidence Interval	
					Lower Bound	Upper Bound
SEG (1)	2	0.057	0.117	1.000	-0.296	0.411
	3	-0.198	0.126	0.765	-0.580	0.183
	4	-0.129	0.112	0.947	-0.469	0.212
	5	-0.317	0.127	0.196	-0.702	0.068
	6	-0.272	0.114	0.253	-0.618	0.075
	7	-0.032	0.168	1.000	-0.541	0.478
	8[2]	0.256	0.155	0.720	-0.215	0.727
FSG (2)	3	-0.256	0.120	0.394	-0.619	0.108
	4	-0.186	0.106	0.647	-0.506	0.134
	5	**-0.375**[3]	0.121	**0.041**	-0.742	-0.008
	6	**-0.329**[3]	0.108	**0.047**	-0.656	-0.003
	7	-0.089	0.164	0.999	-0.585	0.407
	8	0.199	0.151	0.891	-0.257	0.655
ENS (3)	4	0.070	0.116	0.999	-0.281	0.420
	5	-0.119	0.130	0.985	-0.513	0.275
	6	-0.073	0.118	0.999	-0.430	0.283
	7	0.167	0.170	0.978	-0.350	0.683
	8	**0.455**[3]	0.158	**0.076**	-0.024	0.933
SPS (4)	5	-0.189	0.117	0.741	-0.543	0.165
	6	-0.143	0.103	0.862	-0.455	0.169
	7	0.097	0.161	0.999	-0.390	0.584
	8	0.385	0.147	0.151	-0.061	0.831
CAF (5)	6	0.046	0.119	1.000	-0.314	0.406
	7	0.286	0.171	0.708	-0.233	0.805
	8	**0.574**[3]	0.159	**0.007**	0.093	1.055
OAF (6)	7	0.240	0.162	0.818	-0.251	0.731
	8	**0.528**[3]	0.149	**0.009**	0.077	0.979
SRM (7)	8	0.288	0.193	0.813	-0.298	0.874

[1] SEG – mixed prairie, FSG – fescue grassland, ENS – silverberry, SPS – western snowberry, CAF – closed aspen forest, OAF – semi-open aspen forest, SRM – saline riparian meadow, FRM – fresh riparian meadow.

[2] 8 represents FRM-fresh riparian meadows.

[3] Mean difference is significant at the .10 level.

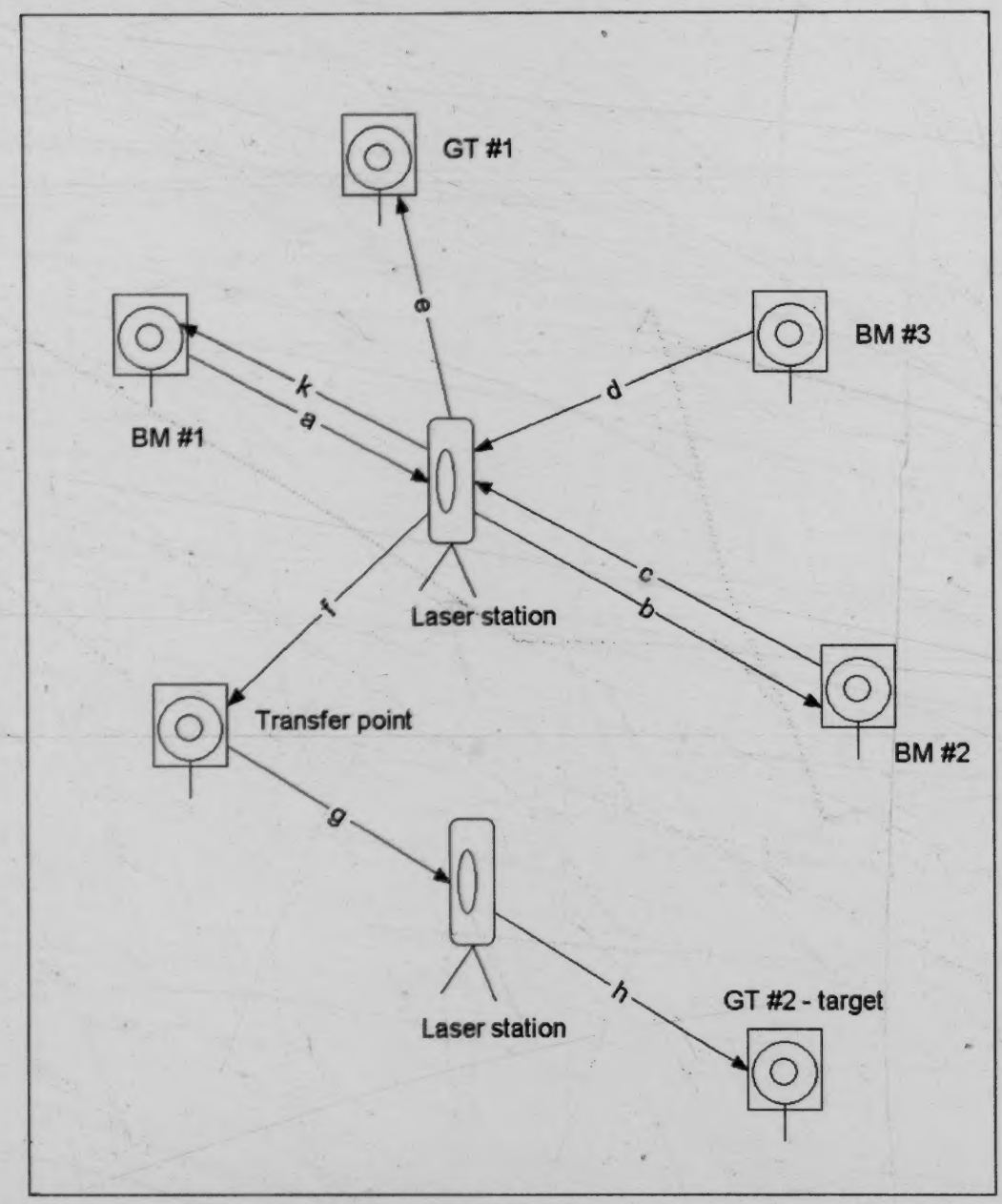

Figure 3-1 Field layout for obtaining elevation measurements on ground truthed points using a total laser station.

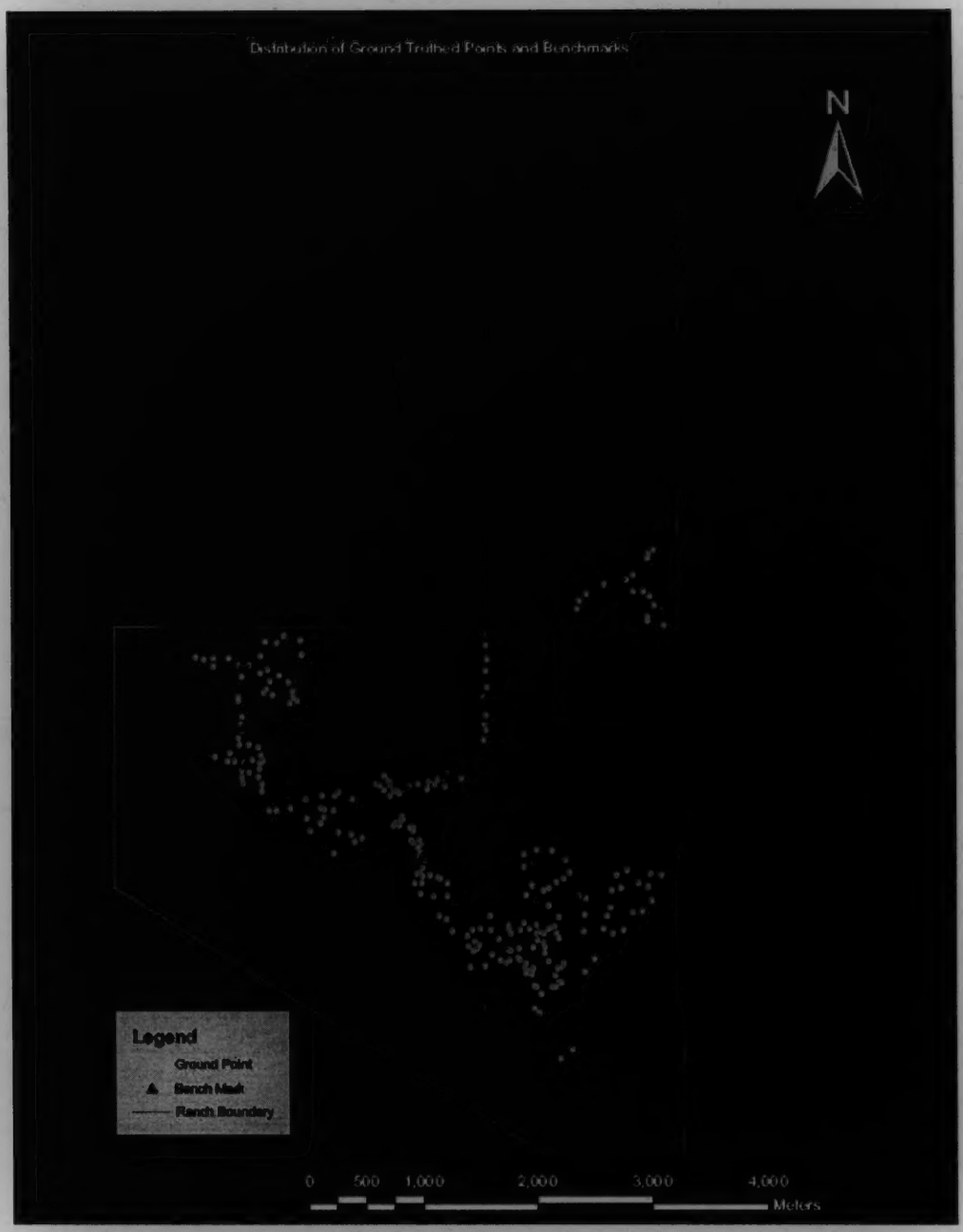

Figure 3-2 The distribution of 27 inter-connected benchmarks and 260 ground truthed data points around those benchmarks.

Figure 3-3 Digital elevation model of the study area with a spatial resolution of 1.5 m obtained using IDW 0.3 interpolation.

a.

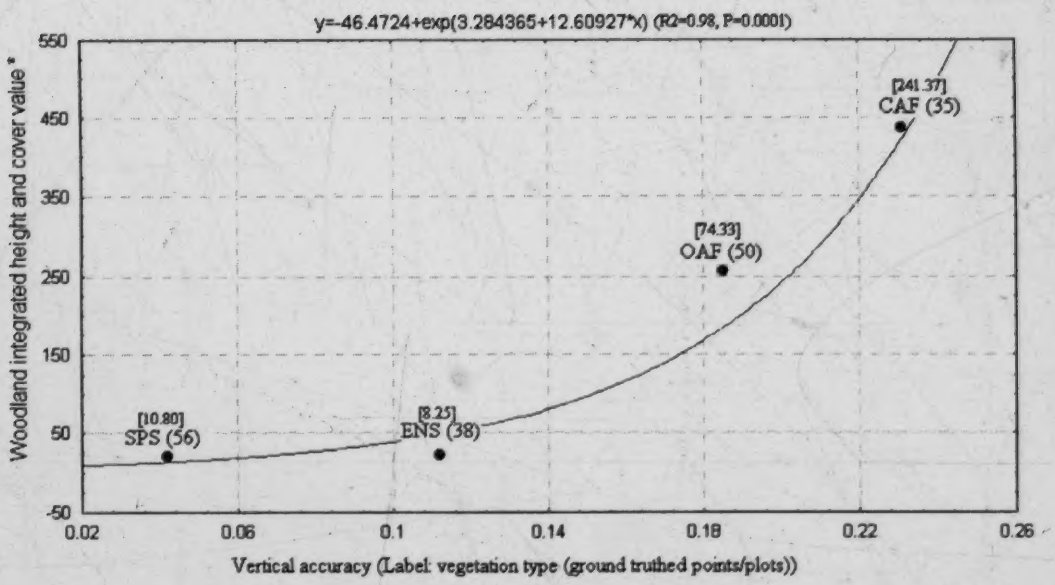

b.

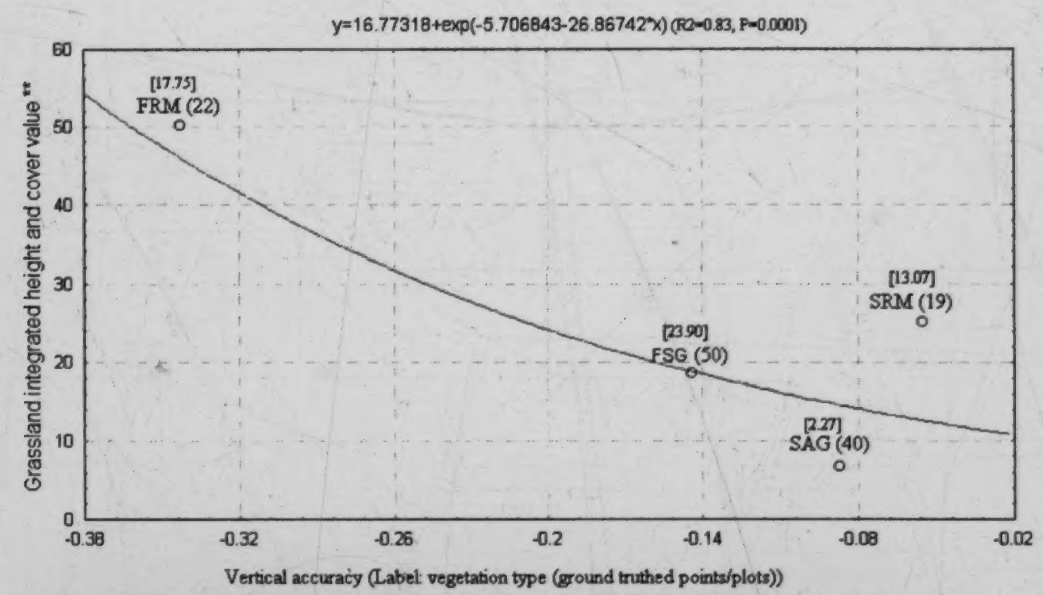

Figure 3-4 The relationship between mean vertical accuracy and integrated vegetation characteristics to the over (a) or underestimation (b) of a LIDAR-derived DEM. [*Woodland integrated height and cover value = (understory cover)·(understory height) + (overstory cover) · (overstory height); **Grassland integrated height and cover value = (grass height) · (grass cover)]. The square brackets represent the std. dev. of the integrated values.

4 Characterization of Aspen Parkland Vegetation Using LIDAR Data

4.1 Introduction

Vegetation spatial structure (i.e., physiognomy), including plant height, cover, and vertical or horizontal heterogeneity, is an important factor influencing biodiversity and the associated exchange of matter and energy between landscape and atmosphere (Dubayah *et al.* 1997). Measurements of land surface (including vegetation) shapes, patterns, and heterogeneity provide data necessary to understand landform changes in space and time (Ritchie *et al.* 2001).

Historical methods of rangeland assessment largely emphasized the use of point-based inventories, intended to collect detailed information on individual plant communities (National Research Council 1994). With this method, primary strata or samples from the entire rangeland were selected, with sub-sampling used to derive select data from a few, stratified locations within the entire land base. This approach represented a type of 'bottom-up' management in that strategically placed random sub-sampling was used to collect detailed information on the species composition, soil type and slope, etc., of representative key areas, with these limited sum-sampling points extrapolated back to the entire rangeland to alter management (West and Smith 1997). Yet other attempts were made to select different sampling points that were thought to represent different successional stages associated with a disturbance. Collectively, these processes were useful in that detailed plant community information could be related

quite readily to the determination of ungulate carrying capacity, as well as the existing models of rangeland condition based on livestock grazing and associated retrogression of vegetation (Clements 1916, Dyksterhuis 1949).

While the use of stratified random sampling (SRS) inventories is highly effectively at providing information on localized plant communities, several problems exist with the use of this method. These problems largely stem around the inability of managers to safely extrapolate local sampling points to the larger, more realistic, and more spatially variable landscape scale at which management actually occurs, as well as the very laborious and costly nature of data collection. Coupled together, these factors have limited the application of SRS for rangeland managers, including the potential for large-scale rangeland condition and trend assessment. In fact, reductions to both the budget and labour pool in many rangeland management, advisory, and regulatory agencies, along with a restricted field season, renders the intensive, prolonged sampling of plant communities altogether unrealistic.

Remote sensing is a potential alternative rangeland monitoring method to gather site-specific data from vast areas. Primary benefits include synoptic (e.g., spatially complete) coverage, high cost-effectiveness (i.e., reducing the cost per unit area examined), and lower labour requirements relative to SRS (Tueller 1989). In addition, remote sensing can provide data on areas that are often inaccessible, as well as highly heterogeneous landscapes, where complex mosaics of vegetation with frequent transitional areas may preclude the use of point sampling. Remotely-sensed data also facilitates, though its complete coverage or stratification, additional forms of analysis such as landscape metrics (e.g., vegetation distribution). The spatially complete nature of

remotely-sensed information on rangelands provides an efficient strategy for rangeland management, and as a result, provides a potential complementary data source to the collection of detailed plant community information. Traditional remotely-sensed systems include aerial photography, videography, as well as airborne and satellite spectral sensors or RADAR.

However, assessing rangeland conditions and their spatial distribution using conventional remote sensing technology provides data of limited spatial resolution. For example, most remote sensing systems (e.g., airborne photography) provide images of the horizontal (2-D) organization of canopies, but do not provide direct information on the vertical (3-D) distribution of canopy elements (Dubayah *et al.* 1997). Current SAR (Synthetic Aperture RADAR) technology offers promise for predicting low levels of vegetation structure and for mapping general vegetation types in floristicly simple (e.g., non-diverse) landscapes (Smith *et al.* 1994, Rignot *et al.* 1994), but is insensitive to and thus, unsuitable, for mapping densely vegetated sites (Waring *et al.* 1995).

More recently, laser altimeter systems have been developed to provide high resolution, geolocated measurements of vegetation vertical structure (Nelson 1997) and ground elevations (Pachepsky and Ritchie 1998). However, little research has fully explored the capability of using LIDAR (Light Detection and Ranging) data to characterize vegetation within structurally complex landscapes that include many different plant communities.

The Aspen Parkland of western Canada forms a broad transition zone between the warm, dry prairies to the south and cool, moist boreal forest to the north (Johnson *et al.* 1995). The Parkland commonly consists of groves of aspen *(Populus tremuloides*

Michx.) alternating with grasslands predominantly of rough fescue [*Festuca halli* (Vasey) Piper] (Wheeler 1976).

The objective of this research was to use LIDAR positional data, and where possible, LIDAR intensity information, to quantify field vegetation height, cover and density of various vegetation types in a portion of the Aspen Parkland, including open grasslands, shrublands, and aspen forests of varied canopy closure.

4.2 Study Area

This research was conducted at the University of Alberta Ranch (53°0' N; 111°31' W) located 150 km SE of Edmonton, Alberta, Canada, within the Aspen Parkland natural sub-region. The Ranch is 2700 ha in size and has a general topography of rolling hills (i.e., knob and kettle terrain) with 5-15 m relief arising from its glacial moraine landform origin. The region has a temperate continental climate, with mean annual precipitation of 433 mm and 100-120 frost-free days (University's Meteorological Station at Kinsella Ranch). North-facing slopes are capable of supporting plant species with greater moisture requirements due to snow accumulation, such as aspen forest and shrublands, while south-facing slopes typically support plant communities tolerant of drier conditions such as grasslands (Wheeler 1976, Coupland 1961). The most common soil type of the area is a Black Chernozem, although Dark Gray Chernozems and Eluviated Chernozems are present as well (Bailey and Wroe 1974, Scheffler 1976). Gleysols and Solonetzic soils also occur, the former confined to poorly drained lowlands. Herbage production is 2251 ± 747 and 2886 ± 993 ($kg \cdot ha^{-1}$, dry matter) in its first and second rotation,

respectively (Asamoah *et al.* 2003), and the major vegetation types at the Ranch are as follows:

(1) Riparian meadows

Meadows are mesic to hygric habitats occupied by grass (*Poaceae* family) and grasslike species primarily of the genera *Carex* and *Juncus*. The primary environmental characteristic affecting meadow vegetation is the high water table during all or part of the year (Benedict 1982). 2 major types of wetlands exist at Kinsella, which include:

A. Saline riparian meadows (SRM) dominated by salt grass [*Distichlis spicata* (L.) Greene], alkali grass [*Puccinellia nuttalliana* (Schultes) Hitchc] and numerous forbs. They were found bordering salt covered lakebeds of discharge origin.

B. Freshwater riparian meadows (FRM) dominated by aquatic sedges (e.g., *Carex atherodes* Spreng., etc), tufted hairgrass [*Deschampsia caespitose* (L.) Beauv.], and some marsh reedgrass [*Calamagrostis canadensis* (Michx.) Beauv.]. These meadows occurred at slightly greater elevations as ground water recharge areas.

(2) Upland grasslands

Grasslands were historically maintained by a combination of periodic fire (Wright and Bailey 1982) coupled with grazing by ungulates including bison (*Bison bison*) (Campbell *et al.* 1994). 2 major upland grassland types at Kinsella Ranch were described by Coupland (1961), and include:

A. Mixed Prairie grassland [Stipa-Elymus (SEG)] dominated by western speargrass (*Stipa comata* Trin. & Rupr.), and northern wheatgrass [*Elymus lanceolatus* (Scribn. & J.G. Sm.) Gould], these xeric grasslands can be found on steep, south-facing slopes (>5°) and hilltops.

B. Fescue grassland [Festuca-Stipa (FSG)] dominated by plains rough fescue [*Festuca hallii* (Vasey) Piper] and western porcupine grass [*Stipa curtiseta* (A.S. Hitchc.) Barkworth], fescue grassland once covered most of the Aspen Parkland. Today, most fescue grasslands have been broken for cereal production or overgrazed (Trottier 1986). At Kinsella, remnants of unbroken or moderately grazed fescue grasslands remain abundant on mesic uplands with gentle slopes (<5°).

(3) Shrublands

Upland shrublands are ecotonal between grassland and adjacent aspen forest. 2 major types of shrublands occur at Kinsella and include (Wheeler 1976):

A. Western snowberry (*Symphoricarpos occidentalis* Hook.) (SPS).

B. Silverberry (*Elaeagnus commutata* Bernh. ex Rydb.) (ENS).

Both snowberry and silverberry reproduce extensively by suckering from creeping underground roots, resulting in dense, closed canopy patches.

(4) Aspen forest

Generally, forested areas at Kinsella are represented by trembling aspen *(Populus tremuloides* Michx.) communities, with an understory of saskatoon [*Amelanchier alnifolia* (Nutt.) Nutt. ex M. Roemer], chokecherry (*Prunus virginiana* L.) and wild rose (*Rosa woodsii* Lindl) shrubs along with a well-developed herbaceous component. Aspen forest has expanded considerably over the last 60+ years (Bailey and Wroe 1974, Scheffler 1976), although periodic outbreaks of tent caterpillars and drought, coupled with prescribed burning have resulted in aspen stands of varied condition across the Ranch. Young (5-30yr) and mature (30-60yr) aspen communities are characterized by closed canopy stands of relatively uniform tree age, height and diameter (Peterson and

Peterson 1995, Stelfox 1995). In contrast, old and decadent aspen communities (>60yr) have often undergone significant canopy break-up and subsequent understory release as well as the emergence of secondary young aspen and shrubs. As a result, aspen communities at Kinsella can be classified into closed (young or mature) (CAF) and semi-open (decadent) aspen forest (OAF) types.

4.3 Materials and Methods

A total of 120 ungrazed circular field plots each with a radius of 6 m were sampled for vegetation height, cover, and where possible, tree density. Corresponding LIDAR data points within each field plot were sampled through the use of a differential-GPS system. LIDAR-derived vegetation height and cover data were then compared with field measurements, and evaluated our ability to characterize vegetation using LIDAR data.

4.3.1 LIDAR Data Acquisition

Airborne scanning laser data were collected over the study area by Optech, a company specializing in the design of laser-based ranging, mapping and detection systems. The laser system was flown at 1700m above sea level, with an average above ground elevation of 1005m (but ranging from 989m to 1027m) in the afternoon of 3 October 2000 during leaf-on conditions (Appendix 1). LIDAR sampling used an across-track scanning system with a Z-shaped ground target path. The wavelength and frequency of the laser pulse were 1.04 μm and 25 KHz, respectively. The mean intensity

was 42% and maximum off-nadir angle 15°. Flight lines were approximately 500m apart, with a total of 19 north-south flight lines covering the entire area (2700ha). Laser measurements are sometimes but not usually affected by other reflections such as sunlight. Optech's scanning laser instruments scan laser pulses within a preferred range of angles. Instruments are designed to operate in daylight (Optech Incorporated 2003).

The initial LIDAR data files consisted of 2 components including the realtime geo-corrected coordinates (UTM easting and northing, as well as Z-elevation) for each laser point on the ground (last return) and the top of the vegetation (first return), as well as the associated intensity readings. LIDAR intensity is the ratio of strength of reflected light to that of emitted light (unit: %). An elevation was calculated by knowing the speed of light (approximately 0.3 metres per nanosecond) and distance to (start pulse) and from (return pulse) the object being measured. The average laser footprint diameter was 0.3m ($0.071m^2$) directly below the aircraft, which increased to 0.31m ($0.075m^2$) at a maximum distance of 250 m off-nadir. The average laser point sampling interval was 1.5m between footprints in the across-track direction and 1.3m in the along-track (i.e., forward) direction. Final LIDAR data sampling densities across the area averaged 0.54 points/m^2, but ranged from 0.28 to 1.35 pts/m^2. The digital elevation model (DEM) developed in Chapter 3 (this volume) was used to calculate vegetation height information for each laser point as the difference between the interpolated ground elevation and corresponding LIDAR first return elevation.

4.3.2 Experimental Design

A preliminary power analysis (Thomas and Juanes 1996) was conducted to

determine the minimum number of ground plots needed to characterize each of the 8 vegetation types described earlier. The vegetation categories included mixed prairie (*Stipa-Elymus*) and fescue (*Festuca-Stipa*) grasslands, closed (young or mature) and semi-open (old-growth or decadent) aspen forests, silverberry and snowberry shrublands, as well as freshwater and saline riparian meadows. Additionally, all field plots were further stratified directly by slope gradient (<=5°; >5°). Power analysis (Thomas and Juanes 1996) indicated approximately 15 plots per vegetation type or a total of 120 field sampling plots (alpha=0.05, effect size=0.15 and power=95%) were necessary to satisfy the correlation analysis between field and LIDAR data (Appendix 1).

Although field plots could not be initially stratified by off-nadir distance because of difficulty identifying these classes within the landscape prior to sampling, the varied spatial distribution of plots ensured both categories (on or near-, and off-nadir) were sufficiently represented (e.g., n=65, <130 m from nadir; n=55, 130-250 m off-nadir).

4.3.3 Field Vegetation Sampling

Within each plot, vegetation was sampled along 2, 10 m long parallel transects (Figure 4-1 a, Appendix 1) in July and August of 2001. Transects were oriented north to south in plots of slope gradient less than 2°; otherwise, they ran parallel to the slope contour. On each transect, 10 uniformly distributed 0.5 x 1.0 m quadrats were sampled for maximum understory vegetation height (herb and shrub separately). In addition, the canopy cover of each species was assessed ocularly in each quadrat, using the method of Daubenmire (1959). In aspen forest, 6 trees from the dominant overstory were measured

for height using a clinometer and tape ruler. Trees nearest the start, middle and endpoint (0, 5 and 10m) of each transect were measured within each plot. Each aspen forest plot was also sampled for the density of over- and middle-story (≥ 1.5 m) aspen stems, as well as other tall trees (height ≥1.5m) within 2, belted transects, each 2x10m, centred on the linear transects. Eco-site data on slope, aspect and landscape position of each plot were also recorded. In total, 120 vegetation-sampling plots with 15 of each of the 8 vegetation types were designated (Table 4-1).

4.3.4 LIDAR Data Compilation

Assessment of the utility of using LIDAR data for characterizing vegetation was achieved by sampling all the LIDAR data within a 12m-diameter (113.1m^2) 3-D theoretical cylinder surrounding the center of each field plot (Figure 4-1 a, b). The centre of each 3-D plot was located using a Leica differential GPS unit (average accuracy 0.53m) and corresponded to the centre point of a field plot. On average, 77 ± 30 LIDAR data points were available in each plot (ranging from 32 to a maximum of 153). In total, 9045 LIDAR data points were used in the analysis of vegetation characterization.

4.4 Analysis

4.4.1 Vegetation Height Characterization Using LIDAR Data

Within each plot, the differential elevation between the first and interpolated last return (i.e., from the DEM) of each LIDAR data point was used to estimate vegetation

height (Fowler 2000). Estimations of vegetation height were initially based on several assumptions, including that the first return LIDAR data had an accuracy similar to the observed last return. Additionally, this approach assumed that the modelled DEM derived from the last return LIDAR data (as described in Chapter 3 - this volume) produced a relatively accurate representation of the ground surface. This approach had the benefit of duplicating what would typically be employed under commercial conditions, where the availability of exact elevation data for individual locations may be unavailable.

During DEM modelling in Chapter 3 (this volume and Appendix 3), last return LIDAR data were found to have an overall mean accuracy of +2 cm (RMSE = 1.21 m) across the 8 vegetation types examined. However, elevations were over-estimated within forested areas by an average of 20 cm (RMSE = 1.05 m), under-estimated (-12 cm, RMSE = 1.36 m) within grasslands (upland and lowland), and most accurate in shrublands (+7 cm, RMSE = 1.15 m). These inaccuracies suggest our capability of using LIDAR data alone to quantify vegetation height may be limited by the accuracy of the last return and its corresponding DEM. While the degree of error may have a negligible effect in estimating the height of vegetation that is tall in stature (e.g., +20 cm DEM inaccuracy in forest that is 6 m+ tall), these errors will increase in importance as the height of a target vegetation type declines (e.g., -12 cm DEM inaccuracy in grassland that is 25 cm tall). As a result, an additional analysis was done where the last return (i.e., modelled ground surface elevation) was corrected using the known DEM error for each plot obtained in the previous study, and the analysis of vegetation height repeated using these corrected data.

For the analysis of aspen forest, division lines between aspen and shrub, and between shrub and herb were determined based on field measurements of average shrub and herb height in the understory (Table 4-1). Frequency histograms were also used to assist in making these decisions (Figure 4-2). 2 values were used representing a conservative and liberal estimate of the understory distribution, including the 95% confidence interval above the mean height for separating understory shrub from the herbaceous layer and 1.5 m division line between understory shrub and overstory tree layer. Within semi-open (decadent) aspen forest, for example, mean herb height was determined to be 26 cm (Table 4-1). The upper 95% confidence interval above this value was 31 cm, which was then used as a decision-rule separating the shrub from herbaceous layers within semi-open aspen forest.

A similar method was used to establish the division line between the overstory shrub and understory herb layer within shrubland plots. Within the silverberry and western snowberry vegetation types, mean understory herb heights were 18 and 19 cm (Table 4-1), and upper 95% confidence intervals were 23 and 22 cm, respectively.

LIDAR estimated height for each vegetation layer within a plot was then determined by calculating the average height of all LIDAR points falling between the minimum and maximum for that interval, as outlined above. For the herbaceous layer of all the 8 vegetation types examined, the minimum height was set to 0 cm. For tree height, the average height of the 6 highest LIDAR points was used to estimate maximum aspen height in that plot.

LIDAR estimated heights for each vegetation layer (herb, shrub, or tree) within each vegetation type, were then regressed against their corresponding field

measurements, with each field plot representing 1 point in the correlation analysis (min. $P<0.10$). All herb and shrub field measurements per plot represented the average of 20 quadrat readings (per growth form), while tree height was obtained from the mean of 6 measurements.

4.4.2 Vegetation Cover Characterization Using LIDAR Data

Vegetation cover (leaf cover) was estimated from LIDAR measurements using canopy height by calculating the proportion of laser measurements in each height class category. This was achieved by dividing the number of laser measurements per height class by the total number of laser measurements for that plot (Figure 4-1 b). For example, closed aspen forest typically consists of stands with relatively similar tree ages, heights and diameters (Stelfox, 1995). Given that the dividing line between the tree overstory and shrub layer was established to be no more than 78cm, the proportion of first return LIDAR data points situated above 78cm was used to estimate the cover of aspen over- and middle-story. Semi-open aspen forest, however, has often undergone significant canopy break-up and subsequent understory release as well as the emergence of secondary young aspen and shrubs, resulting in a more continuous distribution of vegetation with increasing height (e.g., see Figure 4-2). As a result, K-means clustering (Lillesand and Kiefer 2000) was applied to these plots to separate this continuous vegetation into over- and middle story, as well as understory shrub and herbaceous layers. The K-means algorithm starts with an initial partition of the cases into K clusters. Subsequent steps modify the partition to reduce the sum of the distances for each case

from the mean of the cluster to which the case belongs. The modification consists of allocating each case to the nearest of the K means of the previous partition. This leads to a new partition for which the sum of distances is strictly smaller than before. The improvement step is repeated until no more significant improvements occur.

Within the aspen forest vegetation types, cover determination of the understory layers was impeded by the initial interception of LIDAR data points by the overstory tree canopy. As a result, cover determination of the shrub layer could only be estimated by removing those points intercepted by the overstory from the analysis, and calculating cover as the proportion of incoming LIDAR data points reaching the shrub layer. This procedure was then repeated for the herb layer within the understory of aspen stands.

Within shrublands and grasslands, the cover of shrub and herb layers was estimated using a procedure similar to that outlined above for aspen forest.

4.4.3 Vegetation Density Characterization Using LIDAR Data

In this study, the requirement of complete spatial coverage to analyse the whole Ranch made swath overlapping inevitable. By randomly selecting 4 km^2 of data and calculating the laser point density with increasing off-nadir distance (<50m, 50-100m, 100-150m, 150-200m and >200m, respectively), we found that contrary to our expectations, the intensity of LIDAR sampling increased with off-nadir distance (e.g., densities of 0.42, 0.47, 0.59, 0.69 and 0.71 points/m^2, respectively). The linear feature of the number of LIDAR hits (based on off-nadir distance) did not confirm to the circular patch characteristics of the actual vegetation. Also, the relatively sparse LIDAR sampling density ($\overline{X}$ = 0.54 points/m^2) limited the utility of using LIDAR density to

directly examine tree density.

Instead, an alternative approach was used to assess tree density. Natural thinning in aspen development generally decreases tree density (Peterson and Peterson 1995) and changes the cover of over- and middle-story within aspen forest. Because LIDAR estimated cover was a good predictor of actual field tree cover, the changes in tree density were assumed to reflect corresponding changes in LIDAR estimated cover. LIDAR-derived cover was therefore hypothesized to be sufficiently accurate ($P<0.10$) to facilitate its use in further characterizing tree density. Specific analysis included estimating the density of (1) live aspen over-story trees, (2) live aspen over- and middle-story trees, and (3) the total tree over- and middle-story density, including live and dead stems using LIDAR estimated cover.

4.4.4 Assessment of LIDAR Intensity Data

Intensity is defined as the ratio of strength of reflected light to that of emitted light, and is influenced mainly by the reflectance of the target object. Reflectance varies with material characteristics as well as the light used. Influential ground factors (e.g., soil, litter, vegetation and moisture) are known to vary among different vegetation communities, as well as among different vegetation growth forms (Song *et al.* 2002). As a result, we hypothesized different vegetation communities or growth forms would result in detectable variation in LIDAR sample intensity. This hypothesis was tested by (1) comparing LIDAR intensity among the 8 vegetation types described above, (2) correlating LIDAR-derived height with its intensity to evaluate whether sample intensity

may vary among different layers of growth forms within each of the 8 plant communities (e.g., trees vs shrubs vs herbs in aspen forests), and (3) correlating mean LIDAR data intensity of a growth form with its actual field cover.

Finally, at the landscape level, vegetation patchiness reflects the inherent variation of vegetation height and physiognomy (Rietkerk *et al.* 2000). This was also tested by correlating the standard deviation of measured field vegetation height with the variation in LIDAR intensity at the individual plot level.

4.5 Results

4.5.1 Vegetation Height Assessment Using LIDAR Data

Within aspen forest, LIDAR data were found to be effective for characterizing aspen height within both closed (i.e., young or mature) (R^2=0.93, P<0.01) and semi-open (i.e., decadent) (R^2=0.90, P<0.01) aspen forest (Table 4-2, Figure 4-3). However, LIDAR data were not accurate for quantifying the height of their understory shrub (R^2=0.00, P=0.97) or herb (R^2=0.10, P=0.28) strata, even within semi-open aspen forest.

When applied to the 2 shrublands (ENS and SPS), LIDAR data had limited utility for quantifying shrub height within the silverberry community (R^2=0.21, P=0.09, Table 4-2). In contrast, neither western snowberry nor herb height could be estimated (P>0.10) within any shrubland (Table 4-2).

Within the 4 herbaceous vegetation types (2 upland grasslands and 2 lowland meadows), no significant (P>0.10) associations were found between the field measured and LIDAR estimated vegetation height (Table 4-2). Estimations of vegetation height

from LIDAR data were typically overestimated ($\overline{X}$ = +6 ± 5 cm) within mixed prairie type, but underestimated within the fresh ($\overline{X}$ = -35 ± 17 cm) and saline ($\overline{X}$ = -16 ± 14 cm) riparian meadows.

In the DEM accuracy analysis in Chapter 3 (this volume), LIDAR data were found to under-estimate the actual elevations of the 4 herbaceous vegetation types. When the corrected DEM was applied to the height estimations of these 4 herbaceous vegetation types, their vegetation heights were found to be further under-estimated (e.g., $\overline{X}$ = -6 ± 5 cm and $\overline{X}$ = -28 ± 14 cm for the mixed prairie and saline riparian meadow, respectively), rather than improved.

4.5.2 Vegetation Cover Characterization Using LIDAR Data

As with height, the LIDAR data estimate of canopy cover ($0 \leq X \leq 100$, %) within closed (Eq. 4.1) and semi-open (Eq. 4.2) aspen forest was significantly correlated to the actual cover measurement ($0 \leq Y \leq 100$, %):

$Y=126-0.0297X^2+0.0003X^3$; $R^2=0.61$, $F=9.32$, $P<0.01$..... (Eq. 4.1)

$Y=EXP\ (4-12.264/X)$; $R^2=0.84$, $F=63.35$, $P<0.01$..... (Eq. 4.2)

Within the 2 shrublands, however, no significant relationships were identified between the LIDAR estimated and field measured cover ($P>0.10$). LIDAR data were typically found to overestimate the cover of the herb layer, but underestimate the cover of overlying shrubs (Figure 4-5).

Among the 4 upland grassland and lowland meadow community types, LIDAR

data generally underestimated the herb cover present, by as much as 14% in the fescue grassland type (Figure 4-6).

4.5.3 Density Analysis Using LIDAR Data

In closed aspen forest, LIDAR estimated cover ($0 \leq X$, %) was found to have a significant relationship with field measured tree density (trees above 1.5m in height) ($0 \leq Y$, # stems/40m^2), including live and dead trees in both the mid- and overstory (Eq. 4.3 to 4.5).

a) Live aspen over-story density estimation:

$Y=1011*(X)^{-1.908}$; $R^2=0.66$, $P<0.01$..... (Eq. 4.3)

b) Live aspen middle and over-story density estimation:

$Y=303*(X)^{-1.120}$; $R^2=0.54$, $P=0.01$..... (Eq. 4.4)

c) Total middle and over-story vegetation density (live and dead) estimation:

$Y=754*(X)^{-1.443}$; $R^2=0.76$, $P=0.01$..... (Eq. 4.5)

Within semi-open aspen forest, LIDAR estimated cover was only found to be significantly ($P=0.02$) correlated to the total density of live and dead trees (Eq. 4.6).

$Y=10.156*EXP(0.147X)$; $R^2=0.40$, $P=0.02$..... (Eq. 4.6)

4.5.4 Assessment of LIDAR Intensity Data

In comparing the 8 vegetation types, it was found that LIDAR sampling intensity (unit: %) could be used to separate both closed ($\overline{X} = 15 \pm 15\%$) and semi-open ($\overline{X}$ =

27 ± 23%) aspen forest from other vegetation types (e.g., fescue grassland $\overline{X}$ = 52 ± 19%) using the mean and std. dev. information. In contrast, shrublands could not be separated from herbaceous communities using intensity data, and neither of the 2 shrublands nor the 4 herbaceous communities could be separated within their own formations (e.g., western snowberry from silverberry). Additionally, closed aspen forest could not be separated from semi-open aspen forest (Table 4-3).

Neither the LIDAR-derived height nor cover information could be associated with LIDAR intensity to separate different growth forms (i.e., physiographic strata) within any of the 8 plant communities ($P>0.10$). In other words, it was impossible to detect patterns in the proportion of lower and higher intensity LIDAR data reflected from different vegetation layers (e.g., shrub or herb) (Figure 4-7). However, the variance of predicted vegetation height was significantly correlated ($P<0.10$) with the variance of LIDAR intensity data in several vegetation types, including fresh riparian meadows ($R^2=0.44$, $P=0.01$) (Table 4-4 and Figure 4-8) and western snowberry shrublands ($R^2=0.32$, $P=0.03$) (Table 4-4).

Unique LIDAR intensity patterns in relation to sampling height were also identified among the 8 vegetation types based on observed histograms. Closed and semi-open aspen forests displayed a downward exponential pattern (i.e., greater intensities at lower heights) with some distortion in the semi-open aspen forest (Figure 4-7 a, b). Most of the LIDAR data had intensity values less than 20 or 30% within the closed and semi-open aspen forest, respectively. The 2 upland grasslands (Figure 4-7 e, f) and shrublands (Figure 4-7 c, d) were all observed to have bimodal patterns. Though the 2 riparian meadows (Figure 4-7 g, h) also had bimodal patterns, these were distorted and showed

trends of a downward exponential pattern. With the exception of aspen forests, other vegetation types consistently had intensity values greater than 30%.

4.6 Discussion

In our analysis to quantify vegetation characteristics, LIDAR data were found to be effective predictors of vegetation height of aspen forest overstory within both closed and semi-open communities. This was consistent with findings made by Magnussen and Boudewyn (1998) as well as Næsset (1997), who concluded the average maximum height of LIDAR data was a good predictor of field tree height in conifer stands in British Columbia and Norway, respectively. However, unlike Magnussen *et al.* (1999), whose observations were sampled with a probability proportional to displayed crown area and derived from the probability that a laser beam penetrates to a given canopy depth through gaps, no height recovery models were applied in our study. Because determining vegetation height requires differencing the estimated canopy elevation from the estimated surface elevation (Means *et al.* 2000), data collected in leaf-on conditions as we did may be ideal for determining canopy elevation but not ground elevation. Conversely, leaf-off conditions may not provide good estimates of canopy height. The definitive determination of whether a returned pulse is actually the "bald earth" or above-ground cover is still an area of intense research (Hodgsona *et al.* 2003). The recovery models of Magnussen *et al.* (1999) are ideal for analysis of individual trees, which require intensive correction for each measurement, and are therefore less suitable for the study of large areas.

The incapability of using LIDAR data to accurately quantify understory

vegetation height in aspen forest exemplified the limitations of the small-footprint LIDAR we used in leaf-on conditions, because only a small proportion of LIDAR data points penetrated through gaps to the understory. The low number of LIDAR data points penetrating the understory of shrub and herb strata of aspen forests through gaps made the cover estimation of these layers impractical. For example, the mean number of LIDAR data points originating from the shrub and herb layers were only 10 and 8 per plot, respectively, within closed aspen forest. On more open forest plots, these increased to only 26 and 17, respectively. Additionally, the complex interaction of an often angular laser pulse inside vertically distributed vegetation is a concern when trying to determine the exact point of reference for a time-of-flight (small footprint) laser sensor (Flood 2001).

The marked progressive decrease in accuracy of LIDAR data for quantifying vegetation height from aspen forests, upland shrublands, to upland grasslands and lowland meadows was in part, likely due to the increase in DEM error relative to the actual vegetation height being assessed. A constant level of DEM error among vegetation types would introduce greater error in the final prediction accuracy of low structured vegetation compared to taller aspen stands. This might explain why there was no statistical difference between the ground and laser height measurements at the 5% level of probability in sagebrush communities (mean > 30 cm) by Ritchie et al. (2001), but significant differences existed in our mixed prairie and fescue grasslands, whose average vegetation height was about 10cm. Notably, these problems could not be overcome by correcting for the inherent DEM error among vegetation types. Vertical resolution of LIDAR within 20 cm might also be the reason for the over- or under-

estimation of the low structured vegetation. LIDAR estimated height is random regardless of true vegetation height with this 20 cm error range (Figure 4-4, 4-5, and 4-6). Flood (2001) also encountered difficulty in using algorithms to accurately extract the ground surface in areas of low, dense ground cover. For example, a small error of 30cm in the DEM would be negligible in aspen forest, whose average vegetation height was about 9m. In contrast, this degree of error would greatly magnify inaccuracies of herb height within Aspen Parkland upland grasslands. The overestimation of vegetation height in the mixed prairie community was probably also due to the error of DEM interpolation. Most of the mixed prairie communities occupied steep slopes, landscape positions that usually produced the greatest distortion of the DEM (Chapter 3 – this volume).

LIDAR measurements in our analysis significantly underestimated the height of both shrublands, as well as that of 3 of the 4 herbaceous communities (fescue grasslands as well as the fresh and saline riparian meadows). This was consistent with the findings of Ritchie *et al.* (2001), Aldred and Bonner (1985) as well as Weltz *et al.* (1994). Those studies found that laser systems consistently underestimated the height of shrubs and herbs (mainly sagebrush, desert zinnia and gramma grass, respectively). The underestimation was attributed to field measurements being made on total plant height whereas LIDAR measurements typically intersect the sides or "shoulders" of plant canopies (Weltz *et al.* 1994). Indeed, in retrospect this was likely a problem in our investigation as well, because all height measurements assessed maximum rather than median plant height.

The difference in time of data collection could be another contributing factor

limiting our analysis. LIDAR data were collected in early October of 2000 when vegetation, especially herbs, had become predominantly dormant. Field vegetation sampling however, was conducted in July or August of 2001 when vegetation was still in a vigorous growth stage. Perhaps most important, herbaceous communities are prone to rapid changes in biomass and height with other disturbances, including livestock grazing. The fresh riparian meadows, for example, had a mean height of 48 cm at the time of field measurement, but were estimated to be only 10 cm based on the October collected LIDAR data. This difference may well be due to changes in plant growth and/or disturbances such as grazing between years rather than accuracy limitations, although this problem is less likely for shrublands.

Similar to vegetation height characterization, LIDAR data's ability to quantify vegetation cover was also influenced by the collective error of DEM interpolation, equipment operation, and time of data collection. Weltz *et al.* (1994) cautioned against canopy cover estimation from laser data for vegetation with a height less than 30cm (Appendix 4). Many of the herbaceous and shrub communities had a height less than 30cm at the time of LIDAR data collection in early October, and given the low accuracies of cover estimation, this supported the assertion of Weltz *et al.* (1994). Within shrubland, assessing cover in October near the time of leaf fall would also complicate comparison to July or August field data. These differences undoubtedly further impaired our assessment of the utility of using LIDAR data for quantifying vegetation cover in shrublands. Background noise (i.e., signals returning back to a sensor that are emitted from other sources such as those from natural light) to the LIDAR measurement in these plant communities may have been another significant contributing factor. Weltz *et al.*

(1994) concluded that, "the over- or under-estimation of canopy cover in sparsely populated shrub and low height herbaceous communities will not be resolved unless new techniques are available to discriminate the background noise in the laser return signal".

Also, the field sampling distribution might be a contributing factor. In Ritchie *et al.*'s (2001) experiment, the ground data was an average for 6, 30-m transects while the laser data was the average of 3, 1-km transects. In our analysis, measures by laser and ground techniques were compared plot by plot using a high precision differential – GPS system. Ritchie *et al.* (2001) also found canopy cover measured by laser and ground techniques in the Wyoming big sagebrush vegetation differed significantly, but unlike the underestimation of shrub and herb cover in our analysis, they found the laser measure of cover (38.1 ± 21.1 cm) was twice that of the ground measurement.

The negative correlation between field measured vegetation density and LIDAR predicted cover in aspen forest (Eq. 4.3, 4.4 and 4.5) reflected the common phenomenon of vegetation thinning in aspen stands. With increasing stand age, intense competition leads to self-thinning over time (Peterson and Peterson 1995). The greater R^2 in Eq. 4.5 demonstrated that when all live and dead trees were counted together for the over- and mid- stories, they accounted for more of the variance in LIDAR cover data. In other words, LIDAR cover data were more closely associated with the density of all tree stems, regardless of whether they were live or dead. Unlike closed aspen forest, the less consistent positive association between LIDAR cover and measured tree density in semi-open aspen forest (Eq. 4.6) probably reflected understory tree regeneration in those stands following canopy opening. Although the derivation of density information from cover data may be less meaningful ecologically, the link is nevertheless important for the

potential use of LIDAR data on assessing tree density, both live and dead. For example, this finding has implications for inventorying insect- or fire-killed stands of forest vegetation.

The identification of unique LIDAR intensity distribution patterns, including the downward exponential frequency distribution patterns of aspen forests and the bimodal patterns of herbaceous and shrub communities, were inconsistent with Fowler (2000), who claimed that if a vegetation type (e.g., shrubland) were uniformly present, the intensity would be uniform as well. This inconsistency might simply reflect that all our plant communities were not homogeneous despite their appearance to the contrary.

Variation in LIDAR intensity with vertical height, however, was consistent with the findings made by Brock *et al.* (2001), who concluded LIDAR intensity generally decreased as points moved from the ground to the canopy of vegetation in a forest site. The comparatively lower LIDAR intensity values of the 2 aspen forests relative to the other vegetation types were probably due to (1) aspen forest having lower reflectance compared to the other vegetation types, or (2) the other vegetation types having far more reflectance from the ground, which was dry and would have had greater reflectance in early October. The incapability of using LIDAR intensity data to separate different growth forms within any shrubland or herbaceous community indicated both high and low reflectance materials existed in each herbaceous and ground layer within grasslands, or in each shrub and herbaceous layer within shrublands. This might represent the co-existence of dark litter and brighter leaves in each vegetation growth form within a plant community, or it could be the effect of more complicated reflectance, scattering or refraction. Background noise might once again be another limiting factor.

4.7 Conclusion

Land surface and vegetation properties are key for understanding range condition. Ground-based measurements of these properties are difficult and time-consuming. Scanning airborne laser altimeter systems mightbe an alternative method to synoptically quantify vegetation features and properties over large land areas. The agreement between airborne laser altimeter and observed field measurements in vegetation height, cover and density within both closed and semi-open aspen forest indicated this technology is useful for characterizing some forest vegetation properties. The capability of using LIDAR data to quantify understory vegetation characteristics, as well as those of individual shrublands and grasslands, however, was far more limited. Precision accuracies from using LIDAR data could likely be improved if the collective error from LIDAR-derived DEM development, equipment operation or time of data collection could be reduced.

LIDAR intensity data appeared to reflect the material characteristics of objects. While LIDAR intensity does not conform to theoretical reflectance of materials, it does follow relative magnitudes of reflectance. For example, dry land usually has greater reflectance compared to vegetation with more moisture content. Aspen forest has lower reflectance compared to shrubland and grassland. However, more testing will be needed to design and understand LIDAR signals before intensity data are useful for characterizing vegetation more reliably.

Overall, these results support the utility of using LIDAR data for forest characterization in the Aspen Parkland, with limited applications for assessing other

vegetation types that constitute 50-80% of the area. With technology advancement, LIDAR measurements may further improve our ability to quantify vegetation characteristics of shrublands and herblands so that improved management practices and structures can be developed to manage spatially diverse and complex rangelands more effectively. Laser-distancing technology from airborne platforms provides useful data not only for modelling land surface topography (Krabill *et al.* 1984, Ritchie *et al.* 1993b, Chapter 3 – this volume), but also for understanding vegetation properties (Schreier *et al.* 1985, Nelson 1997, Ritchie *et al.* 1992 and 1993a, Chapter 4 – this volume) for large areas. For some vegetation types, profiling and scanning airborne laser systems therefore appear to be an effective alternative to the use of traditional ground-based point measurements, which are difficult and time-consuming to undertake.

4.8 Literature Cited

Aldred, A. H. and G. M. Bonner 1985. Application of airborne laser to forest surveys, Information Report PI-X-51. Canadian Forest Services, Petawawa National. Forest Institute, Chalk River, Ontario.

Asamoah, S. A., E. W. Bork, B. D. Irving, M. A. Price, and R. J. Hudson. 2003. Cattle herbage utilization patterns under high-density rotational grazing in the Aspen Parkland. *Canadian Journal of Animal Science*. 83:541-550.

Bailey, A.W. and R.A. Wroe. 1974. Aspen invasion in a portion of the Alberta parklands. *Journal of Range Management* 27:263-266.

Benedict, N.B. 1982. Mountain meadows: stability and change. *Madroño* 29:148-53.

Brock, J.C., A.H. Sallenger, W.B. Krabill, R.N. Swift, and C.W. Wright. 2001. Identification and mapping of barrier island vegetation with NASA airborne topographic mapper LIDAR surveys. In *International Airborne Remote Sensing Conference and Exhibition*, 5th, San Francisco, September 17-20.

Campbell, C., I.D. Campbell, C.B. Blyth, and J.H. McAndrews. 1994. Bison extirpation may have caused aspen expansion in western Canada. *Ecography* 17:360-362.

Clements, F.E. 1916. Plant Succession. Carnegie Institute Publication 242, Washington.

Coupland, R.T. 1961. A reconsideration of grassland classification in the northern Great Plains of North America. *Journal of Ecology* 49:135-167.

Daubenmire, R. F. 1959. Plants and environment. John Wiley & Sons, Inc., New York, New York.

Dubayah, R., J. B. Blair, J. L. Bufton, D. B. Clark, J. JaJa, R. G. Knox, S. B. Luthcke, S. Prince, and J. F. Weishampel. 1997. The Vegetation Canopy LIDAR mission (pp100-112). In *Land Satellite Information in the Next Decade II: Sources and Applications.* American Society for Photogrammetry and Remote Sensing, Bethesda, Maryland.

Dyksterhuis, E. J. 1949. Condition and management of range land based on quantitative ecology. *Journal of Range Management* 2:104-115.

Flood, M. 2001. Laser altimetry: from science to commercial LIDAR mapping. *Journal of Photogrammetric Engineering and Remote Sensing* 67:1209-17.

Fowler, R. A. 2000. The low down on LIDAR. *Earth Observation Magazine* 9:1-7.

Hodgsona, M.E., J.R. Jensena, L.Schmidtb, S.Schillc, and B. Davisd. 2003. An evaluation of LIDAR- and IFSAR-derived digital elevation models in leaf-on conditions with USGS Level 1 and Level 2 DEMs. *Remote Sensing of Environment* 84:295-308.

Johnson, D., L. Kershaw, A. MacKinnon, and J. Pojar 1995. Plants of the western boreal forest & aspen parkland. Lone Pine publishing and the Canadian Forest Serivce, Edmonton, Alberta.

Krabill, W.B., J.G. Collins, L.E. Link, R.N. Swift, and M.L. Butler. 1984. Airborne laser topographic mapping results. *Journal of Photogrammetric Engineering and Remote Sensing* 50:685-694.

Lillesand, M. T. and R. W. Kiefer 2000. Remote sensing and image interpretation (4th edition). John Wiley and Sons, Inc, New York, New York.

Magnussen, S., P. Eggermont, and V.N. LaRiccia. 1999. Recovering tree heights from airborne laser scanner data. *Forest Science* 45:407–22.

Magnussen, S. and P. Boudewyn. 1998. Derivations of stand heights from airborne laser scanner data with canopy-based quantile estimators. *Canadian Journal of Forest Research* 28:1016-31.

Means, J. E., S. A. Acker, B. J. Fitt, M. Renslow, L. Emerson, and C. J. Hendrix. 2000. Predicting forest stand characteristics with airborne scanning LIDAR. *Photogrammetric Engineering and Remote Sensing* 66:1367-71.

National Research Council. 1994. Rangeland health: New methods to classify, inventory and monitor rangelands. National Academy Press, Washington, DC.

Næsset, E. 1997. Determination of mean tree height of forest stands using airborne laser scanner data. *ISPRS Journal of Photogrammetry and Remote Sensing* 52:49-56.

Nelson, R. 1997. Modeling forest canopy heights: The effect of canopy shape. *Remote Sensing of Environment* 60:327-334.

Optech Incorporated. 2003. About laser RADAR. http://www.optech.on.ca /aboutlaser.htm.

Pachepsky, Y.A. and J.C. Ritchie. 1998. Seasonal changes in fractal landscape surface roughness estimated from airborne laser altimetry data. *International Journal of Remote Sensing* 19:2509-2516.

Peterson, E. B. and N. M. Peterson 1995. Aspen managers' handbook for British Columbia. Joint publication of the Canadian Forest Service and the British Columbia Ministry of Forests.

Rietkerk, M., P. Ketner, J. Burger, B. Hoorens and H. Olff. 2000. Multiscale soil and vegetation patchiness along a gradient of herbivore impact in a semi-arid grazing system in West Africa. *Plant Ecology* 148:207-224.

Rignot, E., J. Way, C. Williams, and L. Viereck. 1994. RADAR estimates of aboveground biomass in boreal forests of interior Alaska. *IEEE Transactions on Geoscience and Remote Sensing* 32:1117-24.

Ritchie, J.C., J.H. Everitt, D.E. Escobar, T.J. Jackson, and M.R. Davis. 1992. Airborne laser measurements of rangeland canopy cover. *Journal of Range Management* 45:189-193.

Ritchie, J.C., D.L. Evans, D.M. Jacobs, J.H. Everitt, and M.A. Weltz. 1993a. Measuring canopy structure with an airborne laser altimeter. *Transactions of the ASAE* 36:1235-1238.

Ritchie, J.C., T.J. Jackson, E.H. Grissinger, J.B. Murphey, J.D. Garbrecht, J.H. Everitt,

D.E. Escobar, M.R. Davis, and M.A. Weltz. 1993b. Airborne altimeter measurements of landscape properties. *Journal of Hydrology Science* 38:403-416.

Ritchie, J. C., M. S. Seyfried, M. J. Chopping, and Y. Pachepsky. 2001. Airborne laser technology for measuring rangeland conditions. *Journal of Range Management* 54: A8-21.

Scheffler, E.J. 1976. Aspen vegetation in a portion of the east central Alberta parklands. M.Sc. Thesis. University of Alberta.

Schreier, H., J. Lougheed, C. Tucker, and D. Leckie. 1985. Automated measurement of terrain reflection and height variations using an airborne infrared laser system. *International Journal of Remote Sensing* 6:101-113.

Smith, A. M., D. J. Major, M. J. Hill, W. D. Willms, B. Brisco, and C. W. Lindwall. 1994 Airborne synthetic aperture RADAR analysis of rangeland revegetation of a mixed prairie. *Journal of Range Management* 47:385-391.

Song, J.H., S.H. Han, K. Yu, and Y. I. Kim. 2002. Assessing the possibility of land-cover classification using LIDAR intensity data. In *ISPRS Commission III, Symposium* 2002. September 9 - 13, Graz, Austria.

Stelfox, J. B. (editor) 1995. Relationship between stand age, stand structure, and biodiversity in aspen mixedwood forests in Alberta. Jointly published by Alberta Environmental Centre (AECV95-R1), Vegreville, AB, and Canadian Forest Service (Project No. 0001A), Edmonton, Alberta.

St-Onge, B., J. Dufort, and R. Lepage. 2000. Measuring tree height using scanning laser altimetry (pp425-32). In *Proceedings of the 22nd Annual Canadian Remote Sensing Symposium*. Victoria, British Columbia.

Thomas, L. and F. Juanes. 1996. The importance of statistical power analysis: an example from Animal Behaviour. *Animal Behaviour* 52: 856-859.

Trottier, G.C. 1986. Disruption of rough fescue, Festuca hallii, grassland by livestock grazing in Riding Mountain National Park, Manitoba. *Canadian Field Nature* 100:488-495.

Tueller, P. T. 1989. Remote sensing technology for rangeland management applications. *Journal of Range Management* 42:442-453.

Waring, R.H, J. Way, E.R. Hunt, L. Morrissey, K.J. Ranson, J.F. Weishampel, R. Oren, and S.E. Franklin. 1995, Imaging RADAR for ecosystem studies. *BioScience* 45:715–723.

Weltz, M.A., J.C. Ritchie, and H.D. Fox. 1994. Comparison of laser and field measurements of vegetation heights and canopy cover. *Water Resources Res*earch 30: 1311-1320.

West, N.E. and E.L. Smith. 1997. Improving the monitoring of rangelands. *Rangelands*, 19:9-14.

Wheeler G. W. 1976. Some grassland and shrubland communities in the parklands of central Alberta. Master thesis, Edmonton, Alberta.

Wright, H. A. and A. W. Bailey. 1982. Fire ecology: United States and Southern Canada. John Wiley & Sons, New York, New York.

4.9 Tables and Figures

Table 4-1 Height and cover characteristics of the 8 vegetation types based on field sampling in July 2001.

Vegetation Type[1]	Plots (#)	Herb		Shrub		Tree		
		Height (cm)	Cover (%)	Height (cm)	Cover (%)	Height (m)	Density (#)	Cover (%)
FRM	15	48 (24-88)	83.5 (63-100)					
SRM	15	24 (8-49)	68.2 (41-87)					
FSG	15	12 (1-44)	63.3 (33-81)					
SEG	15	5 (1-12)	51.8 (6-91)					
SPS	15	19 (8-81)	25.9 (6-52)	45 (25-73)	40.6 (23-69)			
ENS	15	18 (8-41)	40.5 (13-77)	79 (44-122)	35.0 (5-96)			
CAF	15	29 (5-86)	15.4 (1-45)	67 (29-94)	26.2 (8-55)	8.48 (5.01-19.25)	41.1 (14-84)	81.7 (61-96)
OAF	15	26 (16-44)	19.2 (2-27)	62 (40-106)	27.0 (10-43)	9.52 (5.24-15.72)	28.3 (11-83)	37.0 (20-48)
Mean		23	46	63	32.2	9	34.7	59.4

[1]FRM – fresh riparian meadow, SRM – saline riparian meadow, FSG – fescue grassland, SEG – mixed prairie grassland, SPS – western snowberry, ENS – silverberry, CAF – closed aspen forest, OAF – semi-open aspen forest.

Table 4-2 Association between LIDAR measured and field sampled mean vegetation height (m).

Closed aspen forest over- and middle-story	Y=1.2029X-1.7816[1]	**R^2=0.93 P<0.01**
Closed aspen forest understory shrub layer (<1.5 m)	Y=0.0652X+0.7184	R^2=0.00 P=0.97
Closed aspen forest understory herbaceous layer (<0.3m)	Y=-0.5950 X+0.3359	R^2=0.10 P=0.28
Semi-open aspen forest over- and middle-story	Y=1.0048X-0.0837	**R^2=0.90 P<0.01**
Semi-open understory shrub layer (<1.5 m)	Y=0.7141X+0.3380	R^2=0.23 P=0.13
Semi-open understory herbaceous layer (<0.31m)	Y=-0.0957X+0.2758	R^2=0.00 P=0.86
Western snowberry shrub layer	Y=0.0083X+0.4485	R^2=0.00 P=0.98
Western snowberry herbaceous layer	Y=0.0076X+0.1646	R^2=0.00 P=0.99
Silverberry shrub layer	Y=0.5187X+0.5786	**R^2=0.21 P=0.09**
Silverberry herbaceous layer	Y=0.3813X+0.1343	R^2=0.02 P=0.64
Fescue grassland	Y=0.7348X+0.0517	R^2=0.02 P=0.58
Mixed prairie grassland	Y=0.1407X+0.0385	R^2=0.02 P=0.64
Fresh riparian meadow	Y=0.4231X+0.4105	R^2=0.00 P=0.83
Saline riparian meadow	Y=1.4922X+0.1128	R^2=0.06 P=0.38

[1]X-field measured vegetation height (m), Y-LIDAR estimated vegetation height (m).

Table 4-3 Mean LIDAR sampling intensity among different vegetation types.

Vegetation Type	Mean (95% CI) (%)	Deviation (%)
Mixed prairie grassland	45.7 (43.6-47.9)	16.5
Fescue grassland	52.6 (50.0-55.2)	18.1
Closed aspen forest	23.5 (13.7-27.6)	53.5
Semi-open aspen forest	29.4 (21.7-35.9)	33.4
Western snowberry	49.9 (46.5-53.1)	17.4
Silverberry	47.6 (45.3-49.9)	17.3
Saline riparian meadow	51.3 (42.4-59.5)	18.2
Fresh riparian meadow	47.1 (42.0-53.0)	18.4

Table 4-4 Association of LIDAR sampling intensity with field measured vegetation patchiness.

Vegetation Type	Assessment Formula	Significance
Silverberry	Y=26.645X2-20.121X+20.610[1]	**R^2=0.40 P=0.06**
Western snowberry	Y=EXP(3.071-.035/X)	**R^2=0.32 P=0.03**
Mixed prairie grassland	Y=-184.448X2+27.050X+15.761	R^2=0.27 P=0.15
Fescue grassland	Y=16.303X+17.392	**R^2=0.25 P=0.058**
Fresh riparian meadow	Y=51.0317X+14.2134	**R^2=0.44 P=0.01**
Saline riparian meadow	Y=0.095/X	R^2=0.15 P=0.17

[1]X: standard deviation of 40 height measurements in a plot; Y: standard deviation of all LIDAR data intensities positioned in that plot.

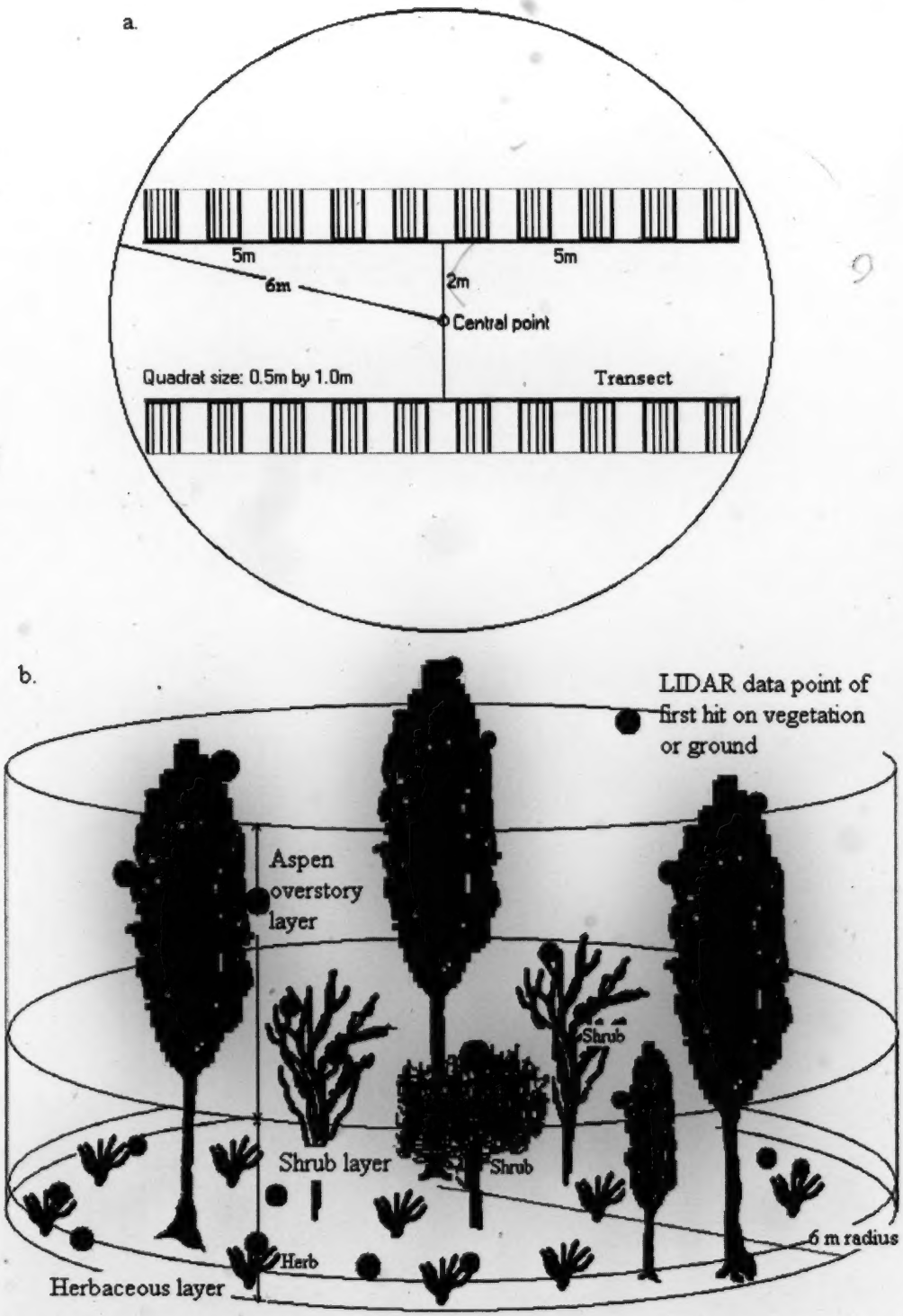

Figure 4-1 Field vegetation and LIDAR data sampling diagram in 2-dimension (a) and 3- dimension (b).

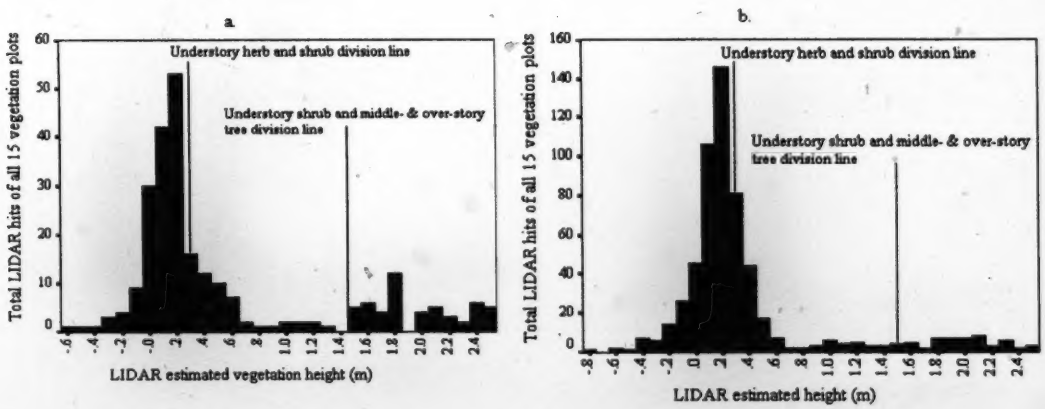
a
Understory herb and shrub division line
Understory shrub and middle- & over-story tree division line
Total LIDAR hits of all 15 vegetation plots
LIDAR estimated vegetation height (m)
b.
Understory herb and shrub division line
Understory shrub and middle- & over-story tree division line
Total LIDAR hits of all 15 vegetation plots
LIDAR estimated height (m)

Figure 4-2 Estimated height division lines between herb and shrub layers, and between shrub and tree layers in closed (a) and semi-open (b) aspen forest.

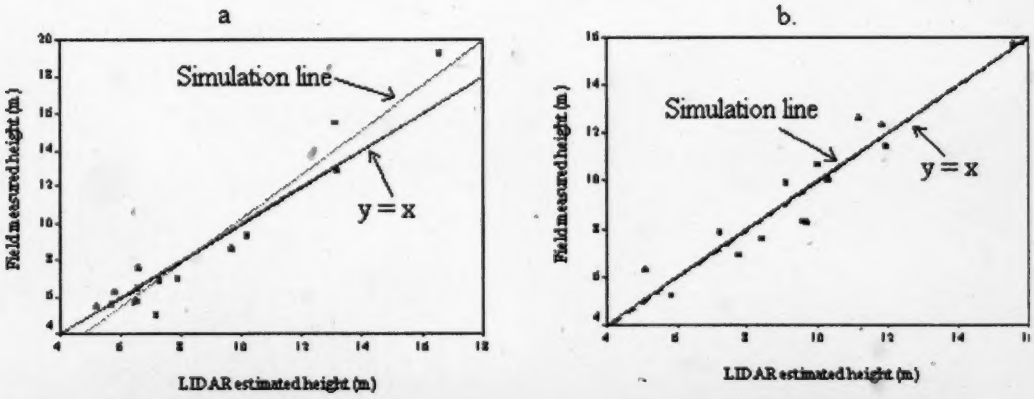

Figure 4-3 Association of LIDAR estimated height with field measured vegetation height within closed (a) and semi-open (b) aspen forest. The field measured vegetation height on the Y-axis was the mean of 6 field height measurements; the LIDAR estimated vegetation height on the X-axis was the mean of 6 tallest LIDAR data points within the same plot.

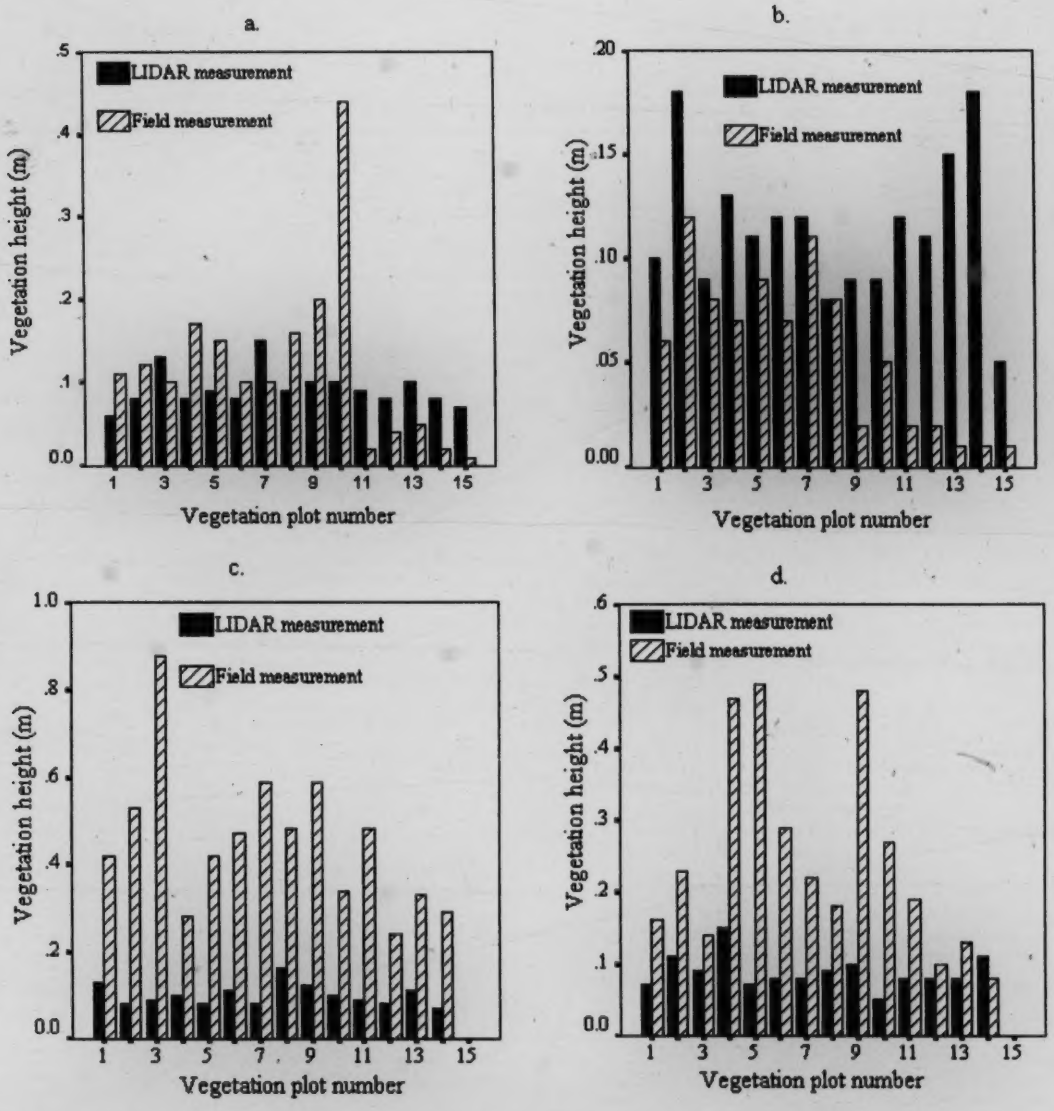

Figure 4-4 Plot by plot comparison between LIDAR estimated and field measured vegetation height within the 4 herbaceous communities, including fescue (a) and mixed prairie (b) grasslands, as well as fresh (c) and saline (d) riparian meadows.

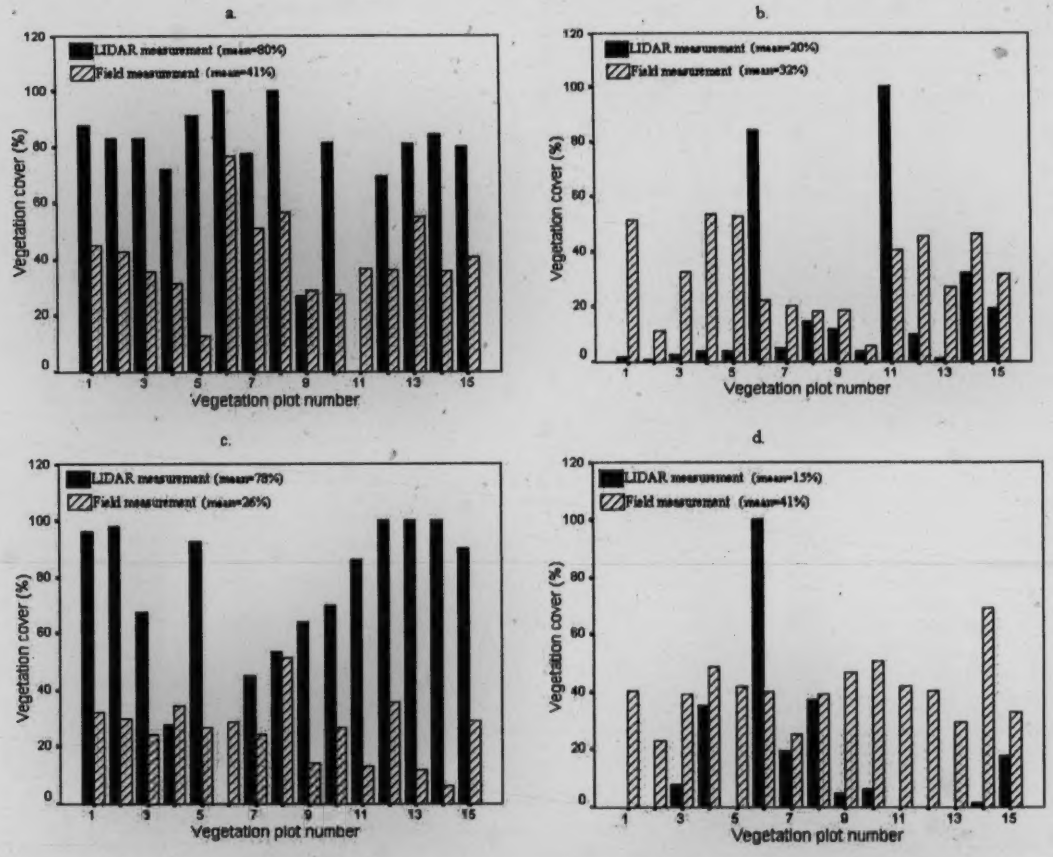

Figure 4-5 Plot by plot comparison between LIDAR estimated and field measured vegetation cover within the 2 shrublands, including herbaceous (a) and shrub (b) layers in the silverberry community, and herbaceous (c) and shrub (d) layers in the western snowberry community.

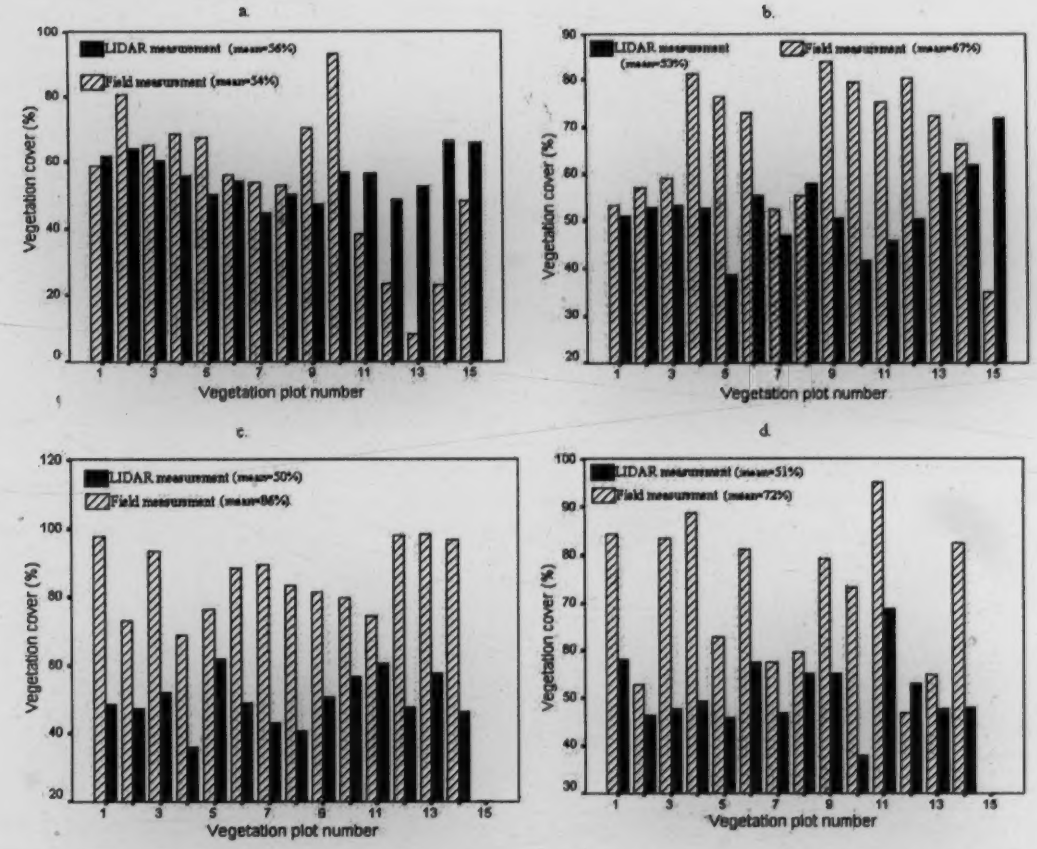

Figure 4-6 Plot by plot comparison between LIDAR estimated and field measured vegetation cover within the 4 herbaceous vegetation types, including mixed prairie (a) and fescue (b) grasslands, as well as fresh (c) and saline (d) riparian meadows.

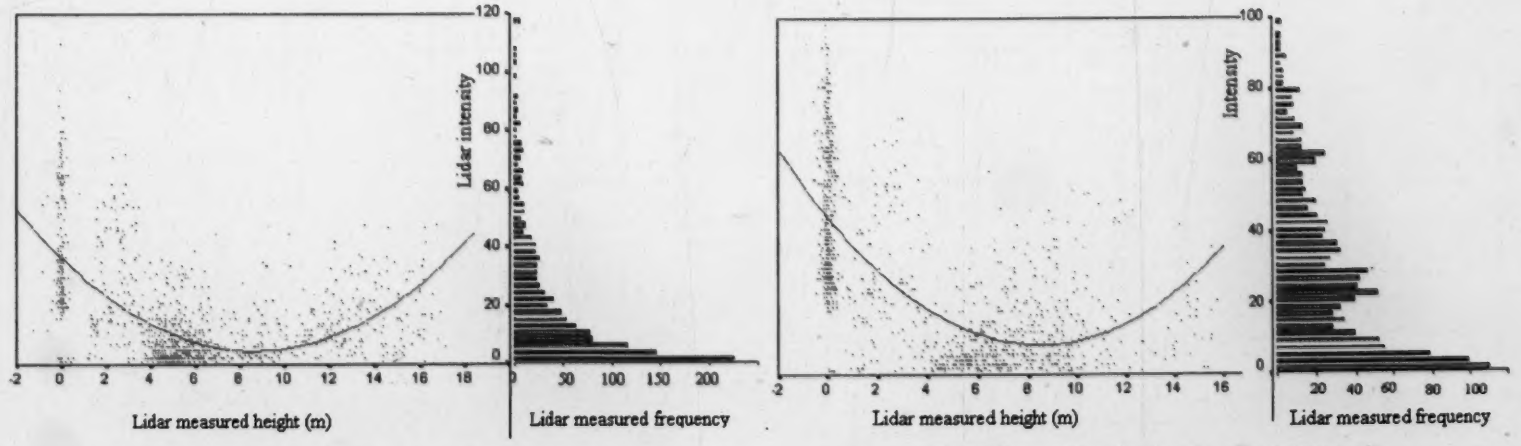

a. Closed (young and mature) aspen forest (1218pts)

b. Semi-open (decadent) aspen forest (1221pts)

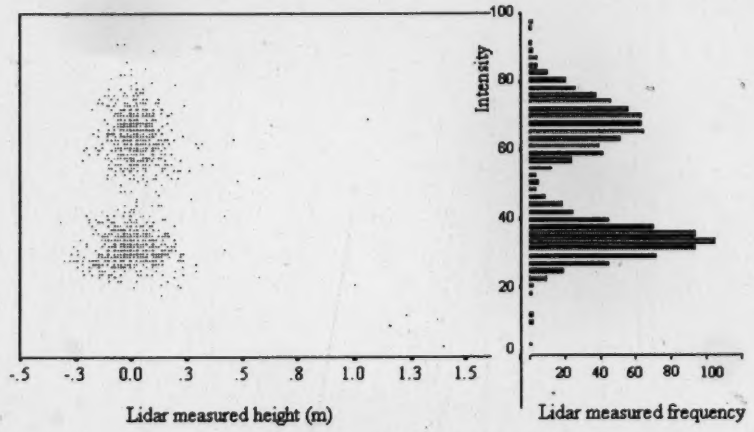

c. Elaeagnus vegetation type (1179pts)

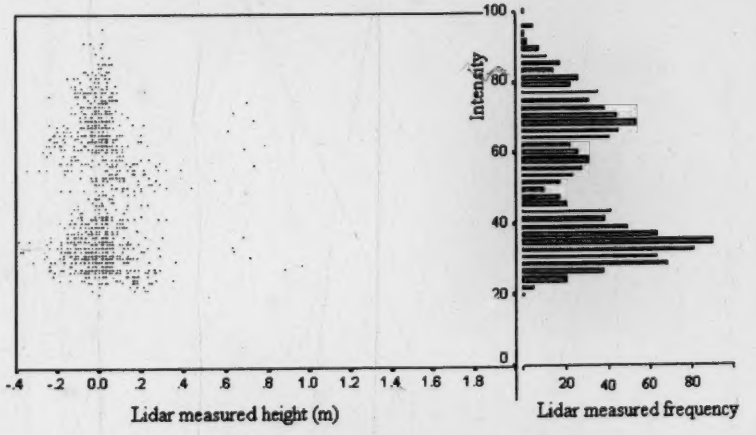

d. Symphoricarpos vegetation type (1142pts)

Figure 4-7 Association between LIDAR estimated vegetation height (m) and individual LIDAR intensity return characteristics.

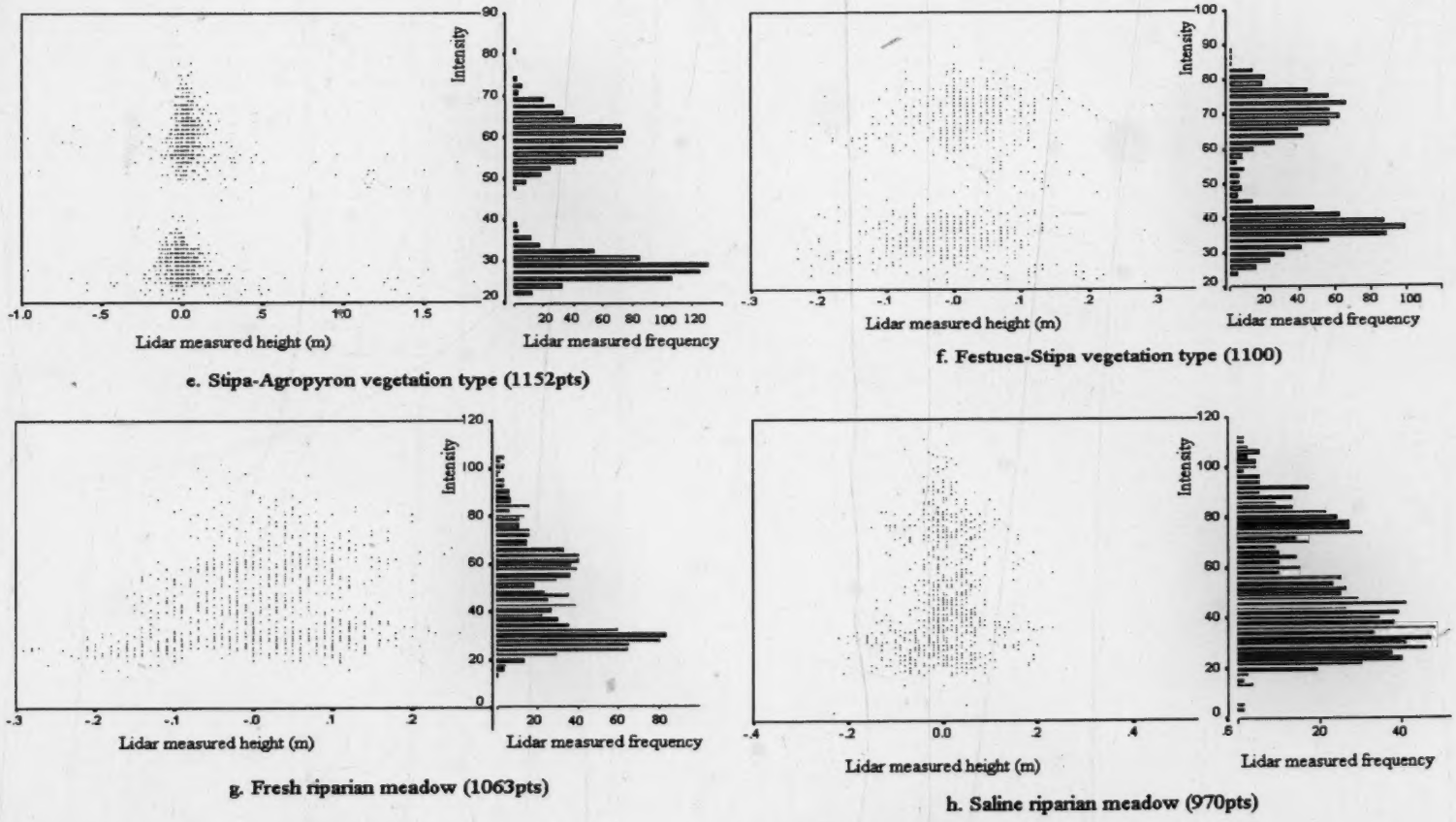
Intensity
Lidar measured height (m)
Lidar measured frequency
e. Stipa-Agropyron vegetation type (1152pts)
f. Festuca-Stipa vegetation type (1100)
g. Fresh riparian meadow (1063pts)
h. Saline riparian meadow (970pts)

Figure 4-7 (*Continued*). Association between LIDAR estimated vegetation height (m) and individual LIDAR intensity return characteristics.

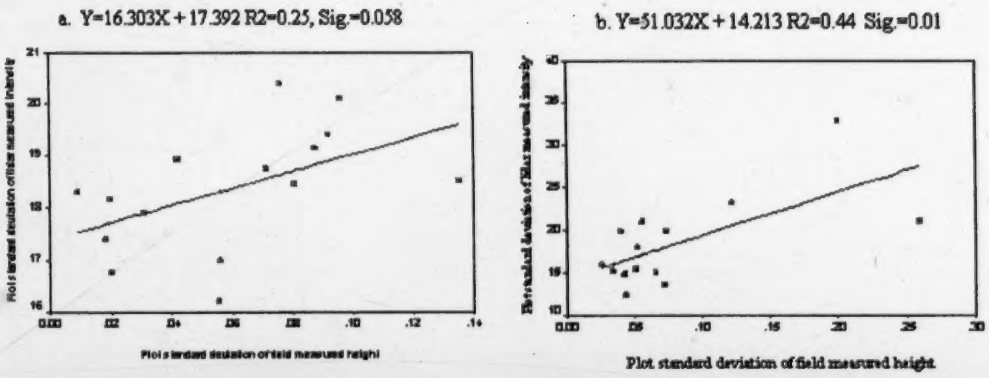

Figure 4-8 Association between variation in field measured vegetation height and variation in LIDAR intensity for the fescue grassland (a) and fresh riparian meadow (b). (X: standard deviation of the 40 field measured vegetation heights in 1 plot; Y: standard deviation of all the LIDAR data points within the same plot).

5 Vegetation Mapping

5.1 Introduction

Recognition of vegetation types is important for rangeland management agencies as it provides a basis for the development and evaluation of management policies and actions. Vegetation classification is the process of identifying and describing areas of relatively homogeneous plant species composition (e.g., communities in a resource inventory), and subsequently mapping the resulting spatial distribution of various vegetation types across the area of interest. Similar plant communities are thought to be both equally susceptible to disturbance, as well as respond to various disturbances in a uniform or consistent manner. Improved vegetation classification accuracy from remotely-sensed data will enhance the ability of managers to develop initial management plans as well as track vegetation responses in a timely manner following specific management activities such as livestock grazing or the use of prescribed fire.

The spatial organization of vegetation canopies is a fundamental boundary condition that influences many ecosystem processes. In particular, information on vertical canopy structure advances studies of the global C cycle (Post 1993), vegetation productivity and biomass estimation (Ryan and Yoder 1997, VCL 2000), habitat use by wildlife and livestock (MacArthur 1958, Schowalter 1995, Carey 1996), and interactions between vegetation, soil moisture and streams (Gregory *et al.* 1991). Canopy structure information is also important for wildfire behaviour prediction (Rothermel 1991).

Despite the value of this information, data on the 3-dimensional (e.g., physiognomic) organization of vegetation canopies is difficult to obtain. Most remote sensing systems, although readily providing information on the horizontal organization of canopies, do not provide direct data on the vertical distribution of canopy elements. Ground observer or *in-situ* measurements of canopy vertical structure are inherently laborious and time consuming, and thus, are often limited in scope.

Traditional remote-sensing techniques have inferred the vertical structure of vegetation by the varying proportions of tree and shadow with changing tree density (Woodcock *et al.* 1994, Cohen *et al.* 1992), or by the increased presence of spectrally unique new scene components (such as lichen) in the vegetation canopy (Cohen *et al.* 1990). Current synthetic aperture RADAR (SAR) technology offers promise for predicting low levels of vegetation cover and for mapping general vegetation types in floristicly simple landscapes (Rignot *et al.* 1994, Smith *et al.* 1994), but is insensitive and thus, unsuitable, for mapping densely vegetated sites (Waring *et al.* 1995).

A new and innovative method of vegetation classification is in using LIDAR (Light Detection And Ranging) data. Unlike microwave and traditional optical sensors, LIDAR sensors do not suffer from this limitation because they directly measure both the vertical location and horizontal distribution of aboveground plant biomass. Recording the distance to the first and last reflective surface for each laser point gives a direct height measurement for each observation. Such techniques have proven useful for predicting canopy height, vegetation structure and biomass (Næsset 1997).

In terms of vegetation classification, airborne photography and videography are well-developed technologies. Within a single image (photo or digital), 2 kinds of image

characteristics can be used for vegetation type identification, the size and shape of the object, or its color and brightness. For an object (e.g., a plant species) to be recognized on an image, the object's size ideally would be similar to or larger than the pixel size (spatial resolution) (Clegg *et al.* 1975). When the spatial resolution exceeds the target size, it may be possible to identify certain plant species through the color and shape of the organism. However, if the brightness of certain objects can be readily distinguished from others, the former object may be identified even if their actual size is considerably smaller than an individual pixel. For example, with color-infrared (CIR) 1:700 aerial photographs, McCormick (1999) successfully mapped the distribution of high-density *Melaleuca quinquenervia*, an aggressive exotic species at a site in the East Everglades. However, the low-density *Melaleuca* seedlings and/or small saplings (secondary and/or tertiary class vegetation) were occasionally difficult to identify.

When multi-spectral images are available, spectral mixing models [usually spectral vegetation indices-(VI)] are used to identify certain objects. The most frequently used VI is the normalized difference vegetation index (NDVI) for contrasting optimum reflection and absorption characteristics of vegetation. Other indices assisting vegetation (and soil) identification include RVI, GVI, DVI, PVI, SAVI, TSAVI, and $SAVI^2$ (Richardson and Everitt 1992). Pickup *et al.* (2000) found that although no single index separated all cover classes from each other, a step-by-step procedure using a limited number of spectral indices could provide a high level of discrimination among classes. However, more sophisticated approaches are available to develop rules for the classification of vegetation types based on training pixels/points, such as the classification of color composite images from band ratioing.

Unlike traditional sensors, LIDAR data have high spatial resolution, accurate vertical properties, and laser return intensity values that provide a unique additional source of information (though the practicality of intensity information is vague) (Fowler 2000). These advantages hold potential for future vegetation classification and characterization using LIDAR data. The intensity value of LIDAR data provides quantitative spectral information that may indicate what the reflection is from, including the type of vegetation, rock, or parent materials. However, most LIDAR data have only 1 wavelength, making the analysis of complex indices for vegetation mapping impossible. For terrestrial mapping, a single band is commonly used from the near-infrared spectrum.

Given the capability of using LIDAR data (though single band) to provide information on vegetation vertical structure, and multi-band images to identify vegetation through its color, shape or indices, our research tested and compared the suitability of using LIDAR and 3-band digital data for classifying spatially complex Aspen Parkland vegetation at the University of Alberta Ranch near Kinsella, Alberta, Canada. 2 vegetation classification systems were tested: (a) one using 3 vegetation classes limited to the major formations of deciduous forest, shrubland and grassland, and (b) a second using 8 detailed vegetation classes including mixed prairie and fescue (upland) grasslands, closed and semi-open (aspen) forests, western snowberry and silverberry shrublands, and fresh and saline riparian (lowland) meadows. In mapping with LIDAR data, the 3-class system used only a vegetation surface elevation model (SEM) that included LIDAR data derived height information, while the second eight-class system integrated height information with a DEM constructed with LIDAR data to incorporate topographic biases in community positioning across the landscape. In mapping using multi-spectral digital

images, the 2 vegetation classification systems were applied to: (a) the original digital image mosaic, (b) a hybrid color composite image from band ratioing and (c) an image from intensity-hue-saturation (IHS) using respective supervised training techniques. In the final step, a classification was developed that integrated information from both digital images and LIDAR data to determine whether the 2 could be combined to improve the final overall accuracy of Aspen Parkland vegetation classification.

5.2 Materials and Methods

5.2.1 Study Area

This research was conducted at the University of Alberta Ranch (53° 0' N, 111°31' W) located 150 km SE of Edmonton, Alberta, Canada, within the Aspen Parkland natural sub-region. The Ranch is 2700 ha in size and has a general topography of rolling hills (i.e., knob and kettle terrain) with 5-25 m relief associated with its glacial moraine landform origin. The region has a temperate continental climate, with mean annual precipitation of 433mm and 100-120 frost-free days (University's Meteorological Station at Kinsella Ranch). North-facing slopes are capable of supporting plant species with greater moisture requirements due to snow accumulation, such as aspen forest and shrublands, while south-facing slopes typically support plant communities tolerant of drier conditions such as grassland (Wheeler 1976, Coupland 1961). The most common soil type of the area is a Black Chernozem, although Dark Gray Chernozems and Eluviated Chernozems are present as well (Bailey and Wroe 1974, Scheffler 1976). Gleysols and Solonetzic soils also occur, the former confined to poorly drained lowlands.

Herbage production is 2251 ± 747 and 2886 ± 993 ($kg \cdot ha^{-1}$, dry matter) in its first and second rotation, respectively (Asamoah *et al.* 2003), and the major vegetation types found throughout the Ranch are as follows:

(1) Riparian meadows

Meadows are mesic to hygric habitats occupied by grass (*Poaceae* family) and grasslike species primarily of the genera *Carex* and *Juncus*. The primary environmental characteristic affecting meadow vegetation is the high water table during all or part of the year (Benedict 1982). 2 major types of wetlands exist at Kinsella, which include:

A. Saline riparian meadows (SRM) dominated by salt grass [*Distichlis spicata* (L.) Greene], alkali grass [*Puccinellia nuttalliana* (Schultes) Hitchc] and numerous forbs. They border salt covered lakebeds of discharge origin.

B. Freshwater riparian meadows (FRM) dominated by aquatic sedges (e.g., *Carex atherodes* Spreng., etc), tufted hairgrass [*Deschampsia caespitose* (L.) Beauv.], and some marsh reedgrass [*Calamagrostis canadensis* (Michx.) Beauv.]. These meadows occurred at slightly greater elevations as ground water recharge areas.

(2) Upland grasslands

Grasslands in the area were historically maintained by a combination of periodic fire (Wright and Bailey 1982) coupled with grazing by ungulates including bison (*Bison bison*) (Campbell *et al.* 1994). 2 major upland grassland types at Kinsella Ranch were described by Coupland (1961), and include:

A. Mixed prairie grassland [Stipa-Elymus (SEG)] dominated by needle and thread grass (*Stipa comata* Trin. & Rupr.), and northern wheatgrass [*Elymus lanceolatus*

(Scribn. & J.G. Sm.) Gould], these xeric grasslands can be found on steep, south-facing slopes (>5°) and hilltops.

B. Fescue grassland [Festuca-Stipa (FSG)] dominated by plains rough fescue [*Festuca hallii* (Vasey) Piper] and western porcupine grass [*Stipa curtiseta* (A.S. Hitchc.) Barkworth], fescue grassland once covered most of the Aspen Parkland. Today, most fescue grasslands have been broken for cereal production or where remaining, been overgrazed (Trottier 1986). At Kinsella, remnants of unbroken or moderately grazed fescue grasslands remain abundant on mesic uplands with gentle slopes (<5°).

(3) Shrublands

Upland shrublands are ecotonal between grassland and adjacent aspen forest. 2 major types of shrublands occur at Kinsella and include (after Wheeler 1976):

A. Western snowberry (*Symphoricarpos occidentalis* Hook.) (SPS).

B. Silverberry (*Elaeagnus commutata* Bernh. ex Rydb.) (ENS).

Both snowberry and silverberry reproduce extensively by suckering from creeping underground roots, resulting in dense, closed canopy patches.

(4) Aspen forest

Generally, forested areas at Kinsella are represented by trembling aspen *(Populus tremuloides* Michx.) communities, with an understory of saskatoon [*Amelanchier alnifolia* (Nutt.) Nutt. ex M. Roemer], chokecherry (*Prunus virginiana* L.) and wild rose (*Rosa woodsii* Lindl) shrubs along with a well-developed herbaceous component. Aspen forest has expanded considerably over the last 60+ years (Bailey and Wroe 1974, Scheffler 1976), although periodic outbreaks of tent caterpillars and drought, coupled with prescribed burning have resulted in aspen stands of varied condition across the

Ranch. Young (5-30yr) and mature (30-60yr) aspen communities are characterized by closed canopy stands of relatively uniform tree age, height and diameter (Stelfox, 1995). In contrast, old and decadent aspen communities (>60yr) have often undergone significant canopy break-up and subsequent understory release as well as the emergence of secondary young aspen re-generation and shrubs. As a result, aspen communities at Kinsella can be classified into closed (young or mature) (CAF) and semi-open (decadent) aspen forest (OAF) types.

5.2.2 LIDAR Data Acquisition

Airborne scanning laser data were collected for the study area by Optech, a company specializing in the design of laser-based ranging, mapping and detection systems. The laser system was flown at 1700m above sea level (average above ground elevation of 1005m, ranging from 989m to 1027m) in the afternoon of 3 October 2000 during leaf-on conditions (Appendix 1), and used an across-track scanning system with a Z-shaped ground target path. The wavelength and frequency of the laser pulse were 1.04 μm and 25 KHz, respectively. The mean intensity was 42% and maximum off-nadir scanning angle 15°. Flight lines were approximately 500m apart, with a total of 19 north-south flight lines covering the entire area (2700ha). Final LIDAR data sampling densities across the area averaged 0.54 points/m^2, but ranged from 0.25 to 1.35 points/m^2. Laser measurements are sometimes but not usually affected by other reflections such as sunlight. Optech's scanning laser instruments scan laser pulses within a preferred range of angles. Instruments are designed to operate in daylight (Optech Incorporated 2003).

Initial LIDAR data files consisted of 2 components including the realtime geo-corrected coordinates (UTM easting and northing, as well as Z-elevation) for each laser point on the ground (last return) and the top of the vegetation (first return), as well as the associated intensity readings. LIDAR intensity is the ratio of strength of reflected light to that of emitted light (unit: %). An elevation was calculated by knowing the speed of light (approximately 0.3 metres per nanosecond) and distance to (start pulse) and from (return pulse) the object being measured. The average sampling interval was 1.5m between footprints in the across-track direction and 1.3m in the along-track (i.e., forward) direction. The average laser footprint diameter was 0.3m ($0.071m^2$) directly below the aircraft, which increased to 0.31m ($0.075m^2$) at a distance of 250 m off-nadir. The digital elevation model (DEM) developed in Chapter 3 (this volume) was used to calculate vegetation height for each laser point as the difference between the interpolated ground elevation and corresponding LIDAR first return elevation.

5.2.3 Digital Image Acquisition

Digital images were collected for the study area at the same time as the LIDAR data (3 October 2000, Appendix 1). Because a real-time GPS system was used for data collection, digital images were orthorectified and projected to the UTM coordinate system (datum NAD 83, zone number 12) at the time of data collection. Resultant images had 3 spectral bands: red (0.63-0.69 μm), green (0.52-0.60 μm) and blue (0.45-0.52 μm) with a spatial resolution of 0.5 m. The flight elevation, off-nadir angle and scan path had the same configuration as for LIDAR data sampling.

5.2.4 Experimental Design

A preliminary power analysis (Thomas and Juanes 1996) was conducted to determine the minimum number of ground plots (each 6 meter in radius) necessary to create signatures for each of the 8 vegetation types described earlier when mapping using digital images. Power analysis indicated that given the heterogeneity of the study area, approximately 120 signatures (alpha=0.05, effect size=0.15 and power=95%, for a total of 15 signatures per vegetation type) were required. The corresponding 120 field plots were further stratified directly by slope gradient (<=5°, >5°) (Appendix 1). Although field plots could not be initially stratified by off-nadir distance because of difficulty in identifying these classes within the landscape prior to sampling, the varied (i.e., approximate random) spatial distribution of plots across the landscape ensured both categories (on/near- and off-nadir) were sufficiently represented (e.g., n=65, <130m from nadir; n=55, 130-260m off-nadir). Using ground-truthed plots facilitated not only the creation of spectral signatures within the area of interest (AOI) necessary for subsequent supervised classification of digital images, but also our measurement of field vegetation height characteristics from LIDAR data.

Another 128 ground-truthed plots with similar vegetation characteristics, slope gradient and nadir distance were sampled for identifying the accuracy of the vegetation maps generated using both LIDAR data and digital images. The comparatively simple spectral class of bare-ground was also identified for mapping of land cover (10 plots for signature and 10 for accuracy assessment). Both fresh and saline water were also sampled (6 for each of them), but only used for final accuracy assessment, not for calibration. The coordinates of the central position of all 280 field-plots (130 for

calibration, 150 for validation) were located using a Leica differential GPS unit (average accuracy = ± 0.53 m).

5.3 Analysis

5.3.1 Digital Image Classification Schedules

The original digital image of the study area was clipped from a mosaic of 16, 2 by 2 km images with a spatial resolution of 0.5 m. Differences in brightness between images were corrected using empirical-derived correction equations based on linear regressions as described by Hall *et al.* (1991). Widespread shadows existed on the mosaic image because of the tilt angle of the camera and scene illumination condition of the Sun (image taken 2pm MST on 3 October 2000). Shadowing was removed using a spectral ratioing algorithm, which conveyed the spectral or color characteristics of image features regardless of variations in scene illumination condition (Holben and Justice 1981). However, surfaces that have different absolute radiances but similar slopes in their spectral curves may have the same ratio results. To avoid this "intensity blind" effect (Justice *et al.* 1981) from spectral band ratioing, a hybrid color composite image was created by displaying 2 ratio images of the primary colors, but using the third primary color to display an individual band of data (Lillesand and Kiefer, 2000). This hybrid color composite image was then used to classify the study area into land cover with 3 and 8 classes of vegetation, respectively (Figure 5-1).

Unlike green healthy vegetation that has greatest reflectance in the green band on RGB digital images, the images in our analysis had on average, lowest reflectance within

the blue band (mean = 40.83), which increased to 41.92 and 45.79 in the green and red bands, respectively. This trend probably reflected the partial senescence of vegetation in early October (Carter and Miller 1994). Given the condition of the vegetation, the red/blue spectral ratio was chosen as the red band for the hybrid composite image. In contrast, the green/blue ratio was comparatively small and chosen as the blue band of the composite. The green band remained unchanged. The creation of a transformed color composite image not only reduced the shadowing effects on images, but also simulated true color images in which the green band had greatest reflectance (Figure 5-2).

Another effective image processing technique to describe colors by their RGB components is the use of the intensity-hue-saturation system. "Intensity" relates to the total brightness of a color. "Hue" refers to the dominant or average wavelength of light contributing to a color. "Saturation" specifies the purity of color relative to gray (Lillesand and Kiefer, 2000). Beauchemin and Fung (1999) used IHS color space as an alternative technique to the transformation of RGB into a color composite. Similar to results from Schowengerdt (1983), they demonstrated that transforming RGB components into IHS components before processing and classification provided more control over color enhancements and shadowing removal. As a result, an IHS image (Figure 5-3) was created in our analysis for comparative use in vegetation and land cover mapping. Both the hybrid color composite and IHS images enhanced the subtle differences within the shadow areas, but also resulted in information loss on the images. Consequently, the original mosaic image was used to classify the study area vegetation and land cover, and compared for accuracy with the vegetation and land cover maps classified from the hybrid colour composite and IHS images.

In supervised classifications, pixel categorization is supervised by specifying numerical descriptions of the various land cover types present in a scene (Lillesand and Kiefer 2000). Supervised classification requires that all spectral classes constituting each information class be adequately represented in the training set statistics used to classify an image. However, the variable landscape of the study area created an environment of complex heterogeneity among the spectral response patterns even within individual land cover types. Unlike the training sets used in traditional supervised methods, these areas were heterogeneous. As a result, 15 supervised subclass signatures were established for each of the 8 cover types (except for bare ground, which had 10 training signatures). Once all sub-spectral classes had been signatured to reflect the variability in landform and vegetation across the study area (except fresh and saline water), the subclass signatures were aggregated back to the original 9 major class signatures (Figure 5-1 and Appendix 2). In a final step, a Mahalanobis classification was performed with the full set of spectral signatures and the 9-class schedule applied to the original mosaic image, the hybrid color composite and the IHS image. The Mahalanobis distance decision rule uses the covariance matrix in the equation. Variance and covariance are calculated so that clusters that are highly varied will lead to similarly varied classes, and vice versa.

The above procedure was also carried out to classify the study area into land cover with only 3 classes of vegetation – forest, shrubland, and grassland, as well as bare ground. Moreover, this system was applied to the classification schedules of the original mosaic image, the IHS image, and the hybrid color composite from band ratioing.

Accuracy assessment (Figure 5-1) was performed by determining the overall classification accuracy for each class, as well as the commission and omission errors

associated with each individual class within the classification schedule. These accuracies were then compared among the 3 classification schedules. Land cover classification results were also compared between the classification system with 3 classes of vegetation and a second with 8 classes of vegetation. A 95% confidence interval was used in their comparison to identify whether significant differences existed among the three classification schedules and between the 2 classification systems.

5.3.2 LIDAR Data Classification Schedule

Mapping with LIDAR data was dependent on the utility of these data to detect meaningful differences in vegetation height, which in turn, depended on adequate height separation among community types. In the study area, rank dominance of vegetation height begins with aspen trees, and progresses through shrublands, to grasslands. Vertical height division lines between tree and shrub, and between shrub and herb were determined based on field measurements of average shrub and herb height (Table 5-1) as well as 95% confidence intervals above the mean height. Mean herb height in grasslands and overstory shrub height in shrublands were determined to be 22 and 62 cm, respectively (Table 5-1). The upper 95% confidence intervals above these values were 30 and 150 cm, respectively. As a result, vegetation with an estimated height between 30 and 150 cm was considered to be of shrubland origin, while vegetation shorter than 30 cm was classified as grassland and that taller than 150 cm classified as aspen forest.

The first step of LIDAR data mapping was to classify vegetation into deciduous forest, shrubland and grassland (Figure 5-4). A surface elevation model (SEM) (Figure 5-5) for classifying the above three general vegetation formations was constructed for the

study area by differentiating between LIDAR data's first and last return elevation, and then interpolated (see Chapter 3, this volume for details). Unlike a DEM that has a smooth ground surface, the SEM was expected to be much more variable because of the intermittent influence of the overstory vegetation. Although splining was initially used, it produced a smooth (and non-representative) surface for the vegetation, and was therefore discarded. Kriging was also dropped due to the excessive computational time required to process the 3 GB of LIDAR data for the study area. Inverse distance interpolation with a weight of 3, which favoured the use of nearer data points rather than those further away, produced a sharper SEM and was therefore chosen for application to the study area. The output pixel size of the final SEM was set to 1.5 m because the discrete LIDAR data points had an average sampling interval of 1.5 m between footprints in the across-track direction and 1.3 m in the along-track (i.e., forward) direction.

Closed aspen forest was further separated from semi-open aspen forest using LIDAR data point density information. Discreet LIDAR data samples corresponding to the 30 aspen forest field plots indicated that in plots of closed aspen forest, LIDAR data points with a height greater than 1.5 m averaged 82% (95% confidence interval 75-88%) of all LIDAR sample points. In contrast, the proportion of LIDAR points above 1.5 m was only 57% (95% confidence interval 43-70%) in semi-open forest. As a result, the value of 73% [=(75+70)/2] was used as a division rule to separate closed from semi-open aspen forests (Figure 5-4). Using the SEM, the total number of neighbouring pixels of a cell within aspen forest was calculated through a 3 by 3 moving-window. If the calculated value was between 1 and 6 (11-67%), the forest type was determined to be

semi-open aspen forest. Alternatively, values from 7-9 (or 78-100%) were classified as closed aspen forest.

Initially, we planned to separate western snowberry from silverberry plant communities using LIDAR-derived densities of the shrub overstory (0.3 – 1.5 m). However, each shrubland vegetation community had only 2% of their LIDAR data points on average with a height greater than 0.3 m. As a result, LIDAR-derived height information alone could not be used to successfully separate western snowberry from silverberry shrublands. Ultimately, this limitation could only be removed by integrating LIDAR data with digital image classification results.

Upland mixed prairie grasslands on the study area were distributed among hilltops and steep, south-facing slopes (>5°). This distribution was determined (Figure 5-4) using LIDAR-derived DEM information developed in Chapter 3 (this volume). Using the DEM, a slope gradient (Figure 5-6) was calculated through surface analysis (Brabyn 1998) with a pixel size of 1.5 m. Each cell was then classified as being flat (< 2°), or having a gentle (2°-5°) or steep (> 5°) slope. Aspect was classified into a 9-class system (Figure 5-7): including a flat class (F) with no aspect due to a slope less than 2°, as well as aspects centred on N, clockwise to NE, E, SE, S, SW, W and NW, in 45° increments. The collective aspects of SE, S and SW (totalling 125°) were then reclassified as south-facing slopes. All land areas with a slope gradient greater than 5° and having a south-facing aspect were classified as upland mixed prairie grasslands.

Relative relief (Figure 5-8) was calculated from the DEM using a neighbourhood range function through a 30-pixel-radius (typical topographic unit size at the study area – 6500 m^2) moving window (Brabyn 1998). Finally, profile typing was used to determine

whether the flat (F) areas (slope<=2°) were above or below the surrounding terrain (i.e., in upland or lowland topographic positions). Upland and lowland profiles were identified by first calculating the maximum elevation surrounding each pixel on a 30-pixel-radius moving window within the DEM (Brabyn 1998). The elevation of the central cell was then subtracted from this maximum elevation, and where this difference was less than half of relative relief for the same cell, the central cell was identified as upland, otherwise the central cell was considered to be lowland (Figure 5-9). If a resulting upland had a vegetation height less than or equal to 0.3 m (from SEM) and a slope gradient less than or equal to 2°, this area was also classified as upland mixed prairie. As there are only 2 major grassland communities within the study area, the remaining grasslands (vegetation height $\leq$ 0.3 m) within upland positions were classified as fescue grasslands.

Similar to the accuracy assessment of classified digital images, the overall classification accuracy, as well as the commission and omission error of each individual class was also examined. Comparisons were also carried out between the classification system with 3 classes of vegetation and a second with 6 classes of vegetation (i.e., 2 aspen forest and upland grassland types, respectively, as well as 1 shrubland and lowland meadow type, respectively). A 95% confidence interval was used in their comparison to identify significant differences between classification systems.

5.3.3 Classification Schedules Integrating LIDAR Data and Digital Images

Due to the inherent error in interpolation of the SEM and equipment error during LIDAR data acquisition, the LIDAR-derived SEM could not be applied successfully to separate bare ground from grasslands. In contrast, bare ground and grassland were

sampled on digital images, and their classification accuracy found to be effective. As a result, we examined whether these digital classes could assist LIDAR data's classification. Additionally, the height of shrubland was found to be consistently under-estimated with LIDAR data in Chapter 4 (this volume), and probably resulted in assigning some shrubland communities into the grassland types. This problem was addressed using digital image classification schedules.

For those classes that could be separated using both LIDAR data (including classification results incorporating topographic characteristics from the DEM) and digital images, their classification results were compared and those producing the best classification result were used to create the final integrated maps through GIS spatial extraction and integration techniques.

5.4 Results

5.4.1 Digital Image Classification Schedules

Among the land cover classification schedules with 3 classes of vegetation and land, classification from the hybrid color composite image displayed the greatest overall accuracy (mean = 74.6%, range 65.7-80.0% among types) and smallest commission error among validation plots (mean = 25.4%, range 20.0-32.3% among types)(Table 5-2). In contrast, classification from the intensity-hue-saturation image produced a lower classification accuracy (mean = 59.4%, range 43.9-75.0% among types) and greater commission error (mean = 40.6%, range 22.2-43.8% among types). Among individual classes, bare ground had the greatest classification accuracy (100%) when using the

original mosaic image. Bare ground, shrubland and grassland could all be effectively separated using the hybrid color composite image as shown by their high classification accuracies (80%, 78% and 76.9%, respectively) and low commission errors (20%, 27.3% and 25%, respectively).

When the digital land cover classification schedules were applied to the 8 classes of vegetation, their overall classification accuracy decreased substantially (by an average of about 24%, Table 5-3). Nevertheless, classification from the hybrid color composite image continued to display the greatest classification accuracy (mean = 59.4%, range 26.3-87.5% among types) and smallest commission error (mean = 39.8%, range 13.3-70.6% among types), while intensity-hue-saturation created the lowest classification accuracy (mean = 42.8%, range 26.7-72.2% among types) and greatest commission error (mean = 52.8%, range 0.0-75.0% among types). Among detailed vegetation types, the silverberry, mixed prairie and fresh riparian meadows could all be effectively differentiated using the hybrid color composite image (classification accuracies of 80%, 72.2% and 87.5%, respectively). However, the silverberry class also had a commission error of 52%. Further examination revealed that 16% of the commission error came from western snowberry, 12% from closed aspen forest and another 12% from fescue grasslands. Fresh riparian meadows could also be classified with an accuracy of 87.5% when using the original mosaic image. Fescue grassland could be largely distinguished using the intensity-hue-saturation image (72.2%), but with a commission error of 58.1%, limiting its practical utility. The commission error was a result of improper inclusion of 16.1% of mixed prairie grasslands, 12.9% of closed aspen forest, 12.9% of silverberry, 6.5% of semi-open aspen forest and 6.5% of western snowberry into the fescue grassland

type. Western snowberry was poorly classified using all images, with the hybrid color composite image providing the best result (57.7%). Finally, low classification accuracies prevented closed and semi-open aspen forest, as well as saline riparian meadows from being correctly mapped using any of the 3 digital classification schedules tested.

5.4.2 LIDAR Data Classification Schedule

The LIDAR data classification schedule with 3 classes of vegetation displayed a mean classification accuracy of 64.8%, but was highly variable among classes (Table 5-2, varied from 0.0% to 100.0%). Aspen forest achieved a classification accuracy of 88.6% and no commission error. Similarly, grassland could also be identified using LIDAR data with an accuracy of 100%; however, grassland included up to 46.4% of other vegetation types, with 42.3% of those commission errors being shrubland. Moreover, this schedule clearly showed that shrublands in this region of the Aspen Parkland could not be mapped using LIDAR data (0% classification accuracy). Overall, it was evident that LIDAR data were superior to the digital classification schedules for their accuracy in mapping aspen forest and grassland, but not shrubland.

The LIDAR data classification schedule with 6 classes of vegetation had an overall classification accuracy of 52.3% (range 0.0-93.8% among types), intermediate to the 3 digital data sets (Table 5-3). Among these 6 classes, however, lowland meadow, closed and semi-open aspen forest, as well as mixed prairie grassland could all be effectively separated from each other with accuracies of 93.8%, 81.3%, 73.7% and 83.3%, respectively. These accuracies were superior to any of those classifications obtained with the digital data by a minimum of 15.4%. Examination of the contingency

table (Table 5-3) indicated that the 40% commission error to the mixed prairie class was not the result of the more accurate classes listed above, but rather an inclusion of shrubland (24%) and upland fescue grassland (16%). Shrubland and fescue grassland, in turn, could not be mapped because of their low classification accuracy and the high commission errors between these classes (Table 5-3).

5.4.3 Classification Schedules Integrating LIDAR Data and Digital Images

Among the classification schedules with 3 classes of vegetation, because LIDAR data classification of aspen forest had a high accuracy (88.6%) and very low commission error (0%), the first step of integrated mapping was the extraction of aspen forest types using LIDAR data. Although classification with LIDAR data had a very high classification accuracy on grassland (100%), it included up to 42.3% of shrubland (Table 5-2). As a result, the second step of mapping was not the extraction of grassland, but rather the identification of shrubland from the remaining part of the study area through the hybrid color composite image (accuracy 78%). In the third step, grassland was isolated using LIDAR data (accuracy ~100%). Bare ground was isolated last because all the commission error associated with this type came from inclusion of grassland. The final map of the study area with 3 classes of vegetation was created through overlaying and integrating the above extracted portions of classification results and assigning unclassified pixels to a majority type in a 3 by 3 moving window. The overall accuracy of the final map was 91% (range 78.0-100.0% among types) based on the independent field validation plots (Figure 5-10).

Among the classification schedules with 8 classes (6 of LIDAR data) of vegetation, closed and semi-open aspen forest were first extracted from the LIDAR data because of their high classification accuracy and low commission errors (Table 5-3). Given that none of the 3 digital image classification schedules nor LIDAR data were able to separate saline riparian meadows from other vegetation and land cover types, fresh and saline riparian meadows were kept as 1 lowland meadow type, and these areas extracted using the LIDAR data classification with an accuracy of 93.8%. Bare ground was then extracted from the image using the original image mosaic. Extracting lowland meadows prior to bare ground (which had 100% classification accuracy) helped prevent improper inclusion of riparian meadows into bare ground.

In order to separate the remaining vegetation types of silverberry, western snowberry, mixed prairie and fescue grassland, mixed prairie was first extracted using the LIDAR data classification schedule. Undertaking this before the extraction of fescue grassland from the intensity-hue-saturation image, avoided the possibility for commission errors of mixed prairie into fescue grassland. The last step of the process was the extraction of silverberry and western snowberry from the hybrid color composite image. Silverberry was extracted last because this minimized the improper inclusion of other types, including fescue grasslands, closed- and semi-open aspen forest, as well as mixed prairie. Through overlaying and integrating the above extracted portions of classification results and assigning unclassified pixels to a majority type in a 3 by 3 moving window, the final product for the study area was an 8-class (7 classes of vegetation and bare ground) map with an overall accuracy of 80.3% (range 57.7-100% among classes) (Figure 5-11).

5.5 Discussion

The greatest overall classification accuracy reported previously in the analysis of multispectral, high spatial resolution, airborne videographic and spectrographic images in the Aspen Parkland was 65% (Franklin *et al.* 2000). These results were derived from classifying both spectral and textural features, and were compared to validated field plots. The digital classification accuracies obtained in our study with 3 classes of vegetation before integration with LIDAR data were similar to those studies. Additional customized multiband processing (e.g., texture or filter algorithm) of image data yielded classification accuracies up to 75% (Franklin and McDermid 1993). These customized processing techniques produced greater classification accuracies compared to our individual classification schedules, but were not superior to our integrated maps with 3 and 8 classes of vegetation. Map integration and the use of biological information derived from LIDAR data were the 2 key factors contributing to the successful classification of the land cover in our study area.

Pickup *et al.* (2000) found that although no single vegetation index separated all cover classes from each other, a step-by-step procedure using a limited number of spectral indices could provide a high level of discrimination among classes. This was also true in our study as no single classification schedule created a highly accurate map for all cover types. Instead, a step-by-step extraction and integration procedure created a map with the greatest classification accuracy. LIDAR data can provide effective quantification of landscape topography, gully and stream-cross sections and roughness, as well as biological properties specific to certain landform features (Ritchie *et al.* 2001,

Dymond *et al.* 1995), which by comparison are difficult to interpret using digital images. For example, mixed prairie grassland in the present study area preferentially occurs on hilltops or steep, south facing slopes (Wheeler 1976). Using this topographic feature, mixed prairie was classified successfully using LIDAR-derived slope, aspect and upland/lowland data with an accuracy of 83.3%; while the greatest classification accuracy for mixed prairie using only digital images in our analysis was 72.2% (from the hybrid color composite image).

Although aspen forest did not appear to be as topographic dependent as mixed prairie grasslands, the SEM derived from LIDAR data had the inherent ability to separate aspen forest from other land cover types based on vegetation height. Moreover, closed and semi-open aspen forest could be successfully separated from each other because of differences in the number of LIDAR data points available within various overstory layers. In contrast, digital images can not provide accurate vegetation height information, nor density or brightness differences large enough to differentiate closed from semi-open aspen forest. Rather than using digital images, LIDAR data were applied to isolate aspen forest for the final land cover mapping. The use of LIDAR data led to increased accuracies by the mean of 34.9% and 59.7%, respectively, for the 3 and 8 classes of vegetation when compared to the greatest classification accuracy obtained solely from digital images.

The underestimation of vegetation height and misclassification of shrublands into grasslands limited the utility of using LIDAR data to classify shrublands. These limitations were partially removed when using digital images such as the hybrid color composite image, as digital images displayed significant spectral differences both within

shrublands and between the shrubland and other vegetation types. Using a hybrid color composite image increased shrubland classification accuracy, for example, from 0% to 78% within the 3 class vegetation schedule.

The individual 3-class vegetation schedules produced classification accuracies of 65.9% (57.1-100.0%), 74.6% (65.7-80.0%), 59.4% (43.9-75.0%) and 64.8% (0.0-100.0%), respectively, from the original mosaic image, hybrid color composite image, intensity-hue-saturation image and the LIDAR data. No single classification could be definitively considered superior to another in the overall classification accuracy, largely due to variation in accuracy among land cover types. However, the extraction and integration of data types achieved a map with an overall accuracy of 91% (78.0-100.0%), and created a classification superior to any of the 4 individual techniques used. Similarly, the overall accuracy of 80.3% (57.7-100.0%) with the 8-class (7 classes of vegetation and bare ground) map was superior to each of the individual classification schedules (47.8%, 59.4%, 42.8%, and 52.3% on the original mosaic image, hybrid color composite image, intensity-hue-saturation image, and the LIDAR data, respectively). This research has achieved comparable results that confirm the effectiveness of integrating LIDAR data and digital images for vegetation and land cover classification.

Despite the high classification accuracy obtained in the study with the 8-class schedule (mean = 80.3%, varied from 57.7% to 100.0%), the above classification could not separate fresh from saline riparian meadows. Perhaps more problematic is that water bodies were classified together with lowland meadows, which resulted in the over-estimation of lowland meadows by up to 54.2%. Detailed examination of the hydrologic characteristics of the study area revealed that fresh water had an elevation below 683 m

and was distributed on the east side of the study area, while saline water had an elevation below 675 m and was distributed on the west side of the study area. Correspondingly, fresh and saline riparian meadows were located on the east recharge and west discharge areas, respectively. Integrating this information into the classification with 7 classes of vegetation, lowland meadows were further classified into fresh and saline water, as well as fresh and saline riparian meadows, with classification accuracies of 100%, 100%, 100% and 75% for the 4 land cover types. Investigation into LIDAR intensity data revealed that intensity could also be used effectively to separate water bodies (25.45 ± 26.96 %) from other land surface features (53.25 ± 22.18 %), though the classification was not as consistent as using elevation information.

A final map with 11 classes of land cover including 8 classes of vegetation, fresh and saline water, as well as bare ground was created for the study area with an overall accuracy of 83.9% (57.7-100.0% among classes) (Figure 5-12). This high classification accuracy further reinforced the utility of using LIDAR data for improving vegetation mapping in the Aspen Parkland.

5.6 Conclusion

Vegetation properties and features are integral parts of the landscape and have to be evaluated at large scales to understand the biological, environmental and hydrologic processes associated with natural and agricultural systems. Measurements of micro and macro surface features contribute not only to the quantification of watershed information (Band 1986) such as slope gradient, aspect, upland and lowland, and discharge and recharge areas, but also to mapping land cover components (Dymond *et al.* 1995). Core

components include canopy properties, canopy distribution across the landscape, as well as a better understanding of micro-climate, animal movement, livestock grazing, and management interests. The high classification accuracies with 3 and 8 classes of vegetation in our analysis were attributed, in large part, to the capability of using LIDAR data to isolate those vegetation types that were topographic dependent. LIDAR data not only offer the potential to measure landscape and vegetation properties over large areas more effectively, but also contribute to mapping accuracy. Such measurements will improve our inventory of natural and agricultural landscapes so that improved management practices and structures can be developed.

However, because LIDAR data mainly depend on elevation and height information for mapping vegetation and land cover, its utility is limited when vegetation does not vary much or is short in height. The use of LIDAR data is also limited by the difficulty in separating different land cover types through spectral brightness information, which is, in contrast, well developed on digital images. The intensity signal of LIDAR provides the sort of "surface texture" information typical of RADAR imagery; however, at the moment, the practicality of intensity information is vague (Fowler 2000) and was incapable of separating different vegetation types in our study. The lack of advanced algorithms and data processing expertise further limits the operational use of LIDAR data. Finally, some vegetation characteristics (e.g., LAI) cannot be determined either directly, or with modelling from LIDAR data alone. In these cases, LIDAR data should be fused with information from passive optical, thermal and RADAR remote sensing techniques to achieve effective vegetation and land cover mapping (Dubayah and Drake 2000). Though LIDAR data and digital imagery use quite different measurements (range

vs. reflection image) and data processing technologies (based on different sampling patterns and information content), the application potential of LIDAR and image fusion is being disclosed (e.g., this Chapter, Popescu and Wynne 2003).

5.7 Literature Cited

Asamoah, S. A., E. W. Bork, B. D. Irving, M. A. Price, and R. J. Hudson. 2003. Cattle herbage utilization patterns under high-density rotational grazing in the Aspen Parkland. *Canadian Journal of Animal Science*. 83:541-550.

Bailey, A.W. and R.A. Wroe. 1974. Aspen invasion in a portion of the Alberta parklands. *Journal of Range Management* 27:263-266.

Benedict, N. B. 1982. Mountain meadows: stability and change. *Madroño* 29:148-53.

Band, L. E. 1986. Topographic partitioning of watersheds with digital elevation models. *Water Resources Research* 22:15-24.

Beauchemin, M. and K. B. Fung. 1999. Intensity-hue-saturation color display transform for hyperspectral data (pp21-24). In *4th International Airborne Remote Sensing Conference and Exhibition/21st Canadian Symposium on Remote Sensing*, Ottawa, Ontario, Canada.

Brabyn, L. 1998. GIS analysis of macro landform (pp16-19). In *SIRC 98 – The 10th Annual Colloquium of the Spatial Information Research Centre*, University of Otago, Dunedin, New Zealand.

Campbell, C., I.D. Campbell, C.B. Blyth, and J.H. McAndrews. 1994. Bison extirpation may have caused aspen expansion in western Canada. *Ecography* 17:360-362.

Carey, A. B. 1996. Interactions of Northwest forest canopies and arboreal mammals. *Northwest Science* 70:72-78.

Carter, G. A. and R. L. Miller. 1994. Early detection of plant stress by digital imaging within narrow stress-sensitive wavebands. *Remote Sensing of Environment* 50:295-302.

Clegg, R.H. and J.P. Scherz. 1975. A comparison of 9-inch, 70mm, and 35mm cameras: *Photogrammetric Engineering and Remote Sensing* 41:1487-1500.

Cohen, W. B., T. A. Thomas, and G. A. Bradshaw. 1990. Semivariograms of digital imagery for analysis of conifer canopy structure. *Remote Sensing of Environment* 34:167-78.

Cohen, W. B., T. Spies, and A. Thomas. 1992. Estimating structural attributes of Douglas-fir/western hemlock forest stands from landsat and SPOT imagery. *Remote Sensing of Environment* 41:1-17.

Coupland, R.T. 1961. A reconsideration of grassland classification in the northern Great Plains of North America. *Journal of Ecology* 49:135-167.

Dubayah, R.O. and J.B. Drake. 2000: LIDAR remote sensing for forestry. *Journal of Forestry* 98:44–46.

Dymond J.R., R.C. Derose, and G.R. Harmsworth. 1995. Automated mapping of land components from digital elevation data. *Earth Surface Processes and Landforms* 20: 131-137.

Fowler, R. A. 2000. The low down on LIDAR. *Earth Observation Magazine* 9:1-7.

Franklin, S. E. and G. J. McDermid. 1993. Empirical relations between digital SPOTHRV and CASI spectral response and lodgepole pine (*Pinus contorta*) forest stand parameters. *International Journal of Remote Sensing* 14:2331-48.

Franklin, S. E., R. J. Hall, L. M. Moskal, A. J. Maudie, and M. B. Lavigne. 2000. Incorporating texture into classification of forest species composition from airborne multispectral images. *International Journal of Remote Sensing* 21:61-79.

Gregory, S.V., F.J. Swanson, W.A. McKee, and K.W. Cummins. 1991. An ecosystem perspective of riparian zones. *BioScience* 41:540-551.

Hall, F. G., D. B. Botkin, D. E. Strebel, K. D. Woods, and S. J. Goetz. 1991. Large scale patterns of forest succession as determined by remote sensing. *Ecology* 72:628-640.

Holben, B.N. and C.O. Justice. 1981. An examination of spectral band ratioing to reduce the topographic effect on remotely sensed data, *International Journal of Remote Sensing* 2:115-33.

Justice, C.O., S.W. Wharton, and B.N. Holben. 1981. Application of digital terrain data to quantify and reduce the topographic effect on Landsat data. *International Journal of Remote Sensing*. 2: 213-230.

Lillesand, M. T. and R. W. Kiefer. 2000. *Remote sensing and image interpretation* (4th ed). John Wiley and Sons, Inc. New York, New York.

MacArthur, R. H. 1958. Population ecology of some warblers of northeastern coniferous forests. *Ecology* 39:599-619.

McCormick, C. M. 1999. Mapping exotic vegetation in the Everglades from large-scale aerial photographs. *Photogrammetric Engineering and Remote Sensing*. 65:179-184.

Næsset, E. 1997. Estimating timber volume of forest stands using airborne laser scanner data. *Remote Sensing of Environment* 61:246-53.

Optech Incorporated. 2003. About laser RADAR. http://www.optech.on.ca /aboutlaser.htm.

Pickup, G., G. N. Bastin, and V. H. Chewings. 2000. Measuring rangeland vegetation with high-resolution airborne videography in the blue-near infrared spectral region. *International Journal of Remote Sensing* 21:339-51.

Popescu, S.C and R.H. Wynne, 2003. (In press). Seeing the trees in the forest: using LIDAR and multispectral data fusion with local filtering and variable window size for estimating tree height. *Photogrammetric Engineering & Remote Sensing*.

Post, W. M. 1993. Uncertainties in the terrestrial carbon cycle (pp116-132). In *Vegetation Dynamics and Global Change* (A. M. Solomon and H. H. Shugrat, Eds.), Chapman and Hall, New York.

Richards, J.A. and X. Jia. 1999. *Remote Sensing Digital Image Analysis.* Springer-Verlag, New York, New York.

Richardson, A. J. and J. H. Everitt. 1992. Using spectra vegetation indices to estimate rangeland productivity. *Geocarto International.* 1:63-9.

Rignot, E., J. Way, C. Williams, and L. Viereck. 1994. RADAR estimates of aboveground biomass in boreal forests of interior Alaska. *IEEE Transactions on Geoscience and Remote Sensing* 32:1117-24.

Ritchie, J. C., M. S. Seyfried, M. J. Chopping, and Y. Pachepsky. 2001. Airborne laser technology for measuring rangeland conditions. *Journal of Range Management* 54:A8-21.

Rothermel, R. C. 1991. Predicting behavior and size of crown fires in the northern Rocky Mountains. Research Article INT-438, USDA Forest Service, Intermountain Research Station, Fort Collins, Colorado.

Ryan, M. C. and B. J. Yoder. 1997. Hydraulic limits to tree height and tree growth. *BioScience* 47:235-242.

Scheffler, E.J. 1976. Aspen vegetation in a portion of the east central Alberta parklands. M.Sc. Thesis. University of Alberta.

Schowalter, T. D. 1995. Canopy arthropod communities in relation to forest age and alternative harvest practices in western Oregon. *Forest Ecology and Management* 78:115-125.

Schowengerdt, R.A. 1983. Digital image classification (chapter 3, pp129-207). In *Techniques for image processing and classification in remote sensing*. Academic Press, Orlando, Florida.

Smith, A.M., D.J. Major, M.J. Hill, W.D. Willms, B. Brisco, C.W. Lindwall, and R.J. Brown. 1994. Airborne synthetic aperture RADAR analysis of rangeland revegetation of a mixed prairie. *Journal of Range Management* 47:385-391.

Stelfox, J. B. (editor) 1995. Relationship between stand age, stand structure, and biodiversity in aspen mixedwood forests in Alberta. Jointly published by Alberta Environmental Centre (AECV95-R1), Vegreville, AB, and Canadian Forest Service (Project No. 0001A), Edmonton, Alberta.

Thomas, L. and F. Juanes. 1996. The importance of statistical power analysis: an example from Animal Behaviour. *Animal Behaviour* 52: 856-859.

Trottier, G.C. 1986. Disruption of rough fescue, Festuca hallii, grassland by livestock grazing in Riding Mountain National Park, Manitoba. *Canadian Field Nature* 100:488-495.

VCL. 2000. Science Objectives of Vegetation Canopy LIDAR (VCL). http://www.geog.umd.edu/vcl/.

Waring, R.H, J. Way, E.R. Hunt, L. Morrissey, K.J. Ranson, J.F. Weishampel, R. Oren, and S.E. Franklin. 1995, Imaging RADAR for ecosystem studies. *BioScience* 45:715–723.

Wheeler, G. W. 1976. Some grassland and shrubland communities in the parklands of central Alberta. Master thesis, Edmonton, Alberta.

Woodcock, C.E., J. Collins, S. Gopal, V. Jakabhazy,X. Li, S. A. Macomber, S. Ryherd, Y. Wu, V.J. Harward, J. Levitan, and R. Warbington. 1994. Mapping forest

vegetation using Landsat TM imagery and a canopy reflectance model. *Remote Sensing of Environment* 50:240-254.

Wright, H. A. and A. W. Bailey. 1982. Fire ecology: United States and Southern Canada. John Wiley & Sons, New York, New York.

5.8 Tables and Figures

Table 5-1 Height characteristics [mean (range)] of the 8 detailed vegetation types based on field sampling in July 2001.

Vegetation Type	Number of Plots	Overstory Vegetation Height		
		Herb (cm)	Shrub (cm)	Tree (m)
Fresh Riparian Meadow	15	48 (24-88)		
Saline Riparian Meadow	15	24 (8-49)		
Fescue Grassland	15	12 (1-44)		
Mixed Prairie Grassland	15	5 (1-12)		
Western Snowberry	15		45 (25-73)	
Silverberry	15		79 (44-122)	
Close Aspen Forest	15			8.48 (5.01-19.25)
Semi-open Aspen Forest	15			9.52 (5.24-15.72)
Mean	15	22	62	9.00

Table 5-2 Contingency table validating accuracy of the 3-class (vegetation) classification schedule using digital images and LIDAR data.

Land Cover Type	Validation Data Set (Known Land Cover Types) (# of plots)[1]											
	AF	SL	GL	BGD	Row Total	Com[2] Error	AF	SL	GL	BGD	Row Total	Com Error
Classified Type	On Original Mosaic Image						On Hybrid Color Composite					
Aspen Forest (AF)	**20**	7	2	0	29	31.0	**23**	3	6	2	34	32.3
Shrubland (SL)	7	**27**	12	0	46	41.3	8	**32**	4	0	44	27.3
Grassland (GL)	8	7	**34**	0	49	30.6	4	6	**40**	0	50	25.0
Bare Ground (BGD)	0	0	4	**10**	14	28.6	0	0	2	**8**	10	20.0
Actual Class No.	35	41	52	10	138		35	41	52	10	138	
Classification Accuracy (%)	57.1	65.9	65.4	100.0		34.1	65.7	78.0	76.9	80.0		25.4
Ommission Error (%)	42.9	34.1	34.6	0.00			34.3	22.0	23.1	20.0		
Overall Accuracy and 95% CI (%)	65.9 (53.5-90.7)						74.6 (68.8-81.5)					
Classified Type	On I-H-S Image						On LIDAR Data					
Aspen Forest (AF)	**18**	11	2	0	31	41.9	**31**	0	0		31	0.0
Shrubland (SL)	5	**18**	9	0	32	43.8	0	**0**	0		0	0.0
Grassland (GL)	12	12	**39**	3	66	40.9	4	41	**52**		97	46.4
Bare Ground (BGD)	0	0	2	**7**	9	22.2						
Actual Class No.	35	41	52	10	138		35	41	52		128	
Classification Accuracy (%)	51.4	43.9	75.0	70.0		40.6	88.6	0.0	100.0			35.2
Ommission Error (%)	48.6	56.1	25.0	30.0			11.4	100	0.00			
Overall Accuracy and 95% CI (%)	59.4 (45.6-74.6)						64.8					

[1]All the validation data were actual field samples different from those used for signatures.
[2]Com Error = Commission error (%) of total within a land cover class.

Table 5-3 Contingency table assessing classification accuracy of the 3 digital images and a LIDAR data classification schedule for 8 classes of vegetation.

Land Cover Type	Validation Data Set (Known Land Cover Types) (# of plots)[1]																				
	CAF	OAF	ENS	SPS	SEG	FSG	FRM	SRM	BGD	Row Total	Com[2] Error	CAF	OAF	ENS	SPS	SEG	FSG	FRM	SRM	BGD	Row Total	Com Error
Classification Data	Classification Schedule of Original Mosaic Image											Classification Schedule of Hybrid Color Composite										
Closed Aspen Forest (CAF)	**4**	3	0	1	0	1	0	0	0	9	55.6	**9**	6	0	2	0	0	0	0	0	17	47.1
Semi-Open Aspen Forest (OAF)	5	**8**	2	4	0	0	1	0	0	20	60.0	3	**5**	0	1	1	1	1	3	2	17	70.6
Silverberry (ENS)	3	1	**9**	5	5	4	0	1	0	28	67.9	3	2	**12**	4	1	3	0	0	0	25	52.0
Western Snowberry (SPS)	2	1	3	**10**	0	2	0	0	0	18	44.4	1	2	1	**15**	0	0	0	0	0	19	21.1
Mixed Prairie (SEG)	0	0	1	0	**7**	0	0	1	0	9	22.2	0	0	1	0	**13**	1	0	0	0	15	13.3
Fescue Grassland (FSG)	2	1	0	3	3	**9**	0	1	0	19	52.6	0	0	1	2	2	**10**	0	1	0	16	37.5
Fresh Riparian Meadow (FRM)	0	2	0	2	0	1	**7**	0	0	12	25.0	0	2	0	1	0	0	**7**	0	0	10	30.0
Saline Riparian Meadow (SRM)	0	3	0	1	2	1	0	**2**	0	9	77.8	0	2	0	1	0	3	0	**3**	0	9	66.7
Bare Ground (BGD)	0	0	0	0	1	0	0	3	**10**	14	28.6	0	0	0	0	1	0	0	1	**8**	10	20.0
Column Total	16	19	15	26	18	18	8	8	10	138		16	19	15	26	18	18	8	8	10	138	
Classification Accuracy (%)	25.0	42.1	60.0	38.5	38.9	50.0	87.5	25.0	100.0			56.3	26.3	80.0	57.7	72.2	55.6	87.5	37.5	80.0		
Overal accuracy and 95% CI (%)	47.8 (31.7-72.1)											59.4 (45.7-77.2)										
Classification Data	Classification Schedule of I-H-S Image											Classification Schedule of LIDAR Data										
Closed Aspen Forest (CAF)	**5**	3	1	3	0	0	1	0	0	13	61.5	**13**	2	0	0	0	0				15	13.3
Semi-Open Aspen Forest (OAF)	3	**7**	0	7	0	0	1	0	0	18	61.1	2	**14**	0	0	0	0				16	12.5
Silverberry (ENS)	1	1	**4**	3	0	2	0	0	0	11	63.6	0	0	**0**	0	0	0				0	0.0
Western Snowberry (SPS)	2	1	4	**7**	3	2	1	1	0	21	66.7											
Mixed Prairie (SEG)	0	0	0	0	**8**	0	0	0	0	8	0.0	0	0	6	**15**	4	0				25	40.0
Fescue Grassland (FSG)	4	2	4	2	5	**13**	0	1	0	31	58.1	1	3	33	3	**10**	1				51	80.4
Fresh Riparian Meadow (FRM)	0	2	2	3	1	0	**5**	2	0	15	66.7	0	0	2	0	4	**15**				21	28.6
Saline Riparian Meadow (SRM)	1	3	0	1	0	1	0	**3**	3	12	75.0											
Bare Ground (BGD)	0	0	0	0	1	0	0	1	**7**	9	22.2											
Column Total	16	19	15	26	18	18	8	8	10	138		16	19	41	18	18	16				128	
Classification Accuracy (%)	31.3	36.8	26.7	26.9	44.4	72.2	62.5	37.5	70.0			81.3	73.7	0.0	83.3	55.6	93.8					
Overal accuracy and 95% CI (%)	42.8 (31.4-59.3)											52.3 (37.3-91.9)										

[1]All the validation data were actual field samples different from those used for signatures. [2]Com Error = Commission error (%)of total within a land cover class.

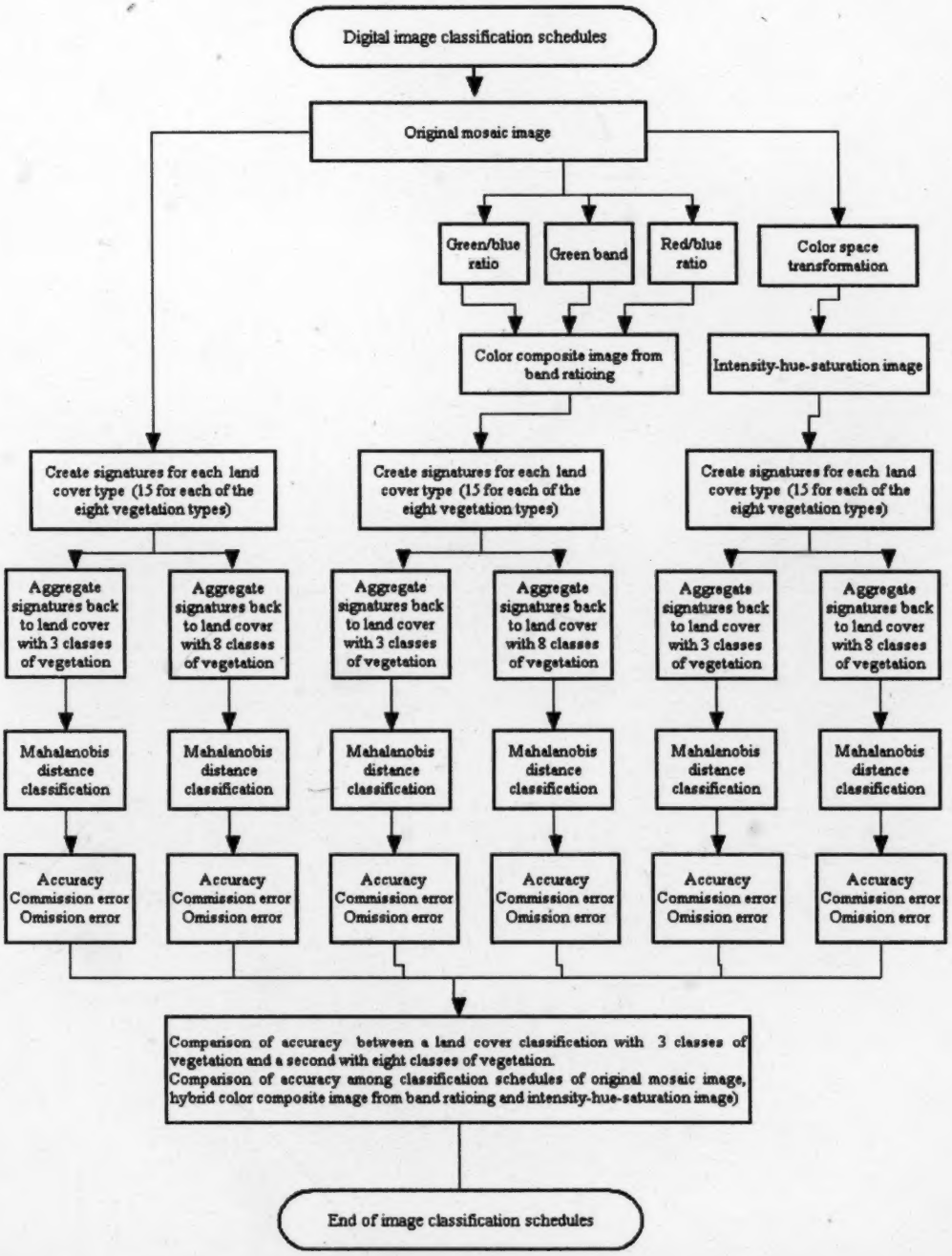
Digital image classification schedules
Original mosaic image
Green/blue ratio
Green band
Red/blue ratio
Color space transformation
Color composite image from band ratioing
Intensity-hue-saturation image
Create signatures for each land cover type (15 for each of the eight vegetation types)
Create signatures for each land cover type (15 for each of the eight vegetation types)
Create signatures for each land cover type (15 for each of the eight vegetation types)
Aggregate signatures back to land cover with 3 classes of vegetation
Aggregate signatures back to land cover with 8 classes of vegetation
Aggregate signatures back to land cover with 3 classes of vegetation
Aggregate signatures back to land cover with 8 classes of vegetation
Aggregate signatures back to land cover with 3 classes of vegetation
Aggregate signatures back to land cover with 8 classes of vegetation
Mahalanobis distance classification
Mahalanobis distance classification
Mahalanobis distance classification
Mahalanobis distance classification
Mahalanobis distance classification
Mahalanobis distance classification
Accuracy Commission error Omission error
Accuracy Commission error Omission error
Accuracy Commission error Omission error
Accuracy Commission error Omission error
Accuracy Commission error Omission error
Accuracy Commission error Omission error
Comparison of accuracy between a land cover classification with 3 classes of vegetation and a second with eight classes of vegetation.
Comparison of accuracy among classification schedules of original mosaic image, hybrid color composite image from band ratioing and intensity-hue-saturation image)
End of image classification schedules

Figure 5-1 Flowchart of digital image classification schedules on original mosaic image, color composite image from band ratioing and intensity-hue-saturation image with 3 and 8 classes of vegetation.

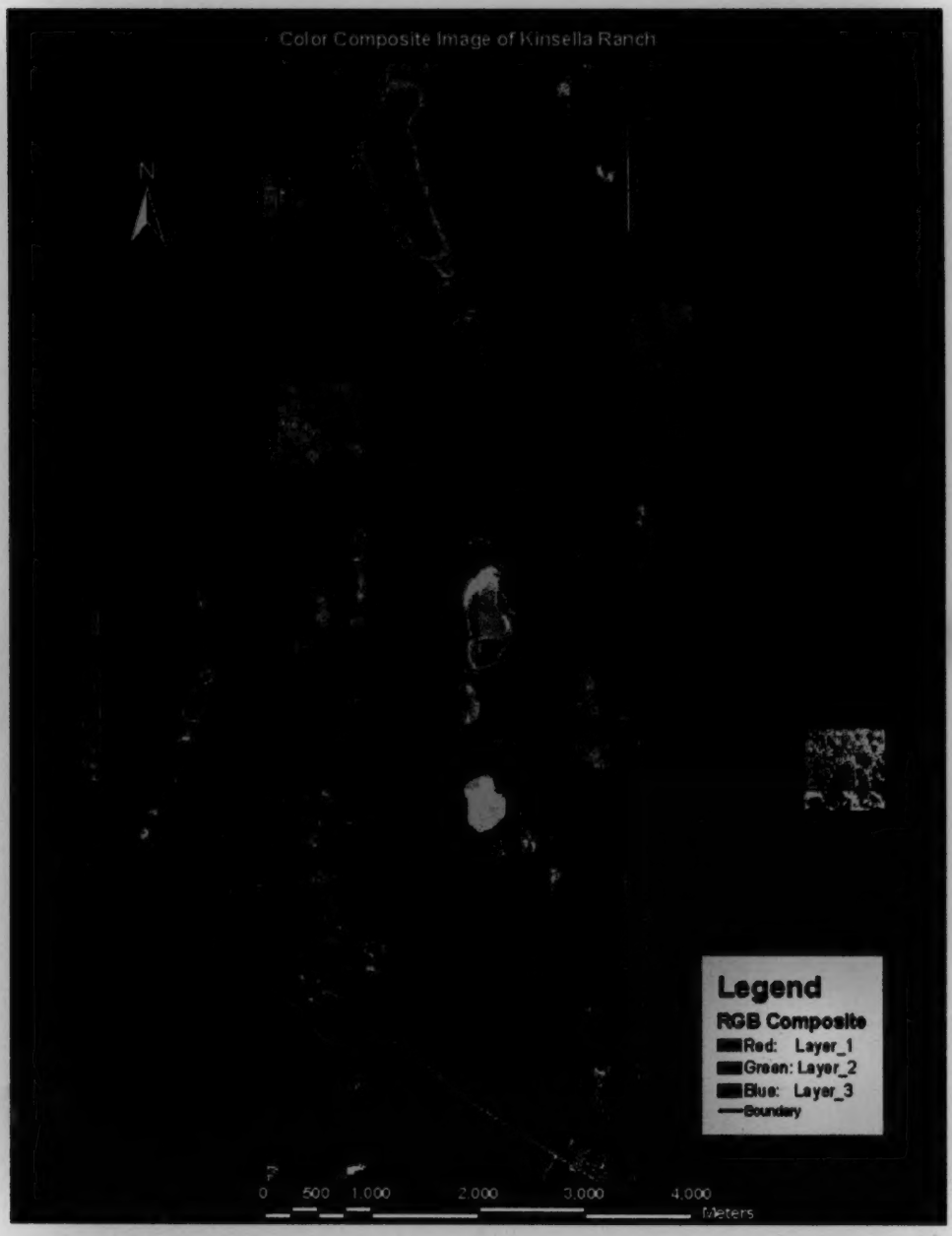

Figure 5-2 Hybrid color composite image of the study area from red/blue ratio, green and green/blue ratio.

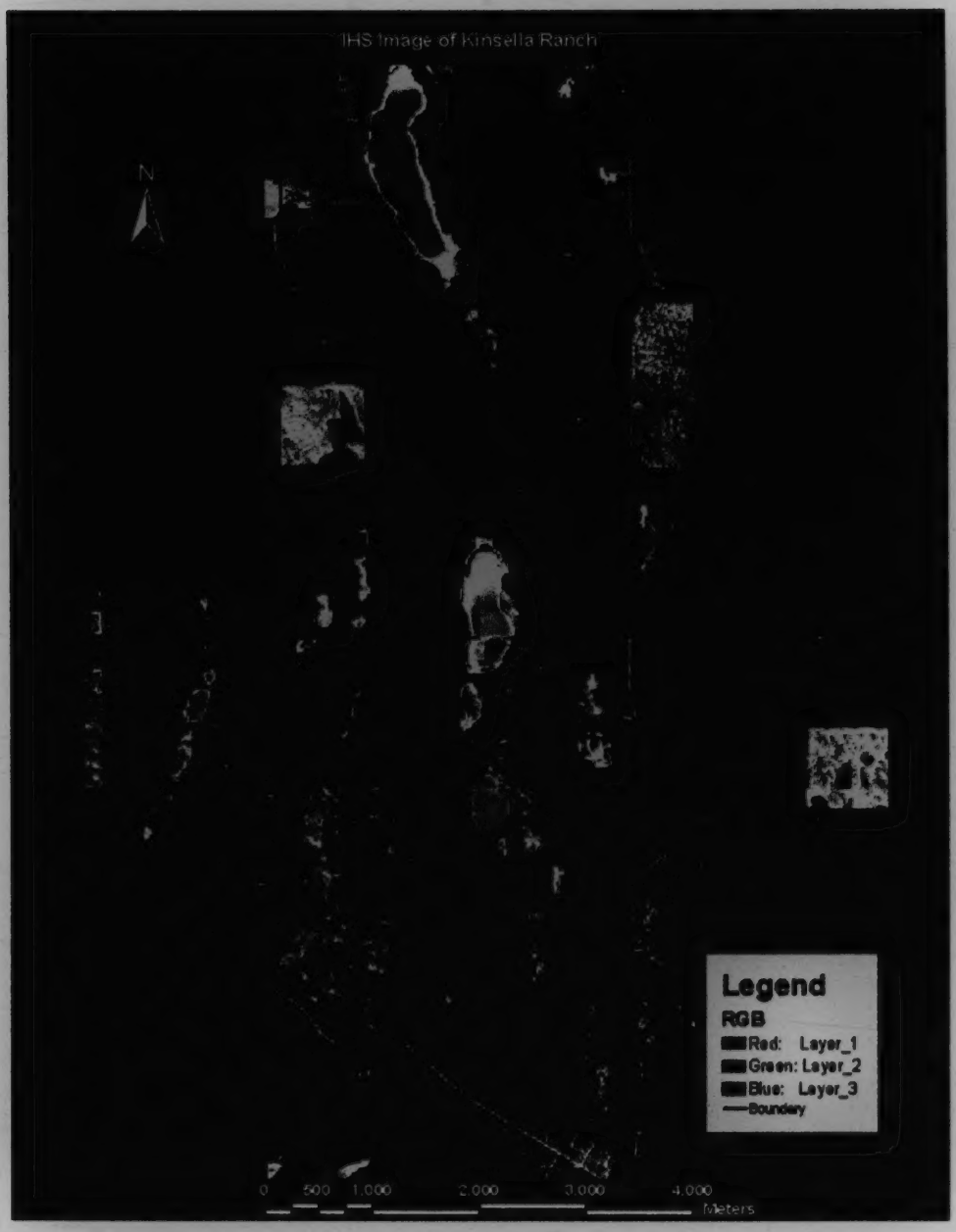

Figure 5-3 Intensity-hue-saturation image of the study area.

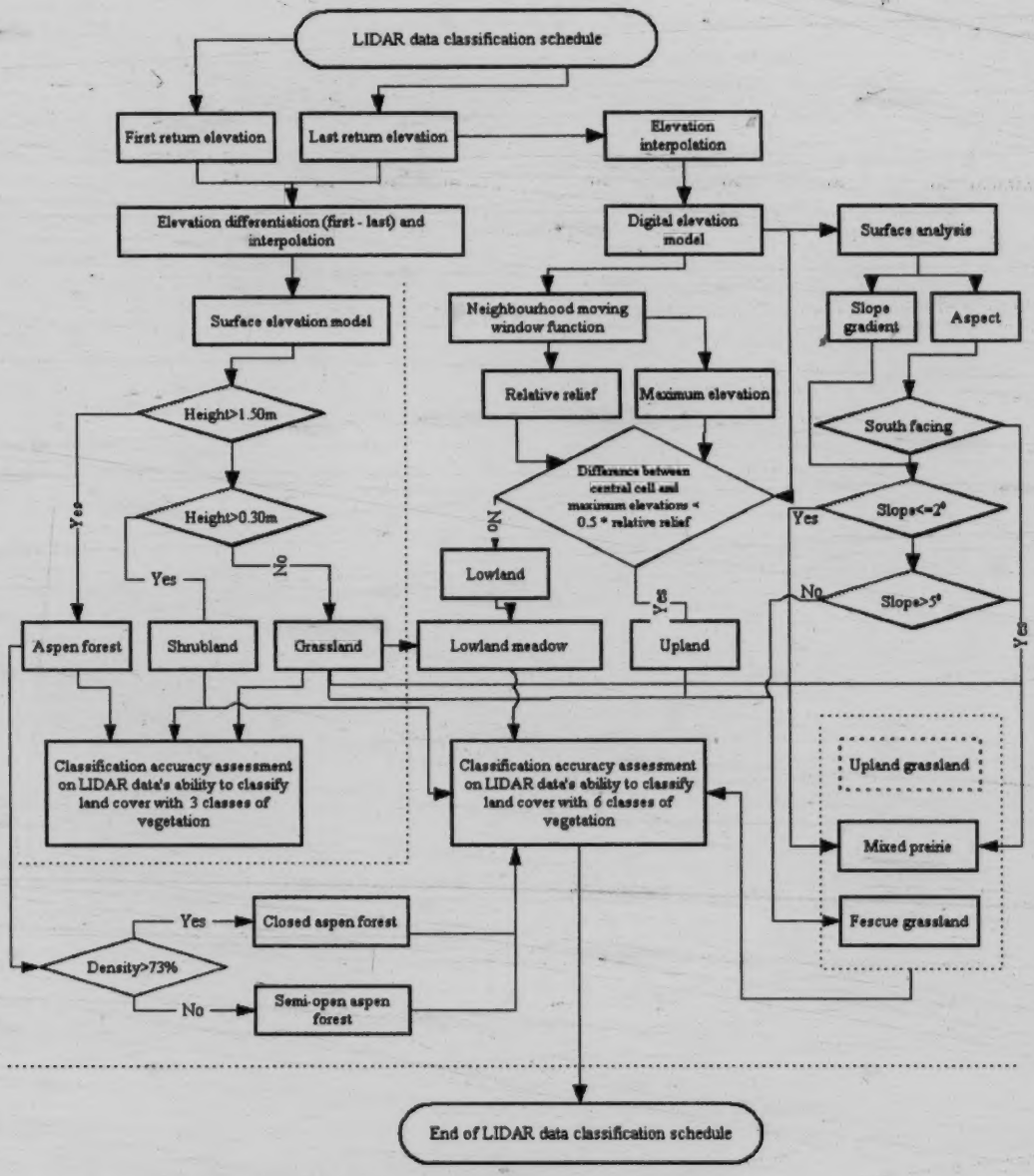

Figure 5-4 Flowchart of LIDAR data classification schedule.

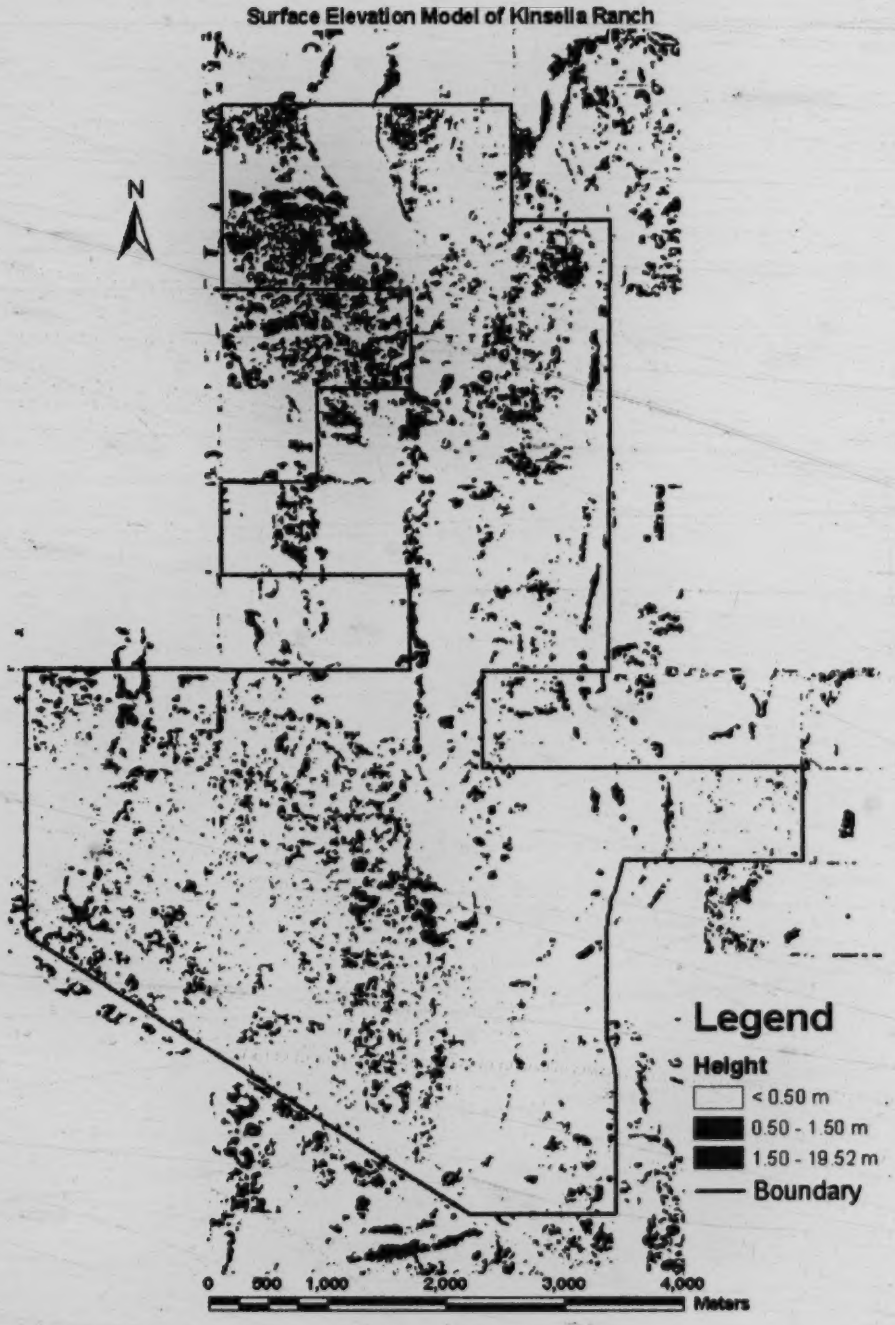

Figure 5-5 Surface elevation model of the study area.

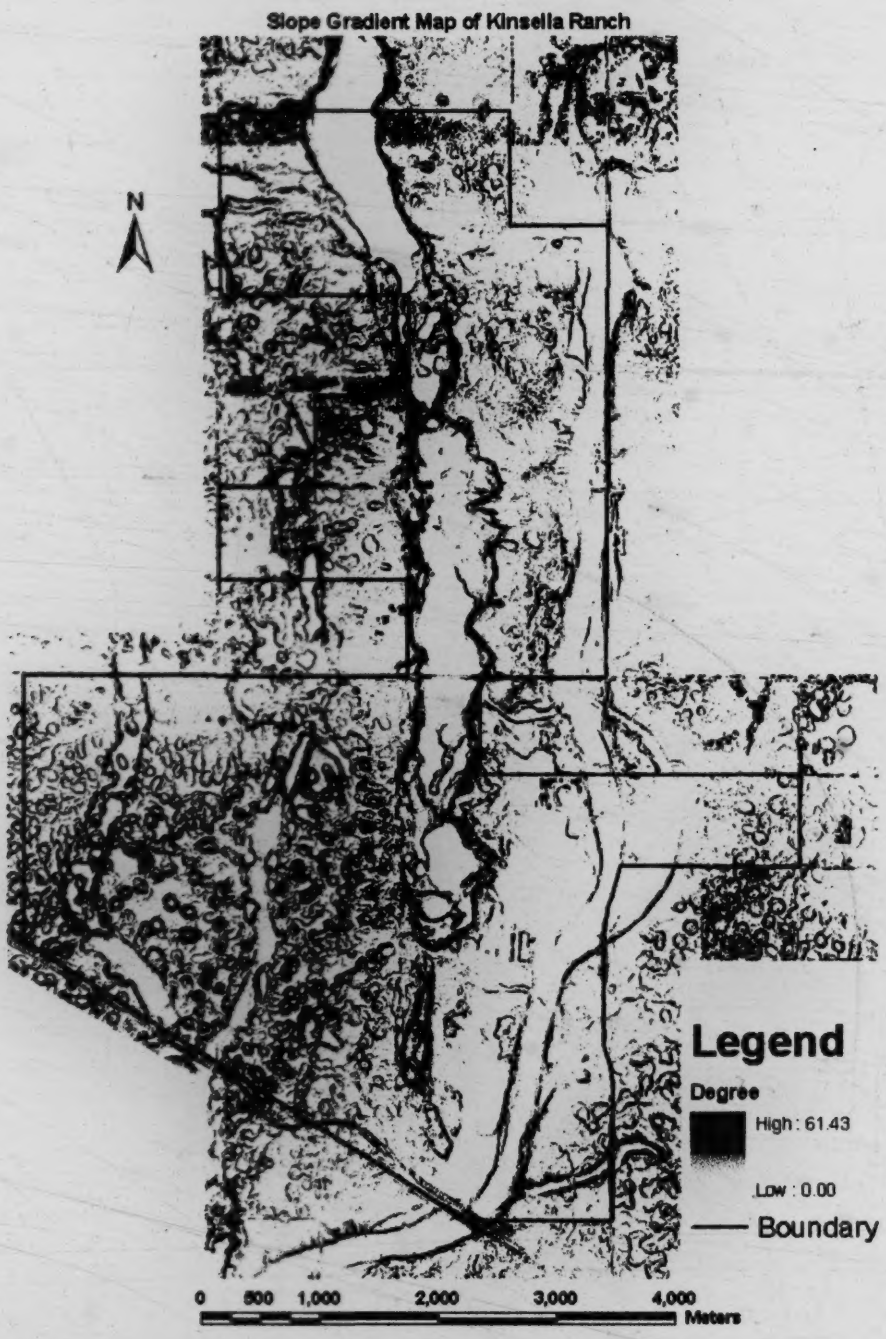

Figure 5-6 Slope gradient map of the study area.

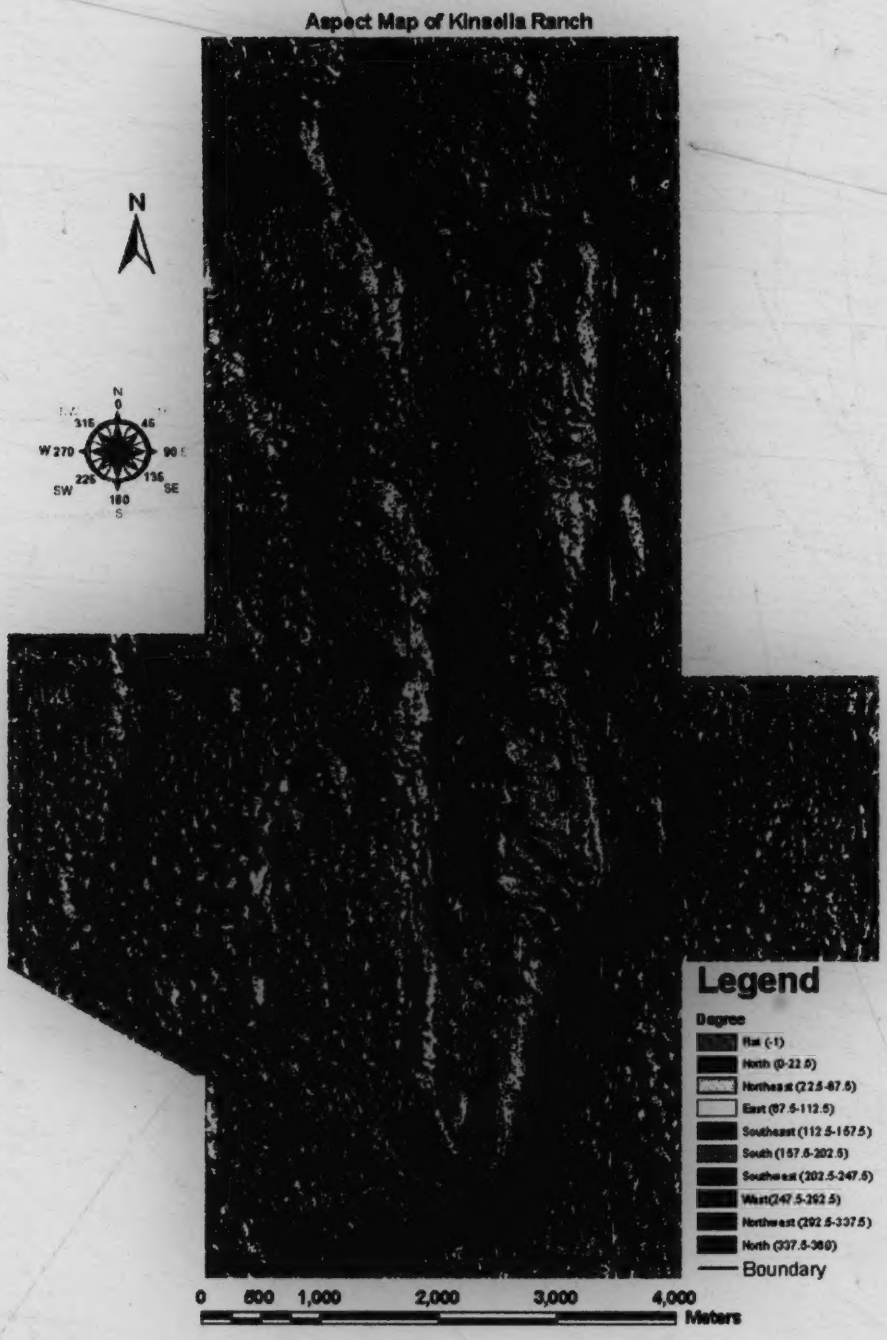

Figure 5-7 Aspect map of the study area.

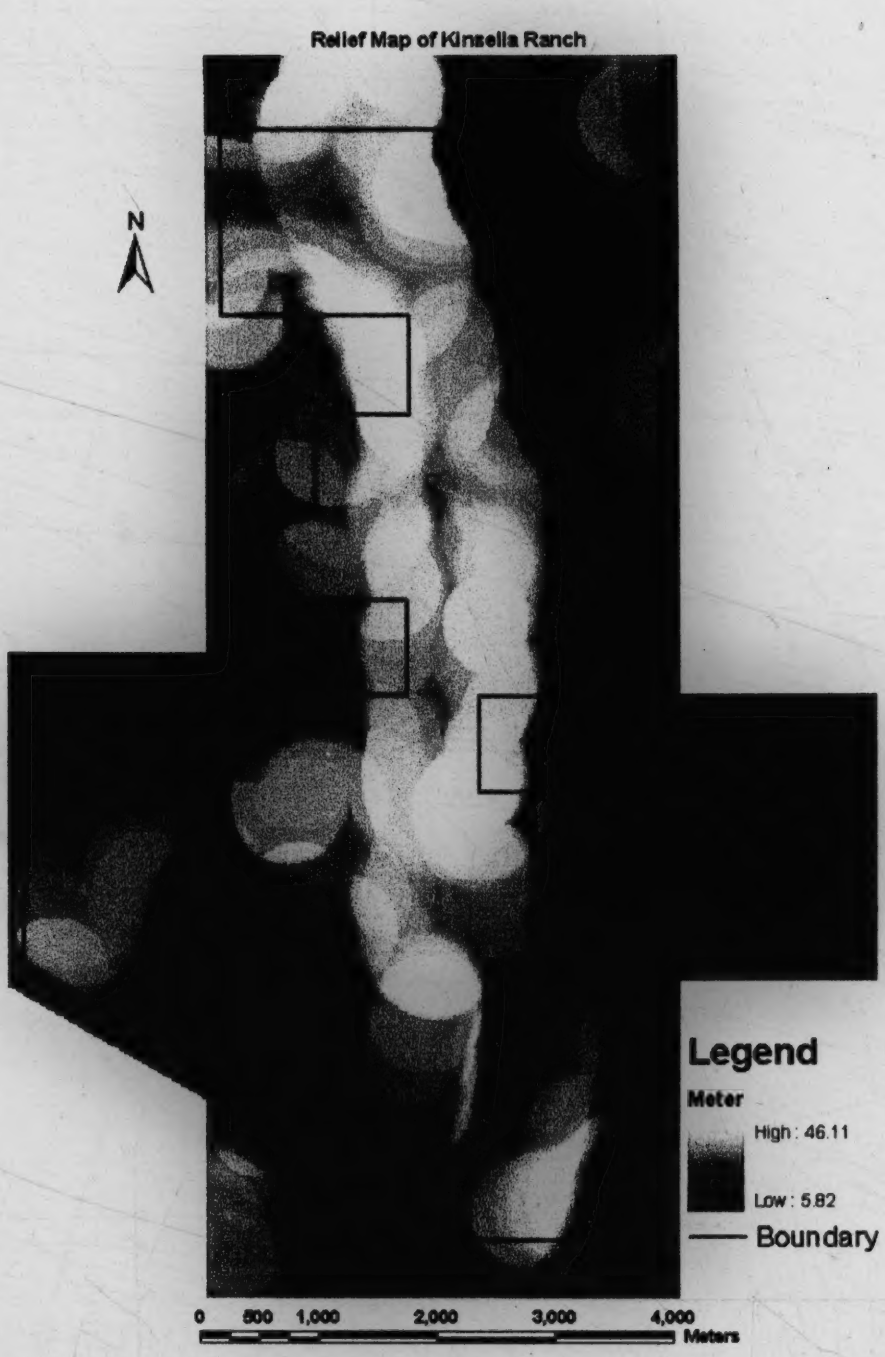

Figure 5-8 Relative relief map of the study area.

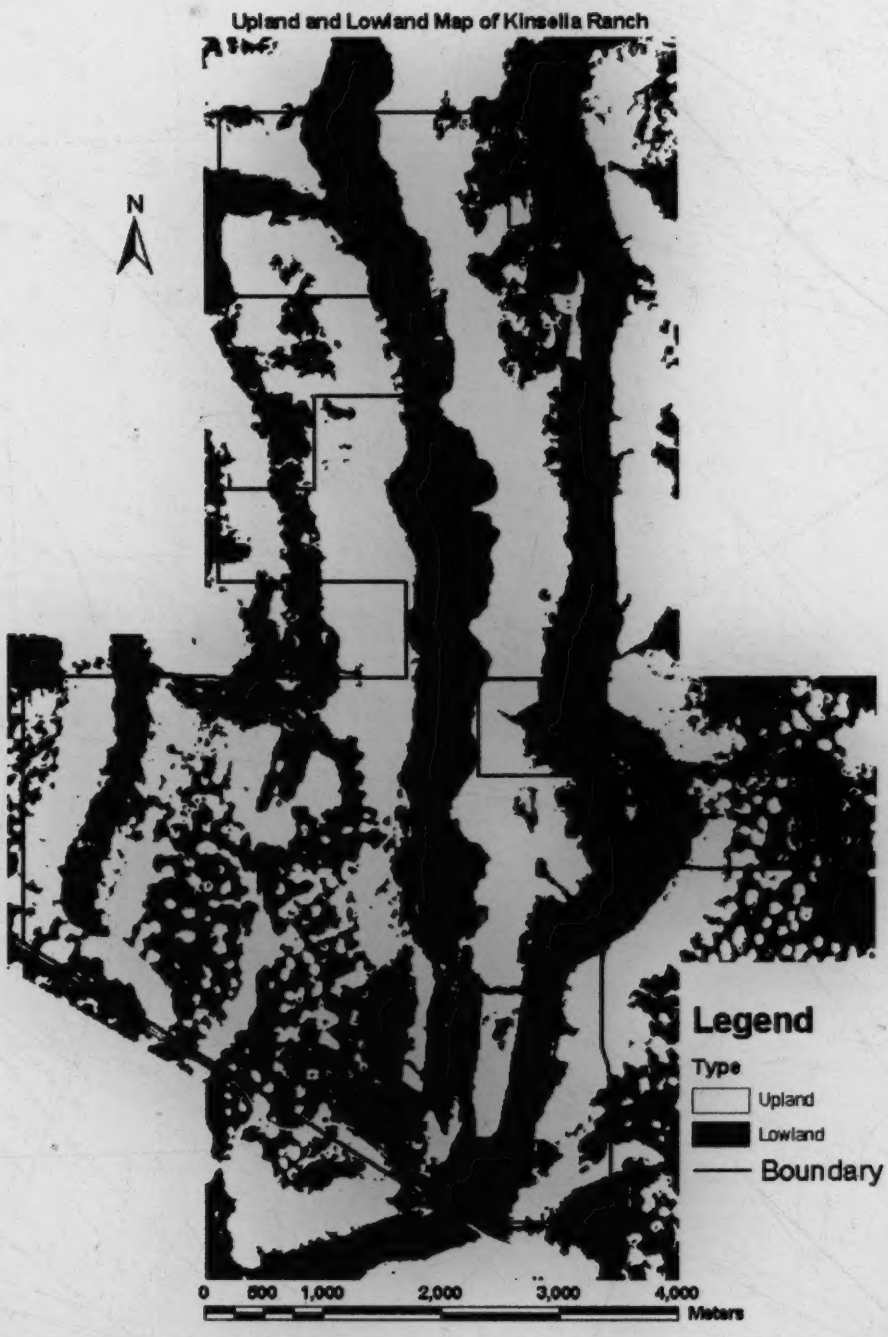

Figure 5-9 Upland and lowland map of the study area.

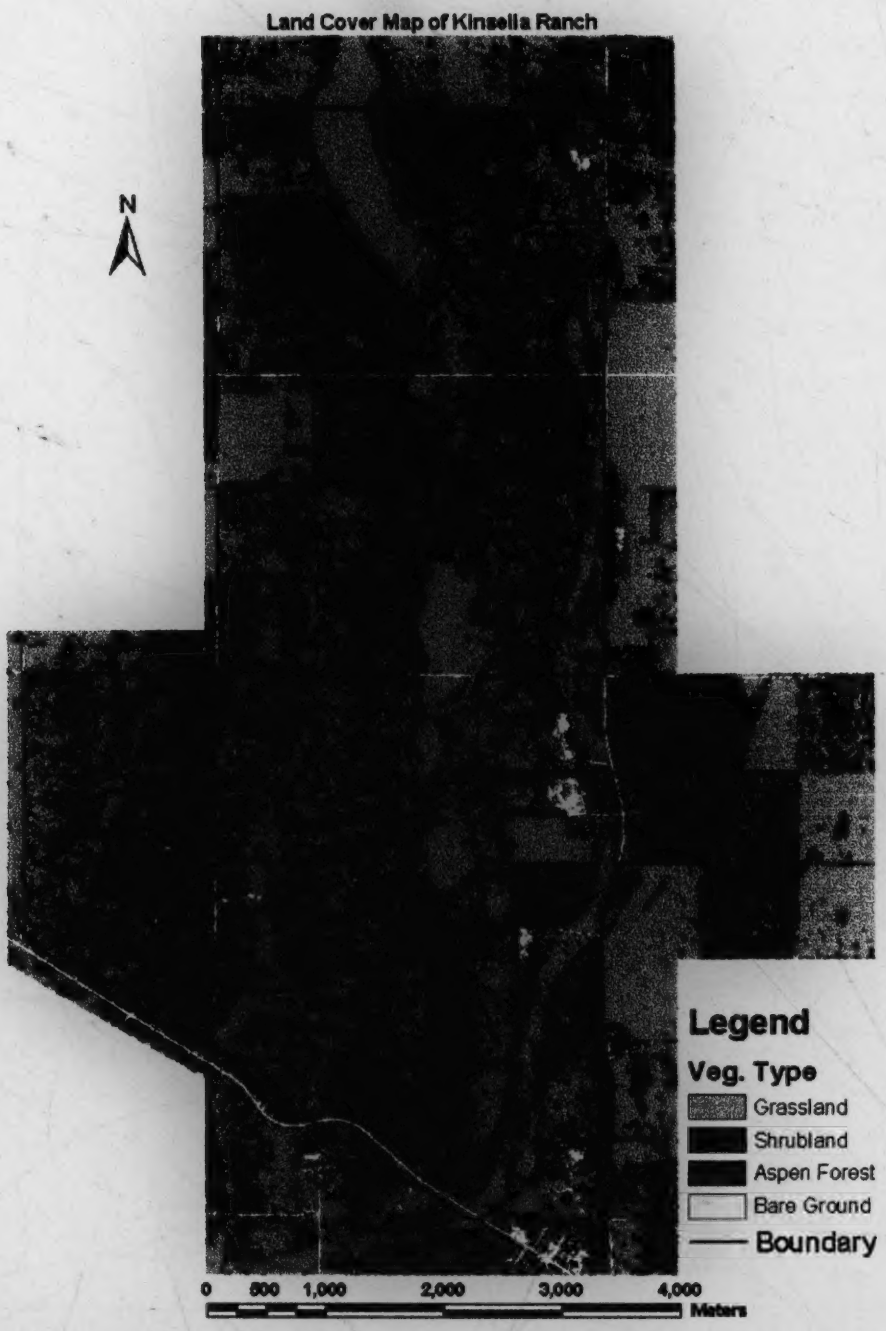

Figure 5-10 Land cover map of the study area produced by integrating LIDAR data and digital image classification schedules with 3 classes of vegetation.

Figure 5-11 Land cover map of the study area produced by integrating LIDAR data and digital image classification schedules with 7 classes of vegetation.

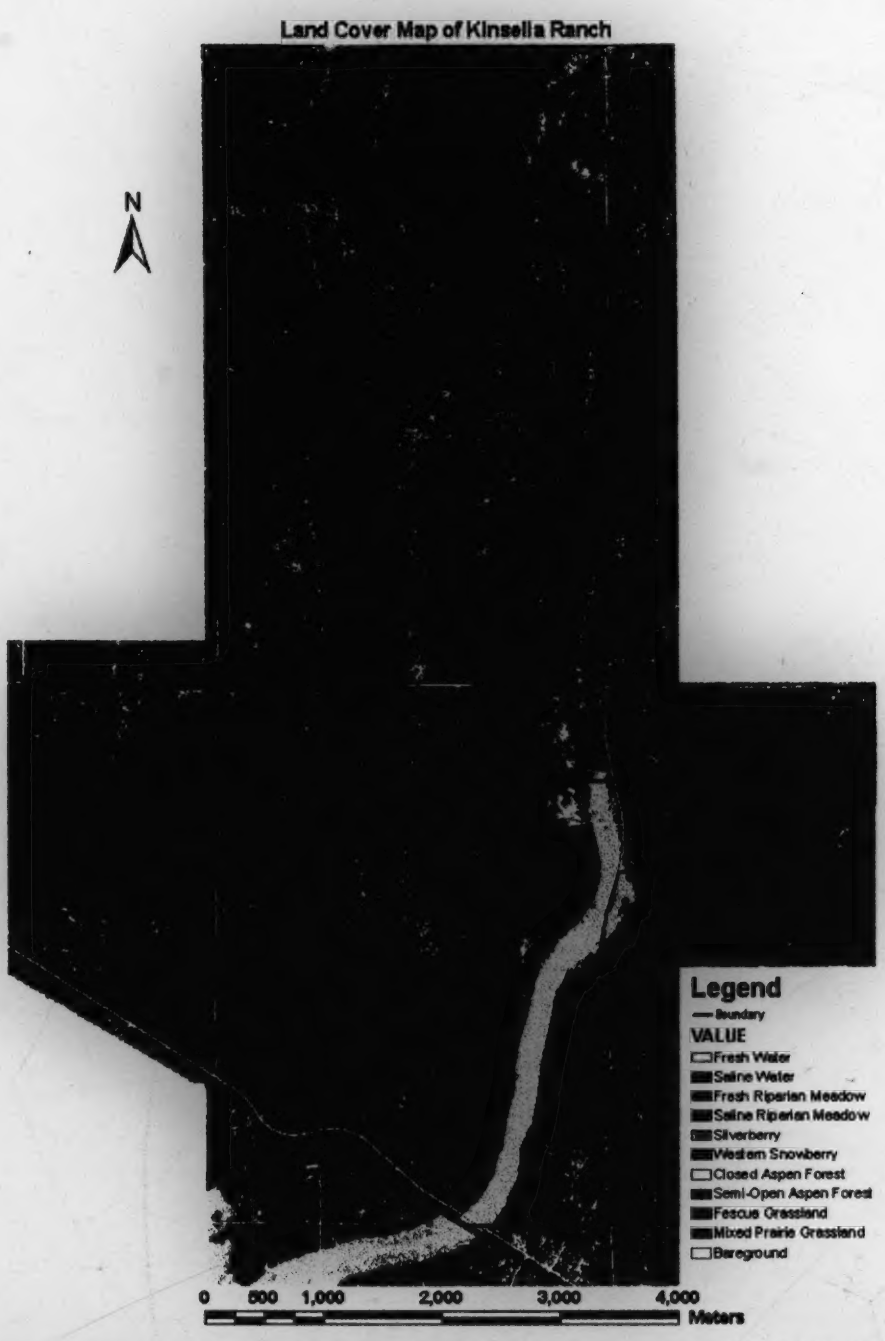

Figure 5-12 Final land cover map of the study area produced by integrating LIDAR data and digital image classification schedules with 11 classes of land cover (including 8 classes of vegetation).

6 Synthesis/Conclusion

Rangelands comprise 60-70% of the global land surface (Everitt 1992). These diverse ecosystems produce a broad array of tangible and intangible products. Physical commodities include those such as forage and habitat for livestock or wildlife, water, minerals, energy, forest products, recreational opportunities, and plant and animal genes, with many of these being economically important rangeland outputs. Rangelands also produce intangible products such as natural beauty and wilderness that satisfy important societal values, many of which can be economically important (Cox *et al.* 1994). Ranchers, land administrators, and range and wildlife conservationists, are collectively interested in monitoring the current condition of rangelands, including their ability to sustainably provide key outputs, which in most areas, include either the provision of high quality livestock forage (Waer *et al.* 1997), wildlife habitat (Weber *et al.* 2002), or both (Arsenault and Norman 2002).

Remote sensing is a potential alternative to traditional rangeland monitoring to gather site-specific data from vast areas (Tueller 1989). Primary benefits include synoptic (e.g., spatially complete) coverage, high cost-effectiveness (i.e., reducing the cost per unit area examined), and lower labour requirements relative to point-based sampling. In addition, remote sensing can provide data on areas that are often inaccessible, as well as highly heterogeneous landscapes where complex mosaics of vegetation with frequent transitional areas may preclude the efficient use of point sampling. Remote sensing data also facilitates, though its complete coverage, additional forms of analysis such as landscape metrics (e.g., vegetation distribution). The spatially

complete nature of remotely-sensed information on rangelands provides a top-down strategy for rangeland management, and as a result, provides a potential complementary data source to the collection of detailed point-based plant community information.

Light detection and ranging (LIDAR) is an active remote sensing system, analogous to RADAR, but using laser light. Unlike most traditional sensors, the laser-based sensor relies on active rather than passive illumination, making shadow effects (e.g., from buildings or trees) not a concern. Since each laser point is individually georegistered, aerial triangulation or orthorectification of data is not required.

LIDAR instruments measure the roundtrip time for a pulse of laser energy to travel between the sensor and target. This incident pulse of energy reflects off the vegetation canopy (branches, leaves) or ground surfaces and back to the instrument where it is collected by a telescope. The travel time of the pulse, from initiation until it returns to the sensor, provides a distance or range from the instrument to the object (hence the common use of the term "laser altimetry" which is synonymous with LIDAR). There are a number of different LIDAR systems made by different manufacturers, but basically they can be classified into 2 categories: scanning and profiling LIDAR. At present, the majority of systems in use are based on the pulse ranging principle and belong to small footprint ($\leq$10 m in diameter) scanning LIDAR. Profiling and scanning airborne laser altimeters have been typically used for terrain mapping, land cover classification and the identification of forest structure, although few applications have been done in rangelands.

Detailed geographic information system (GIS) studies on plant ecology, animal behavior and soil hydrologic characteristics across spatially complex landscapes require

digital elevation models (DEM) with high accuracy. This research demonstrated that, compared to traditional point sampling and remote sensing techniques, LIDAR data could be used to create a DEM of relatively superior quality (overall accuracy +2 cm and RMSE of 1.21 m). This accuracy of DEM is valuable for precision ranching, precision farming and other scientific research that require such a DEM. However, accuracy of the LIDAR-derived DEM did vary with a number of external factors and special consideration should be taken in actual application. Non-vegetational individual factors such as off-nadir distance and slope gradient did not significantly influence LIDAR-derived DEM accuracy; however, when integrated, these factors did have an impact (P=0.05) and should be considered. DEM accuracy normally increased at positions with shorter off-nadir distances and smaller (i.e., flatter) slope gradient.

Vegetational factors had the greatest influence on the LIDAR-derived DEM accuracy. In our analysis, elevations had the tendency of being over-estimated within forested areas, but under-estimated within grasslands (upland and lowland). Forest areas differed significantly from both upland grasslands and lowland meadows with respect to their influence on accuracy of the LIDAR derived-DEM. If a DEM is to be built to its optimal accuracy, LIDAR sampling should be taken in leaf-off condition to reduce vegetation influence. Though the effect of slope gradient could be ignored in our analysis, if the majority of the slope gradient is greater than 10^{o}, this effect might be reconsidered.

Information on land surface and vegetation spatial structure (i.e., physiognomy) is key for interpreting range condition. Ground-based measurements of these properties are difficult and time-consuming. Scanning airborne laser altimeter systems provide an

effective alternative to quantify vegetation characteristics over large land areas. The agreement between airborne laser altimeter and observed field measurements in vegetation height, cover and density within both closed and semi-open aspen forest indicated this technology is useful for characterizing forest vegetation. The capability of using LIDAR data to quantify understory vegetation characteristics, as well as those of individual shrublands and grasslands, however, was far more limited and should be used with caution. When characterizing vegetation within the understory of aspen forest, the available number of LIDAR sampling points reaching the understory should be first examined (best to have >50pts/100m^2). To achieve optimal vegetation characterization accuracies, it is best to use growing season sampling data (e.g., July/August). It is also important to coincide LIDAR data collection with field vegetation sampling to reduce the influenced of animal grazing, phenological changes and other factors on accuracy. Extra caution should be taken when sampling vegetation using LIDAR in areas with vegetation less than 0.3 m in height. The over- or under-estimation of canopy height and cover in sparsely populated shrub and low height herbaceous communities will not be resolved unless new techniques are available to discriminate the background noise in the laser return signal (Weltz *et al.* 1994).

Vegetation types are integral parts of the landscape and have to be evaluated at large scales to understand the biological, ecological and hydrologic processes associated with natural and agricultural systems. LIDAR mapping facilitates the inventory of rangeland resources and range site (topography) identification, benefits on understanding of forage production, animal and wildlife habitats, and assists in setting stocking rates (sustainability) and enhancing overall rangeland management. LIDAR data can be used

effectively to map closed- and semi-open aspen forest as well as upland (e.g., mixed prairie and fescue) grasslands and lowland (fresh and saline riparian) meadows based on the topographic information derived. This requires that the image interpreter has a clear picture of the actual distribution of the above 6 vegetation types and understands their spatial dependence on topography. However, LIDAR data were found to be limited when used to map low stature shrublands (both western snowberry and silverberry).

In this research, neither the individual 3- nor the 8-class vegetation schedules can produce overall classification accuracies definitively considered to be superior. However, the extraction and integration of data types can create accuracies superior to any of the 4 individual techniques used in isolation. Though LIDAR data and digital imagery use quite different measurements (range vs. reflectance image data), integration of these mapping techniques can significantly increase the accuracy of vegetation and land cover mapping. LIDAR data not only offer the potential to measure landscapes over large areas more effectively, but also contribute to mapping accuracy.

The utility of using LIDAR data mainly depends on its unique elevation and height information for DEM modelling, vegetation characterization and mapping. This uniqueness, however, is restricted by the availability of the current technology, such as the lack of algorithms and data processing expertise. The use of LIDAR data is also limited by the practicality of LIDAR intensity information (Fowler 2000) and the difficulty in separating different land cover types through spectral brightness information, which is, in contrast, well developed on digital images. Additionally, there are few LIDAR data sets available. Commercial airborne small-footprint systems are only now becoming available on a cost-effective basis and large-footprint systems are still in the

research phase. These limitations will likely decline with the continuing maturation of technology and fusion with information from other remote sensing systems. The fusion of LIDAR with digital imagery further extends our ability to identify vegetation and landscape characteristics, understand our related resources and improve management practices.

6.1 Literature Cited

Arsenault, R. and O. S. Norman. 2002. Facilitation versus competition in grazing herbivore assemblages. *Oikos* 97:313-18.

Cox, W.J., J.H. Cherney, D.J.R. Cherney., and W.D. Pardee 1994. Forage quality and harvest index of corn hybrids under different growing conditions. *Agronomy Journal* 86:277-282.

Everitt, J.1992. Overview of remote sensing for rangeland management. *Geocarto International* 7:1-15.

Fowler, R. A. 2000. The low down on LIDAR. *Earth Observation Magazine* 9:1-7.

Tueller, P. T. 1989. Remote Sensing technology for rangeland management. *Journal of Range Management.* 42:442-453.

Waer, N. A, H. L. Stribling, and M. K. Causey. 1997. Cost efficiency of forage plantings for white-tailed deer. *Wildlife Society Bulletin* 25:803-8.

Weber, W. L., J. L. Roseberry, and A. Woolf. 2002. Influence of the conservation reserve program on landscape structure and potential upland wildlife habitat. *Wildlife Society Bulletin* 30:888-98.

Weltz, M.A., J.C. Ritchie, and H.D. Fox. 1994. Comparison of laser and field measurements of vegetation heights and canopy cover. *Water Resources Res.* 30:1311-20.

Appendix 1 Target calendar of data collection at Kinsella UA Ranch

Date	Event	Activities
Oct. 3, 2000	LIDAR data acquisition	Collected LIDAR first and last return coordinates (x, y coordinates and z elevations) as well as intensity information.
Oct. 3, 2000	Air photo acquisition	Collected digital images of 3 bands (red, green and blue).
July 15 – Aug. 15, 2001	Benchmarks and ground truthed points setup using total laser station and differential GPS.	a) Set up 27 interconnected benchmarks and measured x, y coordinates along with z elevations. b) Established 260 ground truthed points with x, y coordinates and elevations measured. The slope gradient, aspect, vegetation type and height information of each point were also examined.
July 15 – Aug 15, 2001	Vegetation sampling	a) Created 120 vegetation sampling plots with each sampling plot in a 6 m radius. b) Within each plot, vegetation was sampled along 2, 10m long parallel transects. c) On each transect, 10 uniformly distributed 0.5 x 1.0m quadrats were sampled for maximum understory vegetation height (herb and shrub separately) and cover. d) In aspen forest, 6 trees from the dominant overstory were measured for height using a clinometer and tape ruler. e) Each aspen forest plot was also assessed for the cover and density of over- and middle-story aspen stems, as well as other tall trees (height $\geq$1.5m) within 2, belted transects, each 2x10m, centred on the linear transects. f) Eco-site data on slope, aspect and landscape position of each plot were also recorded.
Sept., 2001 - Dec., 2003	Research on the capability of using LIDAR data to model DEM, characterize and map vegetation	Corresponding findings were presented in Chapter 3, 4 and 5, respectively.

Appendix 2 The mean brightness and std. dev. of the 120 signatures within the 8 vegetation types and bare ground.

Land cover type		I-H-S image*			Original mosaic image			Color composite image		
		Blue	Green	Red	Blue	Green	Red	Blue	Green	Red
Mixed prairie grassland	Mean	0.23	321.62	0.09	51.92	53.93	59.96	1.04	44.79	1.13
	Std. dev.	0.01	86.22	0.02	3.82	5.12	5.61	0.05	3.76	0.08
Fescue grassland	Mean	0.19	316.79	0.11	43.57	47.58	52.74	1.07	44.42	1.12
	Std. dev.	0.02	83.42	0.04	5.67	5.28	11.42	0.05	2.59	0.09
Silverberry	Mean	0.14	274.37	0.08	37.87	39.72	43.23	1.04	36.17	1.13
	Std. dev.	0.02	105.93	0.04	5.11	5.45	7.01	0.04	1.81	0.10
Western snowberry	Mean	0.15	235.33	0.07	35.11	37.82	39.30	1.04	35.87	1.10
	Std. dev.	0.02	119.63	0.04	3.15	6.31	6.31	0.10	4.83	0.11
Fresh riparian meadow	Mean	0.15	98.26	0.08	40.81	38.72	40.23	0.93	36.80	0.96
	Std. dev.	0.03	76.62	0.06	6.16	8.15	9.25	0.07	6.81	0.13
Saline riparian meadow	Mean	0.21	226.67	0.07	45.24	45.64	48.35	1.01	45.04	1.06
	Std. dev.	0.04	112.37	0.04	5.39	5.44	4.76	0.06	4.12	0.09
Close aspen forest	Mean	0.12	72.80	0.13	37.73	38.92	39.65	0.92	29.32	1.01
	Std. dev.	0.03	70.67	0.08	8.98	10.96	7.91	0.14	12.67	0.26
Semi-open aspen forest	Mean	0.13	61.54	0.12	26.63	22.71	26.40	0.87	27.56	0.96
	Std. dev.	0.03	67.16	0.06	3.02	4.64	6.70	0.13	13.64	0.25
Bare ground	Mean	0.35	186.63	0.10	79.79	81.50	91.04	1.04	96.23	1.18
	Std. dev.	0.03	158.24	0.07	12.21	10.92	11.86	0.11	8.94	0.18

* For the I-H-S image, the blue, green and red band correspond to the intensity, hue and saturation of an image.

Appendix 3 The effect of vegetation on LIDAR-derived DEM accuracy (RMSE in parentheses).

(Unit: mean: cm, RMSE: m)
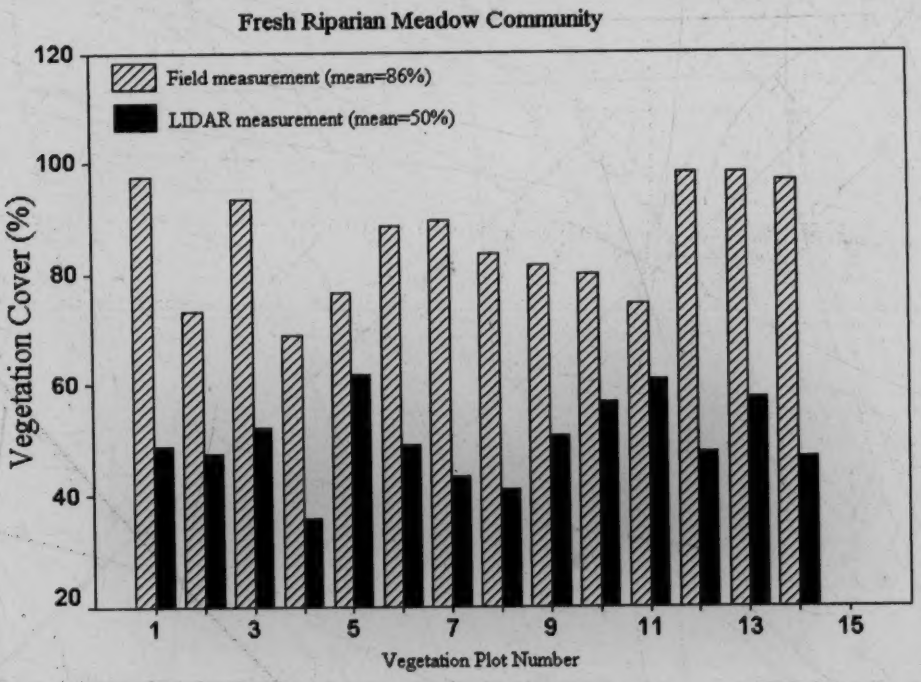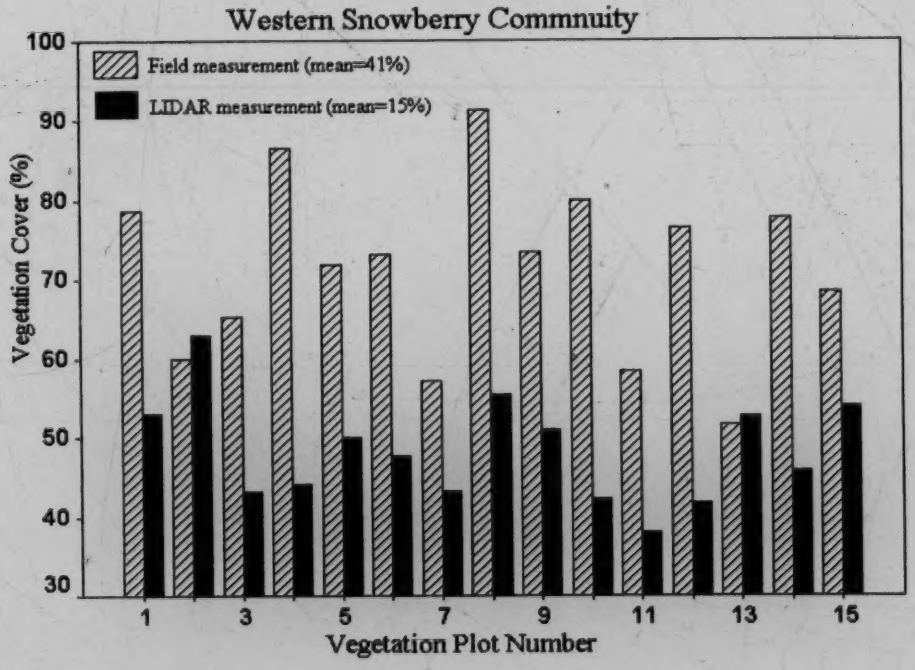
Appendix 4 Comparison between LIDAR-derived and field measured veg. cover.